ANAESTHETIC MODULATION OF ION CHANNEL KINETICS IN BOVINE CHROMAFFIN CELLS

BY

PAUL CHARLESWORTH

Thesis submitted for the degree of Doctor of Philosophy to the Faculty of Science of the University of London

Department of Physiology
Royal Free Hospital School of Medicine
Rowland Hill Street
Hampstead
London NW3 2PF

ABSTRACT

The thesis describes a patch clamp study of the action of anaesthetics on the ion channels primarily responsible for initiating secretion in bovine chromaffin cells. The adrenal chromaffin cell is homologous with sympathetic post-ganglionic neurones and was chosen as a model for studying excitatory neuronal synapses. Pre- and post- synaptic events are modelled by effects on the voltage-gated calcium channels and nicotinic acetylcholine receptor channel respectively.

The overall aim has been to describe anaesthetic depression of excitatory synaptic transmission at the ion channel level. Results of experiments with a representative range of anaesthetic agents are shown.

Modulation of the nicotinic receptor channel has been studied at the level of whole cell currents and single ion channels. Whole cell macroscopic currents were subjected to spectral analysis to derive kinetic parameters of channel gating. These parameters were also calculated from single channel studies and the results used to derive models explaining the modulation of nicotinic acetylcholine receptor channels by anaesthetics. It is shown that while there are common features in the action of different agents, the detailed mechanism by which they inhibit nicotinic gated ion channels varies.

Prior to investigating the action of anaesthetics on calcium channel currents, a study was made using a variety of voltage pulse protocols and selective channel blockers to characterise the macroscopic current and asses the contribution of the various calcium channel sub-types. It is shown that calcium currents in chromaffin cells have two components, probably carried by L and N type channels as described by other workers. Of the anaesthetics studied, all but procaine reduced whole cell calcium channel currents within a relevant concentration range.

A major component of the reduction in ion flux was due to an enhanced rate at which currents decayed after being activated by depolarising voltage pulses. This was observed with all effective agents, though the magnitude of the effect varied and it was not possible to ascribe it to a selective action on either channel type.

Acknowledgements

I wish to thank my supervisors, Chris Richards and Gillian Pocock, for their expert advice and unfailing support throughout this project.

I am also indebted to Ingemar Jacobson for his enthusiastic introduction to electrophysiology.

Many thanks to Hilary for her encouragement, and patience.

The generous financial support of the Wellcome trust is gratefully acknowledged.

LIST OF CONTENTS

List Of Figures And Tables

FIGURES

TABLES

Abbreviations

ACh	Acetylcholine
Bgtx	Bungarotoxin
cAMP	Cyclic adenosine 3', 5' monophosphate
CCh	Carbachol
CNS	Central nervous system
DHP	Dihydropyridine
EPC/P	End plate current/potential
EPSC/P	Excitatory post-synaptic current/potential
f_c	Corner frequency
F_{open}	Frequency of channel opening
GABA	γ-amino butyric acid
IPSC/P	Inhibitory post-synaptic current/potential
IC_{50}	Dose producing 50% inhibition
mAChR	Muscarinic acetylcholine receptor
μM	Micromolar
mM	Millimolar
MEPC/P	Miniature end-plate current/potential
nAChR	Nicotinic acetylcholine receptor
NPY	Neuropeptide Y
pA	Picoamp (Ampere x 10^{-12})
P_{open}	Probability of channel being in open state
PC12	Phaechromocytoma cell line
PKA	Protein kinase A
Ptd Ins	Phosphatidyl-inositols
PTX	Pertussis toxin
S_0	Zero frequency intercept
s.d.	Standard deviation
s.e.m	Standard error of the mean
SP	Substance P
t_{crit}	Critical time constant for channel closure
TEA	Tetra-ethyl ammonium
TTX	Tetrodotoxin
ω-CTX	Omega conotoxin GVIA

1. Introduction

1.1 Molecular Mechanisms of Anaesthesia

The diverse chemical nature and apparent lack of any structure-activity relationships amongst anaesthetic agents has led to an emphasis on physical properties to explain their mode of action. Meyer and Overton (see Meyer 1937) observed that anaesthetic potency correlates with olive oil solubility over a wide range of concentration. This correlation has been refined by varying the polarity of the solvent (Franks & Lieb 1978) and, with few exceptions, has proved to be an enduring empirical rule. While it predicts potency well, the Meyer-Overton rule makes no explicit statement about the mechanism by which anaesthetics act. It does, however, suggest that the likely target sites for anaesthetics have rather permissive structural requirements and are mainly hydrophobic but with some polar character. While such sites could be provided by both membrane proteins or lipids, most early hypotheses of a unitary mechanism for anaesthetics proposed the lipid bilayer as the primary target site.

Mullins (1954) concluded that "narcosis by chemically inert molecules appears to take place when a constant fraction of the total volume of some non-aqueous phase in the cell is occupied by narcotic molecules", providing the first mechanistic explanation of anaesthetic action. Since the molar volumes of anaesthetics vary across a very narrow range compared to their lipid solubilities, it was not possible to test the critical volume hypothesis by correlating anaesthetic potency with molar volume. Support for the theory was instead derived from the antagonism observed between anaesthetics and pressure, leading to the conclusion that anaesthesia occurs as a result of the expansion of a hydrophobic region of the cell membrane and that if the volume of this region can be restored by applied pressure, anaesthesia will be removed (Miller et al

1972). Evidence has been provided (Seeman & Roth 1972, Roth & Seeman 1972, Seeman 1972) that anaesthetics do cause membrane expansion at clinically relevant concentrations, and to a degree predicted from pressure reversal data (Lever et al 1971).

The agreement between the predictions of the critical volume hypothesis and measurements of pressure reversal and membrane expansion has made it popular. However, a number of serious criticisms have been raised. Halsey et al (1978) showed that the relationship between pressure and anaesthetic potency varies for different agents, contrary to any simple interpretation of the hypothesis. It has been noted (Franks & Lieb 1982) that the reversal of anaesthesia by pressure is only a necessary but not a sufficient condition for the validity of the hypothesis and that models involving direct binding of anaesthetic molecules to membrane proteins provide equally good explanations of the data. A fundamental objection is that not all lipophilic molecules are anaesthetics.

In an attempt to overcome some of these difficulties, more specific and testable models have been proposed, suggesting mechanisms by which disruption of the lipid bilayer could be transmitted to sensitive membrane proteins. Anaesthetics have been hypothesised to act by increasing bilayer fluidity (Metcalfe et al 1968, Hubbell et al 1970, Lawrence & Gill 1975, Trudell et al 1973), decreasing the lipid phase transition temperature (Trudell 1977, Lee 1976, Jain et al 1975), or increasing membrane thickness (Ashcroft et al 1977 a&b, Haydon et al 1977 a&b). However, re-examined at relevant anaesthetic concentrations, the magnitude of these effects have been shown either to be small or non-existent (Boggs et al 1976, Lieb et al 1982, Franks & Lieb 1979) and in some cases occur in a different direction to that predicted by the models (Richards et al 1978, Rosenberg et al 1977). Where small changes were observed, these could be reproduced by modest temperature increases. Furthermore, anaesthetic potency

falls with increasing temperature, while all the above models predict that it should rise (Cherkin & Catchpool 1964, & see Richards et al 1978)

If lipid-based unitary hypotheses are unlikely to account for anaesthetic action, as many of the studies mentioned above strongly suggest, mechanisms involving direct interaction with membrane proteins are the most plausible alternative. Further work has both added to the arguments against lipid hypotheses and pointed positively towards direct binding models.

Although a wide range of structurally dissimilar molecules can produce anaesthesia, within classes of anaesthetics significant structure/activity relationships are seen. These are strongest for steroids where the optical isomers of powerful agents are often totally inactive (Phillips 1974), but are also observed with barbiturates (Buch et al 1970), ketamine (Lodge et al 1982) and perhaps most significantly with isoflurane (Franks & Lieb 1991). In addition, mixtures of anaesthetics, which would have strictly additive effects according to any lipid hypothesis, have been shown to act synergistically (Richards & White 1981) while mixtures of active and inactive agents can act antagonistically (Richards & Hesketh 1975). The prediction that equipotent concentrations of different agents should have equivalent actions on specific membrane proteins is not fulfilled (Dilger & Brett 1991b).

All these data are highly suggestive of the existence of binding sites for anaesthetics displaying significant levels of specificity. It is obviously not possible to demonstrate the functional consequences of direct anaesthetic binding to membrane proteins in lipid free systems. The inhibition of firefly luciferase by a variety of anaesthetics (Ueda & Kamaya 1973, Franks & Lieb 1984, Moss et al 1991) does however clearly show that anaesthetic modulation of protein function is not necessarily dependent on surrounding lipid. However, the unambiguous demonstration of direct anaesthetic modulation

of a nerve membrane protein relevant to anaesthesia is still awaited.

1.2 Cellular Mechanisms of Anaesthetics

Irrespective of the molecular nature of the anaesthetic target site, there is little doubt that at a cellular level, neurones, principally central neurones, must be the primary site of anaesthetic action. A fundamental issue in this regard is the relative sensitivity of axonal conduction compared to synaptic transmission. This question was addressed by Larrabee and Posternak (1952), who studied the effect of a range of agents on impulse transmission through cat and rat sympathetic ganglia. By comparing evoked activity in pre- and post synaptic neurons, and in axons which traverse the ganglion without synapse it was shown that many agents, including pentobarbitone and ether, blocked synaptic transmission at lower concentrations than were required to block axonal conduction. The degree of selectivity varied (in relation to potency), being highest (10:1) for pentobarbitone while ethanol was unselective. The finding that excitatory synaptic transmission is selectively blocked by anaesthetics was subsequently demonstrated with a wide variety of agents in the spinal cord (Somjen & Gill 1963), sympathetic ganglia (Nicoll & Iwamoto 1978, Bosnjak et al 1982) and in various regions of the brain (olfactory cortex, Richards 1972, 1973, Richards, Russell & Smaje 1975; hippocampus Richards & White 1975). In each case excitatory synaptic transmission was significantly depressed at relevant anaesthetic concentrations.

However, since the degree of selectivity is not very high and it has been shown that susceptibility to axonal block varies inversely with fibre diameter (Staiman & Seeman 1974) it has been suggested that anaesthetics may inhibit impulse conduction in the fine terminal branches of afferent neurones. While there is evidence that this may account for some of the

depressant effect of anaesthetics (Berg-Johnsen & Langmoen 1986 a&b) there are several reasons to believe it is not generally of great importance. Were impulse conduction in any region of afferent fibres to be inhibited, the latency in EPSP onset after afferent stimulation would be expected to increase, a phenomenon observed with the neuronal blocking agent TTX (Richards 1982), but not with anaesthetics (Richards & White 1975, Richards 1973). While EPSP amplitude is reduced in direct proportion to the attenuation of action potentials by TTX, anaesthetic agents reduce EPSP's before any diminution of the action potential is observed. Furthermore, in some studies no difference was observed in the sensitivity to anaesthetics of axons of varying thickness (e.g Larrabee & Posternak 1952).

Synaptic transmission is now widely accepted as being the aspect of neuronal function most sensitive to anaesthetics. In principle, central depression by anaesthetics could result from attenuated excitatory transmission or enhancement at inhibitory synapses. The work presented in this thesis is primarily concerned with the former and the following survey will concentrate on this aspect of anaesthetic action.

There are a number of processes involved in synaptic transmission, all or a subset of which may be sensitive to the action of anaesthetics.

1) The release of transmitter from pre-synaptic terminals.
2) The response of post-synaptic cells to transmitter.
3) The excitability of post-synaptic neurones.

1.2a Transmitter Release

Various studies have examined the effect of anaesthetics on evoked release of neurotransmitter. Mathews & Quilliam (1964) showed that a range of agents inhibit the electrically evoked release of acetylcholine from sympathetic ganglia. Experiments

investigating the depolarisation induced release of (putative) amino-acid transmitters from brain slices have produced variable results, release being decreased, increased, or remaining unchanged depending on the transmitter, anaesthetic and its concentration (Minchin 1981, Kendall & Minchin 1982).

Quantal analysis of EPSP's has been used to determine the effect of anaesthetics on transmitter release. From such a study on spinal motoneurons Weakly (1969) concluded that the predominant action of barbiturates is to inhibit release since quantal content was reduced while the amplitude of a 'unit' EPSP was unaffected. Zorychta et al obtained similar findings for the action of ether (1978) and halothane (1975). Kullmann et al (1989) also concluded that both thiopentone and halothane reduce quantal content, not quantal size, at 1a afferent synapses, implying a depression of transmitter release. In contrast, Nicoll & Iwamoto (1978) found the opposite for the action of pentobarbitone on sympathetic ganglion cells: quantal size was reduced while the number of quanta was unaffected indicating a solely post-synaptic site of action.

Calcium influx is known to be a prerequisite for transmitter release. Parallel measurements of the evoked uptake of calcium ions and secretion of transmitter from neuroendocrine cells have been made (Pocock & Richards 1987 & 1988, Kress et al 1991, Yashima et al 1986, Takara et al 1986, Stern et al 1991). Such studies have shown that a range of anaesthetic agents inhibit the inward calcium flux and consequent secretion, (although the sensitivity of K-depolarisation induced events is often less than those initiated by receptor activation). Several of these studies have demonstrated the absence of any effect of anaesthetics on stimulus-secretion coupling following the initial rise in intracellular free calcium (Ca_i). Using electropermeabilised chromaffin cells Pocock and Richards (1987 & 1988) showed that secretion was determined solely by free Ca_i in the presence of varying

concentrations of a range of agents. Kress et al (1991) and Stern et al (1991) found that secretion due to the release of calcium from internal stores was unaffected by anaesthetic, again implying no disruption to the exocytotic process.

Barbiturates have been shown to depress voltage-gated calcium currents in dorsal root ganglion cells (Werz & Macdonald 1985, Gross & Macdonald 1988) and *Helix* neurones (Nishi & Oyama 1983 a&b). More recently halothane has been found to inhibit calcium currents in hippocampal neurones (Krnjevic & Puil 1988) and clonal pituitary cells (Herrington et al 1991) (also in cardiac myocytes; Terrar & Victory 1988, Bosnjak et al 1991). The possible mechanism of these effects will be examined later (Section 1.4).

1.2b Post-Synaptic Receptors

Anaesthetics also affect the conductance changes caused by post-synaptic receptor activation. The response of central neurones to iontophoretic application of excitatory amino-acids has been shown to be depressed by a range of agents encompassing all classes of anaesthetics (Galindo 1969, Crawford 1970, Richards et al 1975, Richards & Smaje 1976, Oshima & Richards 1988, Barker & Ransom 1978, Lodge et al 1982, Sawada & Yamamoto 1985). A notable exception would appear to be halothane which did not inhibit responses in a number of the above studies (Richards & Smaje, 1976, Crawford 1970, Galindo 1969).

The effect of anaesthetics on muscarinic cholinergic responses has received some attention. In central neurones Crawford (1970) found that a variety of agents inhibited muscarinic excitation while Smaje (1976) found that only alphaxalone did so, other agents having an excitatory effect or none at all. No effect was seen on the muscarinic response of sympathetic ganglia (Nicoll & Iwamoto 1978) or PC12 cells (Kress et al 1991).

The effects of anaesthetics on peripheral nicotinic cholinergic receptors have been the subject of many studies. The marked extra sensitivity of catecholamine secretion from chromaffin cells evoked by carbachol compared to direct depolarisation clearly indicated a direct effect of anaesthetics on the activation of the nicotinic acetylcholine receptor. (Pocock & Richards 1987 & 1988, Yashima et al 1986, Takara et al 1986). In all cases blockade of the receptor/channel was shown to be non-competitive with agonist.

At the muscle end-plate barbiturates, local anaesthetics and volatile agents have been shown to modify the decay of miniature end plate currents (Kordas 1970, Adams 1976, Gage & Hamill 1976, Torda & Gage 1977). The suggestion that this effect is the result of a selective blockade of open channels has been investigated in many subsequent studies which will be discussed in detail later (Section 1.3).

1.2c Post-synaptic Excitability

Whilst many studies found no effect of anaesthetics of any class on the resting membrane potential and non-synaptic excitability of post-synaptic neurones, a number of reports have suggested that alterations of resting conductances may contribute to the action of anaesthetics.

Barbiturates, steroids and etomidate can directly activate GABA chloride conductance and this would be expected to hyperpolarise and therefore decrease the excitability of post-synaptic neurones. This was the finding of Nicoll and Madison (1982), who showed that barbiturates caused a bicuculline sensitive hyperpolarisation of frog motoneurones. Volatile anaesthetics also hyperpolarised neurones, but this was due to an increase in resting K conductance, a finding supported by Berg-Johnson and Langmoen (1990) who found that isoflurane produced a small hyperpolarisation of rat hippocampal and human neocortical neurons by increasing a K

conductance. MacIver and Kendig (1991) however, reported variable effects of volatile anaesthetics on hippocampal neurones. While halothane hyperpolarised neurones and increased a resting K^+ conductance, enflurane did not produce a consistent effect.

It should be noted that many K channels have been identified in central neurones (Halliwell 1990) and differential effects on separate conductances may lead to the variable effects observed. Indeed Southan and Wann (1989) suggested volatile anaesthetics may have a dual action on hippocampal CA1 neuronal K conductance : increasing a resting K conductance leading to hyperpolarisation and a decrease in excitability and inhibiting $K_{(Ca)}$ thus blocking accommodation and promoting repetitive firing.

Franks & Lieb (1988) showed that volatile anaesthetics activate a novel K conductance in *Lymnea* neurones, completely blocking spontaneous firing at relevant concentrations. The effect was restricted to certain neurons and thus appears to represent a highly specific action on a single channel type.

1.2d Inhibitory Mechanisms

Central depression may occur as a result of the enhancement of inhibitory synaptic transmission. Studies have in fact shown this to be enhanced (Nicoll 1972, Pearce et al 1989) or depressed (el-Beheiry & Puil 1989). This variability is perhaps not unexpected since the strength of post-synaptic inhibitory responses will depend on transmitter release and preceding excitatory contacts, both of which are depressed by most agents. However the increased duration of IPSP's in the presence of barbiturate, steroid and volatile agents (Nicoll et al 1975, Scholfield 1980, Gage & Robertson 1985) is most likely due to an effect on post-synaptic receptors.

The major inhibitory transmitters in the CNS thus far identified are GABA and glycine and most work has focused on the former. In those studies in which the influence of anaesthetics on glycinergic transmission has been studied no effect was seen (Barker & Ransom 1978, Barker et al 1987). In contrast many studies on cultured neurones and chromaffin cells have demonstrated that barbiturates (Barker & Ransom 1978, Peters et al 1988), steroids (Cottrell et al 1987, Barker et al 1987) and more recently inhalation agents (Jones et al 1992) enhance responses to GABA. In addition, barbiturates, steroids, and etomidate (Evans & Hill 1978) were found to activate GABA chloride currents directly. Anaesthetic induced enhancement of GABA currents appears to result from an increase in the mean open time of channel events; Macdonald et al (1989) showed that barbiturates increased the proportion of the longest of three GABA chloride channel open states.

1.3 Mechanisms of nAChR Blockade

Of the models proposed to explain the action of anaesthetics on nicotinic receptor channels, those based on blockade of the activated conducting state of the receptor channel complex have been the most enduring. A formal model on these lines was first proposed by Steinbach (1968) to explain the effect of xylocaine (and derivatives) on EPP's. As observed by other workers, (Kordas 1970, Katz and Miledi 1975, Ruff 1977) EPP and MEPP decay became biphasic in the presence of local anaesthetics; after unaltered growth, currents initially decayed rapidly and then more slowly. The model can be formalised as follows:

$$C \underset{\alpha}{\overset{\beta}{\rightleftharpoons}} O^* \dashrightarrow O' \quad \text{(partially conducting)}$$

α = rate of channel closure

β = rate of channel opening

(Only states marked * are conducting in this and later equations. C = closed state, O = open state).

According to this kinetic scheme, current decays steeply due to the rapid formation of the xylocaine-activated receptor complex, but then shows a prolonged, slowly decaying component due to the relative longevity of this partially conducting complex.

Adams (1975 & 1976), studying the effect of procaine on the frog end-plate, later modified this scheme, proposing that the complex of activated receptor with procaine was in fact non-conducting and that the sustained EPC component was the result of the re-opening of blocked channels. This model can be represented as follows:

$$C \underset{\alpha}{\overset{\beta}{\rightleftharpoons}} O^* \underset{b}{\overset{f.c}{\rightleftharpoons}} O\text{-}B$$

O-B = blocked open state
f = forward blocking rate constant
b = channel unblocking rate constant
c = concentration of blocker

Indeed, depending on the relative values of the parameters, channels could undergo a number of cycles of blockade and re-opening before returning to the resting state. The essential features of this sequential blocking model were succinctly described by his conclusion that only open channels can block and blocked channels can only open.

Strong support for the model was provided by Neher and Steinbach (1978). Recordings of the single channel acetylcholine receptor currents in frog muscle in the presence of QX222, clearly showed the repetitive blockade postulated by the model. Uninterrupted rectangular pulses of current due to channel openings were chopped into bursts of brief pulses in the presence of drug. The length of bursts increased, and the duration of individual pulses decreased, with increasing

concentration of QX222 as predicted. Results confirmed that intervals were non-conducting. Ruff (1977) also favoured a sequential scheme for the action of QX222 on Ach induced current noise. The equations describing the behaviour of channel currents as predicted by the sequential blocking model are as follows :

Single channel	(M)EPC decay *
Mean open time $1/(\alpha+f.c)$	$r_f = (\alpha+b+f.c)-\alpha.b/(\alpha+b+f.c)$
Mean burst time $(1+f.c/b)/\alpha$	$r_s = \alpha.b/(\alpha+b+f.c)$
Mean blocked time $1/b$	$A_s = b-r_s/(r_f-r_s)$

It is worth describing some of the central predictions of these equations. At the level of single channel observations, burst length must increase linearly with drug concentration and mean open time decrease. Blocked times should be a single exponentially distributed population with mean independent of drug concentration. The total time spent in the conducting state should not be altered. Correspondingly, the area under an EPC should be constant and the slow component of EPC decay should be prolonged with respect to the control (equivalent to burst length increasing).

Neher and Steinbach found essentially total agreement with the model and were not compelled to introduce any further channel states or allowed transitions to explain their data adequately. However, a variety of studies showed that the model in its simplest form was not generally applicable. A re-examination (Neher 1983) of the effect of QX222 on single channel currents at greater resolution (Hamill et al 1981) showed that at higher concentrations burst length decreased and two gap time populations appeared.

Work with other agents revealed further deficiencies in the sequential blocking model. Gage and Mackinnon (1985) found burst length to be independent of pentobarbitone concentration while blocked time increased. Pennefather and Quastel (1980)

* r_f = time constant of fast phase of decay
r_s = time constant of slow phase of decay
A_s = relative amplitude of slow component

(see Gage & Sah 1982)

examined the influence of a vast range of agents (including alcohols, volatile anaesthetics, barbiturates and local anaesthetics) on MEPC's finding a great variety of effects, many incompatible with the sequential blocking model (Many agents depressed MEPC area and did not prolong decay.) This was also the conclusion of Gage and Sah (1982) from work on the effect of excitant analogues of central depressants on MEPC's. Amplitude was reduced and in some cases the rate of current decay was enhanced. Adams (1977) found that the steady-state current evoked by low concentrations of agonist at the frog end-plate was reduced by procaine, a result contrary to the predictions of the sequential model.

The simplest extension to the model which accommodates these findings is the existence of a pathway from the blocked state to the closed state without passing through the open state. This extended sequential blocking model can be represented as follows :

$$C \underset{\alpha}{\overset{\beta}{\rightleftharpoons}} O^* \underset{b}{\overset{f.c}{\rightleftharpoons}} O\text{-}B \xrightarrow{\alpha'} C\text{-}B$$

α' = Rate of blocked channel closure

Re-opening of closed-blocked channels is assumed to occur at a very slow rate. Since long-lived closed states are experimentally indistinguishable no explicit statement can be made about the C-B → C pathway, which may involve a number of transitions. The model predicts the following*:

Mean open time $1/\alpha+f.c$, as for the simple model
Mean burst length $1+(f.c.b/(b+\alpha')^2)/(\alpha+(f.c.\alpha'/(b+\alpha')))$
Mean blocked time $1/b+\alpha'$
Open time per burst $1/\alpha+(f.c.\alpha'/(b+\alpha'))$

This kinetic scheme makes predictions which are in marked contrast to the original model. Depending on the relative

*See appendix 1

values of the rate constants, burst length may rise or fall with increasing drug concentration, while total conducting time must fall, owing to the curtailment of bursts by entry into the closed-block state. Corresponding equations describing MEPC behaviour are complex, but the model predicts decreased area with a biphasic decay rate.

Recent studies at the single channel level have shown that the actions of primary alcohols and volatile anaesthetics on muscle acetylcholine receptors are well fitted by the extended block model. Dilger & Brett (1991b) and Murrell et al (1991) found that as a homologous series of primary alcohols was ascended, b, the unblocking rate constant, fell progressively and α', the rate of blocked channel closure, increased until no clusters of openings were observed. Results with volatile anaesthetics (Wachtel & Wegrzynowicz 1991, halothane, isoflurane; Brett et al 1988 and Dilger & Brett 1991b, ether, isoflurane, enflurane.) in which marked 'flickering' is seen are explained by values of $b \approx \alpha'$.

These results are qualitatively and quantitatively in accord with the results of Pennefather and Quastel (1980) and McLarnon et al (1986) on MEPC decay.

1.3a Site of Action

Neither form of the sequential model requires assumptions to be made about the site of drug action. This could be the result either of direct pore occlusion, or binding to an allosteric site causing channel closure indirectly. Results with QX222 suggested that binding and channel blockage are the same molecular event. Calculations based on the voltage dependence of its action (Neher & Steinbach 1978) suggested that the QX222 binding site is located about three quarters across the membrane.

Strong support for the QX222 binding site being located within the channel pore towards the cytoplasmic side has come

from studies of nicotinic acetylcholine receptors expressed in oocytes from subunits altered by site-directed mutagenesis. (Leonard et al 1988, Charnet et al 1990.) Mutations from polar serine to apolar alanine residues at a specific location in the M 2 membrane spanning domain (which lines the channel pore - Imoto et al 1986) were made in the α and/or δ subunits (Leonard et al 1988). In this way nicotinic acetylcholine receptors were expressed with 0,1,2 or 3 ser→ala mutations. The unblocking rate constant, b, increased monotonically with the number of ser→ala changes, indicating progressively weaker binding. The forward blocking rate constant, f, and the voltage dependence remained unchanged. Charnet et al (1990) obtained opposite results for mutations at a site on the adjacent turn of the M2 α-helix: ser/thr→ala mutations resulted in weaker binding. The likely explanation is that the charged quaternary ammonium group and the hydrophobic aromatic moiety of QX222 interact with adjacent turns of the pore-lining M2 α-helix.

The evidence is strong for permanently charged QX 222 (at concentrations up to $\sim K_d$) acting solely by entering the channel pore, binding to a site within it and thereby occluding it. It is less clear that this is the case for other agents.

Uncharged local anaesthetics block the nicotinic acetylcholine receptor in a similar fashion to QX222 (Ogden et al 1981). It also now appears unlikely that the charged form of procaine is the only active species : the voltage dependence of its action is much less than that of QX222 (e-fold for 32mV, Neher & Steinbach 1978 QX222; e-fold for 86mV, Gage et al 1983 procaine) Furthermore procaine is equally effective at pH 7.4 and 9.9, though slower acting at the higher pH at which it exists predominantly as a neutral species. Interestingly, the voltage dependence of its action is the same at both pH's (Gage et al 1983). These results suggest that neutral procaine probably accesses the channel

complex via the membrane and that the voltage dependence of procaine's action is not due to the movement of procaine into the open channel pore, but possibly due to an alteration in the binding site itself.

Many neutral, highly lipophilic, agents block the nicotinic acetylcholine receptors according to the extended block model. Murrell et al (1991) calculated (from K_d vs. chain length) a binding energy of 3.3 kJ/mol for alcohols up to octanol. This represents a highly hydrophobic site, though this could still theoretically reside in the M2 membrane spanning domain which has a stretch of apolar residues.

While charged QX222 (at concentrations up to $\sim K_d$) fits a simple sequential blocking model well, all neutral 'blockers' deviate markedly and generally fit an extended block model in which the tendency to enter the long closed-block state correlates with oil/water partition coefficient. This is suggestive of a two (multi-) site model, in which binding at a hydrophobic site promotes channel closure while binding to another site causes, directly or indirectly, channel blockade. It is of course possible that the two sites are identical.

Work with channel blocking anaesthetics provides powerful, although not conclusive, evidence against lipid based theories of anaesthesia. The concentration of n-alcohols reducing P_o by 50% correlate directly with their oil/water partition coefficient (and are very similar to $E.D_{50}$'s for general anaesthesia), which is consistent with lipid based theories. However, as noted by Dilger & Brett (1991b), such theories would predict equipotent concentrations of alcohols, and indeed other agents, to have similar actions. This is clearly not the case - at doses equieffective in terms of conductance reduction, butanol induces bursts of very brief openings while decanol gives rise to individual, moderately brief openings. Furthermore Dilger and Brett (1991a) showed that over a temperature range of 20 - 35°C, while channel gating kinetics

changed, flickering behaviour was not induced. As mentioned earlier, very small temperature changes mimic most of the effects on bulk lipid produced by relevant concentrations of anaesthesia.

1.4 Mechanisms of Inhibition of Neuronal Voltage-gated Calcium Channels

In comparison to the study of nAChR-anaesthetic interactions, less work has sought to elucidate the molecular mechanisms of the blockade of voltage gated calcium channels by anaesthetics. Barbiturates have received most attention. Nishi & Oyama (1983a) showed that pentobarbitone accelerated the inactivation of calcium currents in *Helix* neurones, an effect they interpreted as open channel blockade analogous to that seen at end-plates. After further work however (Nishi & Oyama 1983b) an enhanced rate of voltage-dependent inactivation was proposed as the mechanism for the enhanced decay. Werz & Macdonald (1985) also found that clinical levels of pentobarbitone and phenobarbitone enhanced calcium current decay in cultured mouse ganglion cells and suggested either mechanism could be responsible.

Subsequently, three calcium channel types were described at whole cell and single channel level in chick sensory neurones (Fox et al 1987 a&b). These have been found in other neuronal and endocrine cell types. The presence of multiple channel types, with different activation and inactivation properties complicates the interpretation of drug effects on whole cell currents in the absence of corroborative studies at the single channel level.

Gross and MacDonald (1988) clearly showed that the low threshold current carried by T-type channels is unaffected by

pentobarbitone in mouse dorsal root ganglion cells, while the decay rate of the high threshold current (N & L channels) was markedly increased, as previously observed. On the basis of multi-exponential curve fitting a differential action on N and L channels was proposed. It was concluded that L-current amplitude was reduced, while its decay rate remained constant, whereas N-current amplitude was unchanged but its decay rate enhanced. They interpreted this in a scheme in which barbiturates prevented L-channel opening and either blocked or increased the inactivation rate of N-channels. This interpretation is however problematic (see discussion).

Halothane reduces peak inward calcium current and enhances decay in hippocampal CA1 neurones (Krnjevic & Puil 1988). In clonal pituitary cells (GH_3) (Herrington et al 1991) the high threshold calcium current was strongly inhibited by levels of halothane similar to those found in the blood during anaesthesia. The sustained current component showed greater sensitivity than the inactivating current, possibly reflecting a greater sensitivity of a non-inactivating channel type (L). This is supported by the finding that the degree of inhibition correlated inversely with the proportion of inactivating current seen in the control. The low threshold current was less sensitive to halothane, and voltage dependent sodium and potassium conductances much less so. No conclusion was drawn as to whether blockade required channel opening.

It appears therefore that in the case of the barbiturates, open channels are the anaesthetic target, but whether the increased decay rate is due to open channel block or enhanced inactivation is not clear. There is little conclusive evidence to suggest one particular channel type is especially sensitive to anaesthetics. Detailed molecular mechanisms and demonstration of differential action of anaesthetics on different channel types is probably dependent on single channel studies.

1.5 Background To This Study

As described above, the work of Pocock & Richards (1987 & 1988) using the bovine adrenal chromaffin cell as a model for excitatory synaptic transmission suggested that general anaesthetics depress the secretion of neurotransmitter by a direct effect on the plasma membrane. Evoked secretion, and the associated ion fluxes, were inhibited by clinically relevant concentrations of anaesthetics, while no significant effect was observed on the intracellular events preceding exocytosis. It appeared therefore that the nicotinic acetylcholine receptor and voltage-gated calcium channels are key target sites mediating the action of anaesthetics on the secretory response of adrenal chromaffin cells. The aim of the study presented here was to investigate the molecular nature of the interaction of anaesthetics with these ion channels, employing the patch clamp technique (Hamill et al 1981).

The anaesthetics selected for this study were: procaine (a local anaesthetic), methoxyflurane (a potent halogenated ether inhalation agent), methohexitone (a short-acting barbiturate) and etomidate (a potent injectable non-barbiturate).

Adrenal chromaffin cells are derived from embryonic neural crest tissue and are homologous with sympathetic post-ganglionic neurones. They express nicotinic receptors and voltage-gated calcium channels of neuronal type and are thus a highly suitable model for investigating the mechanism of excitatory synaptic transmission.

1.6 Properties of the Bovine Adrenal Chromaffin Cell

In vivo, acetylcholine released from splanchnic nerve terminals stimulates secretion of catecholamines from adrenal medullary (chromaffin) cells (Feldberg et al 1934). The sequence of events initiated by acetylcholine leading to catecholamine release, termed stimulus-secretion coupling (Douglas & Rubin 1963), has been intensively studied as a model for neurosecretion.

Experiments performed on isolated cells have defined many of the essential features of stimulus-secretion coupling in these cells (Schneider et al 1977; Trifaro & Lee 1980; Holz et al 1982; Knight & Baker 1983; Cena et al 1983). These may be summarised as follows. There is an absolute dependence on extracellular calcium for secretion to occur in response to cholinergic stimulation or direct depolarisation by elevated potassium. Secretion increases with increasing external Ca^{++} up to a saturating level (~10mM) and evoked Ca^{++} uptake is proportional to the quantity of catecholamine released in response to stimuli (Holz et al 1982). Muscarinic cholinergic agents were unable to evoke secretion, nor could atropine inhibit secretion stimulated by mixed nicotinic-muscarinic agonists. Blockers of autonomic ganglion nAChR, such as hexamethonium (mainly channel block) and mecamylamine (Holz et al 1982) (receptor block), inhibited acetylcholine-evoked catecholamine release, while α-bungarotoxin, a potent inhibitor of the muscle nicotinic receptor which is ineffective at autonomic ganglia, did not (see also section 3.1a).

Veratridine, which activates voltage-dependent Na^{+} channels, was able to trigger secretion, and this response was inhibited by TTX (Cena et al 1983, Knight & Baker 1983). However, the ability of TTX to inhibit release in response to nicotinic agonists was either variable (Knight & Baker 1983) or absent (Cena et al 1983, Pocock & Richards, unpublished data). Table 1.1 briefly describes the functional

neurotransmitter/modulator receptors which have been characterised in bovine adrenal chromaffin cells.

These studies therefore defined the sequence of events in the stimulus-secretion coupling process. Nicotinic cholinergic agonists acting on neuronal-type nicotinic acetylcholine receptors cause opening of the associated ion channel, influx of sodium ions, and membrane depolarisation. This in turn leads to the opening of voltage-gated calcium channels and calcium entry which triggers secretion. Depolarisation induced by nicotinic stimulation probably leads to activation of voltage gated Na^+ channels (Fenwick et al 1982b) and the triggering of action potentials, but this does not appear to be an essential feature of the stimulus-secretion coupling process. Further work has sought to define the nAChR gated cation and voltage-gated calcium currents in more detail, both because of their central role in chromaffin cell function, and more generally as neuronal channel types analogous to those involved in synaptic transmission.

These two conductances of the bovine adrenal chromaffin cell are of central relevance to the work presented in this thesis and are discussed in some detail in the introductions to chapters 3 and 4.

Table 1.1

Functional neurotransmitter/modulator receptors on bovine adrenal chromaffin cells

* indicates a direct effect on the channel.

Table 1.1

Functional Neurotransmitter/modulator Receptors on Bovine Adrenal Chromaffin Cells

Receptor	Direct effect of activation	Effect on I_{ACh}	Effect on I_{Ca}	2nd messenger involvement	Selected References
nAChR	↑ cation conductance				Fenwick et al 1982a Cull-Candy et al 1988
$GABA_A$	↑ chloride conductance				Bormann & Clapham 1985 Peters et al 1988
$GABA_B$	---		↓	PTX-sensitive G-protein	Doroshenko & Neher 1991
mAChR	↑ Ca_i (internal			PI linked	Kao & Schneider 1985 Cheek et al 1989
	↑ cGMP	↓		cGMP	Derome et al 1981
Dopamine					
D_2			↓		Bigornia et al 1988
		↓*	↓	PTX-sensiitve G-protein	Sontag et al 1990
D_1			↑	cAMP & PKA	Artelajo et al 1990
NPY_2		↓		PTX-sensitive	Nôrenberg et al 1991
Opiates		↓			Kumakura et al 1980
Substance P		↓*			Clapham & Neher 1984b Livett et al 1979

2. Materials and Methods

2.1 Isolation and Culture of Chromaffin Cells

(Pocock, 1983)

Bovine adrenal glands were obtained from a local abattoir. They were removed from the animals within 30 minutes of slaughter and dissected free of fat and connective tissue. Glands were then perfused via the adrenal vein with ice cold Locke's solution containing 0.5% bovine serum albumin (BSA) (fraction V, Sigma) before being transported to the laboratory on ice, whereupon all subsequent procedures were performed in a laminar flow hood using sterile materials.

The gland was first bisected. The medulla, readily distinguished from the cortex by its paler colour, was then cut into narrow strips using an aligned stack of razor blades. The strips were cut from the gland with scissors, washed several times with cold Locke's solution to remove the albumin and brought to 37^0C in a shaking water bath.

Enzymatic dissociation of the cells was then begun by adding protease (Sigma type XIV) to give a final concentration of 0.1% (w\v). After 15 minutes of digestion the softened tissue was drawn up and down a wide bore 5ml pipette tip for about 60 seconds. This trituration was repeated at 5 minute intervals. When the tissue flowed freely, progressively narrower bore tips were used. After 30-40 minutes, protease action was halted by adding an excess of BSA (0.2%). Collagenase (Sigma typeII) (0.1%), hyaluronidase (Sigma type I-S)(0.1%) and DNAase I (Sigma type IV)(0.01%) were then added to the incubation medium and periodic trituration resumed for a further 20-30 minutes.

The dissociated cells were then separated from undigested debris by straining through nylon mesh and the resulting suspension was centrifuged (3 min at 1000g). Further cycles of resuspension in Locke's solution followed by centrifugation

were performed until the supernatant was clear. The pellet was then resuspended in the culture medium (DMEM/Ham's F12 1:1 mixture supplemented with 2-10% newborn bovine serum, penicillin (100 I.U./ml), streptomycin (0.1mg/ml), and cytosine arabinoside (10μM)). The concentration of cells in this suspension was determined using a haemocytometer and diluted to $1.5x10^6$ cells/ml. Differential plating was then used to purify the chromaffin cell suspension (see Waymire et al 1983). Aliquots of the diluted cell suspension were placed in glass prescription bottles (30ml/bottle) in a CO_2 incubator for 3-4 hours. Purification of the chromaffin cell preparation is achieved owing to the more rapid adherence of contaminating endothelial cells to the glass than chromaffin cells. Gentle rocking then resuspends the chromaffin cells which can be decanted off.

The cell suspensions were pooled after differential plating and viability was tested by the ability of cells to exclude trypan blue stain. Typically >95% of cells excluded dye. A portion of the pooled suspension was diluted with the culture medium described above to $0.25x10^6$ cells/ml. This fraction was transferred to plastic petri dishes ($2x10^6$ cells/dish) containing poly-L-lysine coated glass coverslips (10^5 cells/coverslip) which were then placed in a humid 5% CO_2 incubator maintained at 37°C. The remainder of the cells were centrifuged and resuspended at a concentration of $1x10^7$ cells/ml in cell freezing medium (Sigma: fetal calf serum containing 10% DMSO as cryoprotectant). 1ml aliquots were placed in cryovials (Nalgene) and transferred to a -70°C freezer for medium term storage (<3 months).

When required for experiments, frozen aliquots were thawed rapidly (<1min) in a 37°C water bath, diluted in Locke's solution and centrifuged to remove the freezing medium. The pellet was then resuspended in culture medium at $0.25x10^6$ cells/ml and plated as described above. Cultured cells were used for recording 1-6 days after plating during which time the morphology of most cells remained unchanged.

2.2 Electrophysiological Methods

Experiments were carried out using three variants of the patch-clamp recording technique of Hamill et al (1981). The configurations used were whole cell recording under voltage clamp, recording from cell attached patches and recording from excised outside-out patches.

Experiments were performed on phase-bright spherical chromaffin cells with a smooth, regular outline. The capacitance of cells recorded from in the whole cell configuration was measured using the calibrated capacitance cancellation circuitry of the patch clamp amplifier. Values ranged from 3 to 28 pF but the great majority of cells lay in the range 5 to 10 pF. Assuming a specific capacitance of $1\mu f/cm^2$, this corresponds to cell diameters in the range 12-18 μm. This compares well to the mean diameter of 18μm measured using a Coulter counter (Pocock 1980) but shows cell selection was biased towards smaller cells, which permitted better voltage clamping.

Patch pipettes were fabricated from thick-walled filamented borosilicate glass (Clarke Electromedical GC150F) using a List L/M 3PA electrode puller and had tip diameters of 1-2 μm. The electrode tips were fire polished on a microforge before filling with recording solution. Filled electrodes were dipped briefly in Sigmacote prior to use. This procedure deposits a hydrophobic film on the electrode which repels bathing solution which would otherwise be drawn up the outside of the electrode and give rise to a capacitative artifact. Electrode resistances ranged from 3-15 MΩ and the series resistance in whole cell mode was usually between 10 and 20 MΩ.* All experiments were performed at room temperature (18-24°C).

In early experiments signals were recorded with a List electronic EPC-5 patch clamp amplifier and stored on magnetic tape (bandwidth DC-2.5Khz) using a Racal Store 4. Later an

* Series resistance was not compensated. The worst voltage errors were c. 12 mV at peak I_{Ba}.

Axopatch 1D amplifier was employed. Signals recorded from agonist-activated channels were stored on tape cassettes (recording bandwidth DC-20 kHz, although signals were usually filtered at 2 kHz before storage on tape) using a modified Sony DAT recorder. Voltage-gated currents were digitised on-line and stored on the hard disc of a Tandon PCA computer coupled to a Cambridge electronic design 1401 interface, which also controlled the voltage pulse sequence used to elicit the currents.

2.3 Solutions and Perfusion Apparatus

Locke's solution was used as the external bathing medium for all experiments on the nicotinic receptor (see table 2.1 for composition). 1μM tetrodotoxin (TTX) was used to suppress any voltage gated Na channel activity (experiments described in chapter 4 and the findings of Fenwick et al (1982b) show that TTX-insensitive Na channels are absent in bovine chromaffin cells). Locke's solution, supplemented with 10 or 20 μM carbachol and 1μM TTX, was also used to fill the electrode for recording from cell-attached patches.

The composition of solutions used to fill electrodes for whole cell and outside-out patch recordings of nicotinic channel activity are also shown in table 2.1. Solution C was used for outside-out patch recordings. Due to the absence of Na^+ ions in this recording solution it was not possible to define the sodium equilibrium potential. To allow definition of both the sodium and potassium equilibrium potentials recording solutions A or B were used. These differed principally with respect to the chloride equilibrium potential they set. Solution B was used for experiments in which there was the possibility of a chloride conductance being activated. Since E_{Cl} for this solution is similar to the holding potential used for whole cell experiments any chloride conductance activated would have negligible amplitude and not interfere with analysis of the nicotinic channel current.

Table 2.1

The composition of electrode solutions and bathing solution (Locke's) for recordings of nAChR channels.

	Recording Solutions			
	A	B	C	Locke's
KCl	120	---	140	5
K Glutamate	---	120	---	---
NaCl	20	---	---	140
Na Glutamate	---	20	---	---
$MgCl_2$	2	2	2	2
$CaCl_2$	1	1	1	1
EGTA	11	11	11	---
HEPES	---	---	---	15
Glucose	---	---	---	5.5
pH	7.2	7.2	7.2	7.4
E_K	-80.2	-80.2	-84.1	
E_{Na}	+49.1	+49.1	?	
E_{Cl-}	-0.8	-86.0	-0.8	

Concentrations in mM. Equilibrium potentials in mV, calculated relative to Locke's solution according to the Nernst equation.

Recordings of whole cell voltage activated calcium currents were made using bathing medium of the following composition (mM):

Tetraethylammonium chloride (TEA-Cl) 120, $CsCl_2$ 5, $BaCl_2$ 10, HEPES 10, glucose 10, TTX 1. pH was adjusted to 7.4 with TEA-OH.

Barium was used as the charge carrier in order to maximise the currents flowing through voltage gated calcium channels (see Nowycky et al 1985).(Some experiments were also performed using calcium as the charge carrying ion, in which case 10mM $CaCl_2$ was used in place of the $BaCl_2$). The recording electrode contained (mM):

CsCl 120, EGTA 10, $MgCl_2$ 5, HEPES 40, ATP 2, GTP 0.3, pH 7.2 using CsOH.

The presence of intra- and extracellular Cs ions and external TEA served to block voltage dependent potassium channels, while external TTX and the absence of sodium ions suppressed possible interference from Na conductances.

Two systems were used to apply control and drug solutions to cells and patches. In early experiments test solutions were applied by pressure ejection from micropipettes fabricated from thin walled glass capillary (Clarke Electromedical GC150TF), with tip diameters 2-5 μm. Most experiments however were performed using the method of Krishtal & Pidoplichko (1980) to microperfuse cells. A U-shaped glass capillary with a hole of about 50 μm diameter at the apex was connected to 1 of 5 solution reservoirs via a multi-way valve (Rheodyne). Pressure and suction were applied such that there was influx of bath solution into the hole. Reducing the suction by raising the syphon then caused flow through the hole to invert and perfuse the preparation. The U-tube structure was mounted on a micromanipulator and positioned with the orifice about 100 μm from the cell which allowed rapid local solution changes. All components of the perfusion apparatus were constructed from nylon, PTFE or glass to reduce the possibility of adsorption of drugs.

2.4 Analysis

2.4a Nicotinic receptor channel currents

Records of nicotinic acetylcholine receptor channel currents activated by carbachol were analysed to determine mean current flow and kinetic parameters of channel gating. Two analytical approaches were used, appropriate to the different types of experiment performed.

1) Whole cell macroscopic currents elicited by 10-25 μM carbachol, due to the simultaneous opening of many channels, were subjected to spectral analysis.

2) Analysis of single channel events was performed on records in which individual channel openings were clearly resolved.

Three types of experiment generated data for single channel analysis:

i) Cell attached patch recordings.

ii) Excised outside-out patch recordings.

iii) Recordings from small whole cells activated by low concentrations of agonist (1-2 μM carbachol).

These two analytical methods are described in detail below.

2.4a(i) Spectral analysis of whole cell current noise

For analysis of carbachol induced current fluctuations the signal from the tape recorder was filtered with a 7-pole Cauer elliptical filter (Frequency Devices model 675, bandwidth DC-1 KHz) and digitised at 2.56 KHz. This filter has a very steep attenuation rate above the cutoff frequency (-94 dB at 2 KHz, -31 dB at the Nyqvist frequency (1.28 KHz)) eliminating aliasing effects. Power spectral densities were calculated on 1024 point (0.4s) data sections, and the mean power spectrum was calculated by averaging the spectra from 50-75 consecutive time blocks. The mean background noise spectrum obtained prior to application of agonist was subtracted from this to obtain the spectrum due to agonist alone.

This distribution was then fitted by either a single or double Lorentzian function using a least-squares Levenberg-Marquart algorithm with proportional weighting of the data points. In some cases, the spectrum was truncated at the high frequency end . This was done when the signal:noise ratio was low (less than 2:1) and the error in the data points of the background subtracted noise spectrum was correspondingly high.

The quality of the fitted curve was judged from the value of χ^2 and the random distribution of residuals. The following parameters were derived from the fitted Lorentzian curve: (See appendix 2)

i) **Corner frequency (f_c).** This is the frequency at which the power in the spectrum has fallen to half its maximum value and is related to the mean lifetime of the open channel (τ) according to the following equation:

$$\tau = \frac{1}{2.\pi.f_c}$$

ii) **The zero frequency (y-axis) intercept (S_0).** The maximum power in the spectrum. A^2S^{-1} density

The mean inward current was determined independently from an all-points histogram of current amplitude and the single channel conductance was calculated according to the equation:

$$\gamma = \frac{S_0.f_c.\pi}{2.I.(V_m-V_r)}$$

V_m = holding potential
V_r = reversal potential
I = mean inward current

2.4a(ii) Single channel events

For the analysis of single channel events segments of data (15-300s) were replayed, low-pass filtered at 1 KHz* (four-pole Bessel) and digitised at either 10 or 5 KHz. An all-points histogram of current amplitude was constructed and Gaussian distributions fitted to the peaks. The detection threshold for channel opening was then set at half of the mean single channel amplitude, determined from the Gaussian curve fit.

After automatic detection of channel openings was complete, each transition was inspected. Obvious noise artifacts were

* Since $1/(f_{final})^2 = 1/(f_1)^2 + 1/(f_2)^2$, the effective overall filtering was ≈ 890 Hz.

re-classified as closed states if brief, or rejected if of longer duration. This was done so as not to bias the closed state distribution unduly. Multiple channel openings were infrequent and were rejected from the transition list. In most experiments a substate opening to 70% of the full conductance was observed, usually at a low frequency. Such openings were re-classified and initially excluded from further analysis (procaine experiments). However, after it was shown that the kinetics of these openings were essentially the same as full conductance openings (see results), all openings were used for analysis.

The characteristics of the Bessel filter used were determined by measuring the attenuation of the amplitude of rectangular current pulses of varying width. It was found that the filter reduced the amplitude of a 0.25ms pulse by 50%. The minimum resolvable time of single channel events was thus taken as the smallest multiple of the sampling rate greater than 0.25ms. This was 0.3 ms and 0.4ms at 10 KHZ and 5 KHz sampling rates respectively. Shorter events were considered unresolved.

After editing of the open/closed state transition list, the following parameters were calculated:

i) Mean open channel lifetime.
ii) Frequency of channel opening (F_o).
iii) Probability of the channel being in the open state (P_o).

Frequency distribution histograms of open and closed state durations were constructed from the edited transition list. Curve fits to these histograms excluded bins up to and including the minimum resolvable time.

Bursts of openings separated by brief closures were analysed by first calculating a critical closed time duration (t_{crit})

below which a closure is classified as being a closure within a burst (Clapham & Neher, 1984; Colquhoun & Sakmann, 1983, and see section 3.6.1). This is calculated so that the proportion of short intervals misclassified as closures between bursts was equal to the proportion of long intervals misclassified as closures within bursts. The mean burst duration and the mean duration of closures within bursts was calculated from such analysis, and the results were also expressed as frequency distribution histograms. Figure 2.4.1 illustrates the measurement of openings and closures within bursts, and the burst length.

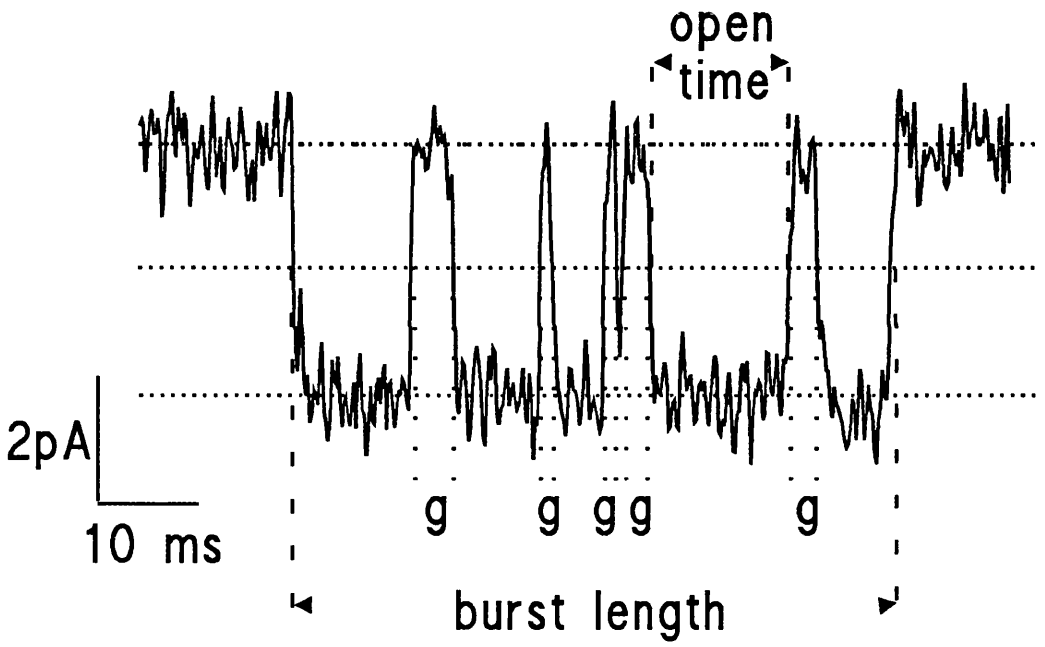

Figure 2.4.1

Detail of a burst of channel openings, describing the measurement of individual openings, the burst length, and closures within the burst (labelled g, for gap)

2.4b Whole cell voltage-gated calcium currents

Signals elicited by voltage steps were normally digitised on-line at a rate of 2.5 KHz. Prior to analysis records were usually adjusted to account for leak currents flowing in response to hyperpolarising voltage steps. Leak currents were generally very small however (0.2-0.5 pA per mV step)

Three main types of voltage pulse protocol were employed to elicit currents:

i) Depolarising voltage pulses (duration 100-300 ms) delivered from a fixed holding potential (-60 to -100 mV) to varying test potentials (-40 to +50 mV; 3-5 mV increments). The results of such experiments allowed current -voltage plots to be drawn.

ii) Depolarising voltage pulses (100-300 ms duration) delivered from varying holding potentials (-40 to -100 mV) to a fixed test potential, equal or close to the potential evoking the maximal current response (usually 0 mV). From these experiments steady-state inactivation curves could be drawn.

iii) Sequences of depolarising pulses (100-300ms duration) from a fixed holding potential (-80 mV) to a fixed test potential (0mV), delivered at low frequency (0.1 Hz). This protocol was employed to produce time courses of the effect of drugs on the calcium channel currents.

iv) Depolarising voltage pulses of 20 ms duration delivered from a holding potential of -80 mV to varying test potentials (-50 to +50mV; 5 mV increment). The currents evoked using this protocol were digitised at 25 KHz, in order to permit analysis of tail currents.

Whole cell calcium channel currents decayed during voltage pulses. This decay was quantified by measuring the peak, late and inactivating components of individual traces (see inset of fig.4.1.2 for description) and by fitting curves (1-2 exponentials, with or without residual) either to raw current records, or to averages of a small number of equivalent consecutive records .

Tail currents recorded at the offset of test pulses were fitted by exponential functions, extrapolated back to the end of the test depolarisation.

Statistics

The Student's t-test was used to assess the statistical significance of differences between sets of results. In most cases, the test was applied to the mean and standard deviation of the differences between paired (control and drug) experiments. For the data obtained from cell-attached patches with procaine (section 3.2c(i)), in which the controls were independent experiments, un-paired t-tests were performed on the two sample means.

Computer Software

The spectral noise analysis (SPAN), channel transition detection (PAT), voltage clamp analysis (VCAN) and voltage pulse generator (VGEN) programmes were kindly supplied by Dr. John Dempster, University of Strathclyde.

Patch and voltage clamp software from Cambridge Electronic Design was also used to control and analyse experiments on whole cell voltage gated currents.

Curve fitting was performed using PFIT from Biosoft.

3. Currents Gated By The Nicotinic Acetylcholine Receptor And Their Modulation By Anaesthetics

3.1 Characteristics of the Nicotinic Acetylcholine Receptor

3.1a Introduction

Cloning studies have identified genes coding for neuronal nAChR subunits, and expression of these genes in oocytes has shown that functional neuronal nAChR are, or can be, composed of two types of subunit: α-subunits (agonist binding, homologous with muscle α) and β (or non-α; homologous with muscle β)-subunits. Subunits assemble to form a pentameric structure with $\alpha_2\beta_3$ stoichiometry (Cooper et al 1991) (c.f the stoichiometry of the muscle receptor: $\alpha_2\beta(\gamma \text{ or } \varepsilon)\delta)$*. To date, 6 α and 3 β neuronal nicotinic receptor subunits have been isolated and cloned. It is clear that there may be many subtypes of neuronal nAChR expressed *in vivo*, made up of different combinations of the genetic isoforms of the α and β subunit. It is possible that the same cell type may express more than one type of receptor.

Many studies are being performed to characterise nAChR expressed in oocytes from various combinations of subunit genes and to determine the tissue location of the different subunits.(See for example: Papke et al 1991, Charnet et al 1992, Connolly et al 1992, Gross et al 1991).

One result of these studies has been to shed light on the variable blocking effect of bungarotoxins. α-bungarotoxin potently blocks all muscle nAChR, but is ineffective on nearly all neuronal nAChR; α-Bgtx insensitivity has been used to define 'classical' neuronal nAChR. A minor component of B.multicinctus venom, named κ-Bgtx (toxin F, Bgtx 3.1) was found to block many ganglionic nAChR (Steinbach & Ifune, 1989, Loring et al 1984), while being ineffective on the muscle receptor. However, not all α-Bgtx insensitive receptors are

---

* Subscripts are used to denote stoichiometry and non-subscripted suffixes to denote genetic isoforms of a subunit.

blocked by κ-Bgtx, the bovine adrenal chromaffin cell nAChR being an example (Higgins & Berg 1987). Neuronal nAChR subunit expression experiments have shown that some combinations are highly sensitive to κ-Bgtx (α3β2), some partially blocked (α4β2), and others insensitive (α2β2, α3β4) (Deneris et al 1991). Of particular relevance here is the finding that the predominant subunit genes expressed in autonomic ganglia are α3, β2 and β4, (Papke et al 1991) hence the α3β2 and α3β4 may represent two ganglionic receptor types, sensitive and insensitive respectively to κ-Bgtx.

Unambiguously assigning particular subunit combinations expressed *in ovo* to receptor types found *in vivo* on the basis of single channel properties has proved difficult: it is possible that unidentified subunits are missing, more than two types of subunit are required or some form of post-translational modification is not performed by the oocyte.

Currents gated by the nicotinic acetylcholine receptor have been recorded from the bovine adrenal chromaffin cell in various studies (Fenwick et al 1982a, Clapham & Neher 1984 a&b, Cull-Candy et al 1988, Jacobson et al 1991). The single channel conductance of the receptor associated ion channel is approximately 40 pS, reported values being: 44 pS (Fenwick et al 1982a), 33 pS (Clapham & Neher 1984a), 39 pS (Cull-Candy et al 1988), 37 pS (Jacobson et al 1991) and see following results. Other conductance levels were observed, but at low frequency and not in all preparations and were apparently not investigated in detail. Cull-Candy et al, for example, found subpopulations of channels with conductances ~5 pS higher and ~6 pS lower than the main conductance level. The 2/3 conductance level commonly observed throughout this study (see results) was not reported (Gage & McKinnon (1985) found channels with conductances of 32 and 46 ps - approximately the same ratio - but this was in extrajunctional regions of chronically denervated rat skeletal muscle). Values of the single channel conductance calculated from Lorentzian curve fits to noise spectra produced lower values than when unitary

events were measured directly e.g 24 pS vs 39 pS (Cull-Candy et al 1988), 30 pS vs 37 pS (Jacobson et al 1991).

The single channel conductance of nicotinic gated channels of sympathetic (and also parasympathetic) ganglion neurones is very similar (35 pS Mathie et al 1990; 38 pS Fieber & Adams 1991) which might be expected considering the close homology that exists between these cells and chromaffin cells. The strong inward rectification of currents gated by nicotinic receptors in ganglion cells (Mathie et al 1990, Fieber and Adams 1991, Yawo 1989)) is also seen in adrenal chromaffin cells (Hirano et al 1987) and PC12 cells (Ifune & Steinbach 91).

Reversal potential data show little or no selectivity for Na^+ over K^+ ions, or indeed other monovalent cations. Vernino et al (1992) have shown the calcium permeability of the bovine adrenal chromaffin cell nAChR to be similar to that of cesium ions, and much higher than is the case for the muscle receptor.

Mean channel lifetime can be difficult to compare between studies since differences in recording bandwidth affect this parameter enormously; at limited bandwidth brief channel closures,or brief openings, are unresolved and hence the mean channel open time overestimated. For this reason the slow time constant of the burst length distribution probably allows the fairest comparison, since it represents the average duration of individual activations of the receptor (Colquhoun & Sakmann 1981) inclusive of brief closures, whether these are fully resolved or not, but excludes very brief activations, which also may or may not be resolved. On this basis, ~10 ms appears to be the approximate mean duration of the lifetime of the channel (11ms Mathie et al 1987; 9.5 ms Cull-Candy et al 1988, and see results). This figure also agrees well with the time constant of the Lorentzian fitted to control spectra, suggesting this value represents burst length (Jacobson et al

1991 calculated time constants of 10ms for CCh and 17ms for ACh; Cull-Candy et al 1988 obtained 11ms using ACh, and see results). These values are also similar to decay time constants for EPSC's.

The following section describes the data obtained from control experiments with the nicotinic acetylcholine receptor performed throughout the present study.

3.1b Results

Currents gated by nicotinic agonists were recorded in bovine adrenal chromaffin cells using various configurations of the patch clamp technique:

i) cell attached patches
ii) excised outside-out patches
iii) whole cell recording

Recordings were analysed as described in Methods (section 2.4) to yield values for the conductance and kinetic parameters of the channel.

The agonist used throughout this study to evoke nicotinic currents was carbamylcholine (carbachol; CCh), a stable analogue of the physiological ligand acetylcholine (ACh). In a few cells the characteristics of currents gated by ACh and CCh were compared (see fig. 3.1.1) and found not to differ qualitatively, although ACh was approximately five times as potent as CCh.

At -80 mV holding potential, the mean sustained inward current elicited by 10 μM CCh was 1.58 $\pm$ 0.58 pA (n=7) and 4.47 $\pm$ 2.24 pA (n=12) for 25 μM CCh. Desensitisation at these agonist concentrations was modest, and currents usually reached a sustained steady level after about 30 s.

3.1b(i) Conductance of the nAChR channel

The single channel conductance and reversal potential of channel openings evoked by carbachol were calculated by plotting the mean of the Gaussian curve fitted to all points open histograms against holding potential. Conductance varied between experiments, but within individual cells channel amplitudes showed little variability, the standard deviation of the Gaussian fitted to the open points histogram rarely being 25% greater than the closed channel distribution (c.f Mathie et al 1987). The reversal potential calculated by extrapolation depended on the pipette solution used (see methods); it was -13mV for Cl^- and 0mV for glu-*.(see fig. 3.1.1). (A value of E_{rev} = -3 mV was calculated assuming equal permeability of Na^+ and K^+ ions.) These figures are calculated assuming linearity of the I/V relationship at negative potentials. Single channel conductance was not significantly different for the two internal media and was 44.8 pS ± 3.6 (n=27).

In addition, a subconductance level was commonly observed. The frequency of sub-state channel openings varied greatly from cell to cell, and to some degree with time in a single cell. Where sub-state openings were numerous enough to fit a Gaussian curve to the amplitude distribution, it was found that the sub-state conductance expressed as a percentage of the full open conductance from the same cell was very consistent, being 64.5 ± 1.5%. (see fig 3.1.1).

Conductance estimated from noise spectra (see methods) was 32.1 ± 3.9 pS (n=33). This value is somewhat lower than the directly measured figure, as was the case in previous studies (see above). Here, it may be partly explained by the presence of the subconductance level.

* A proportion of this apparent difference in reversal potential can be accounted for by the junction potential change (measured as +7-8 mV) associated with glu- filled recording electrodes.

3.1b(ii) nAChR channel gating kinetics

Open state and burst length distributions were calculated from the combined* results of cell-attached (see figs 3.2.3 and 3.2.4), small whole cell (see fig. 3.1.2) and excised outside-out patch experiments. In each case both distributions are well fitted by the sum of two exponentials, with parameters shown in table 3.1.1. Brief closures within bursts were very infrequent and consequently the open and burst distributions are similar, although as can be seen in figure 3.1.2 a small rightward shift is seen in the longer time component of the burst distribution as compared with the open time distribution. All three experimental configurations give essentially similar distributions.

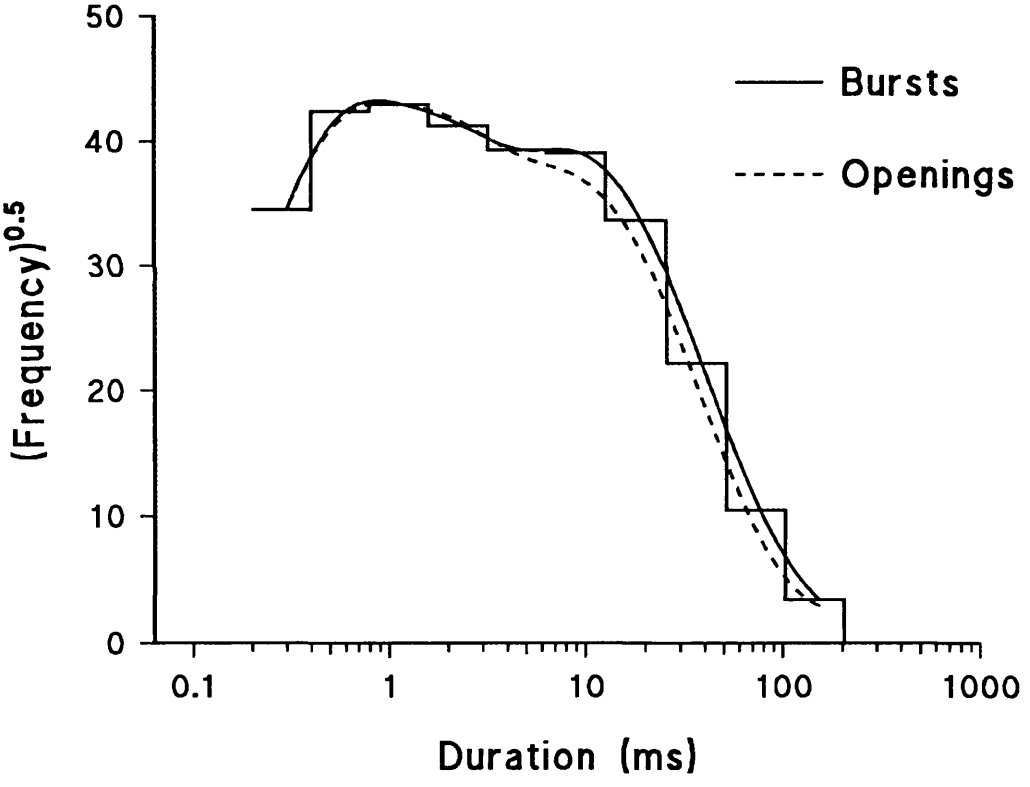

Figure 3.1.2

The frequency distribution of nAChR channel openings/bursts evoked by 1-2 μM CCh in small whole cells. (Combined data from 31 cells; 12299 openings, 11346 bursts). Steps represent bursts.

*Pooling data reduced the number of zero bins in the frequency distributions and improved the confidence of the exponential curve fits.

Spectra calculated from carbachol-induced currents were well fitted by a single Lorentzian component. In some cases, a marginally better fit could be obtained using the sum of two components, however the second, high frequency, component was rarely more than 1% of the magnitude of the main component. For simplicity, control spectra were routinely fitted to single Lorentzian functions and the mean corner frequency of these was 15.6 $\pm$ 2.9 Hz (10 µM CCh) and 18.7 $\pm$ 3.9Hz (25 µM CCh), from which channel closing rate constants of 10.2 and 8.5 ms are calculated. These rate constants probably represent the burst length, and agree well with the slow time constant of the single channel burst length distributions.

In some cells where large numbers of both full and sub-state openings were recorded, open state distributions were calculated for both conductance levels. After exclusion of brief openings (<0.8ms), which are attenuated by the 1KHz filter and thus hard to categorise unequivocally to either conductance level, the distributions for the two conductance levels were found to be essentially the same.

Table 3.1.1

Parameters of exponential curve fits to open time/burst length frequency distributions for control recordings

	Cell-Attached	Outside-Out patch	Small Whole Cell
OPEN STATE			
Mean Open Time (ms)	7.32 ± 1.56	5.80 ± 2.20	5.31 ±0.25
τ_{fast} (ms)	1.07 ± 0.11	0.47 ± 0.05	0.95 ± 0.07
τ_{slow} (ms)	6.94 ± 0.68	6.70 ± 0.11	9.23 ± 0.47
$Area_f/Area_s$	0.54	1.61	1.34
BURST PARAMETERS			
Mean Burst Length (ms)	8.40 ± 1.78	7.34 ± 3.10	6.01 ± 0.29
τ_{fast} (ms)	2.08 ± 0.13	0.88 ± 0.04	0.92 ± 0.04
τ_{slow} (ms)	10.57 ± 1.03	14.60 ± 4.80	10.06 ± 0.26
$Area_f/Area_s$	0.87	2.14	1.22

Values shown ± standard error. τ_{fast} and τ_{slow} are the time constants of the exponential curves fitted to the open state/burst length frequency histograms compiled from pooled dat

Figure 3.1.1

Nicotinic gated currents in bovine adrenal chromaffin cells

The top panel describes the current voltage relationship for single channel currents recorded using whole cell voltage clamp from a small (4.1 pF) chromaffin cell.

Glutamate recording solution was used and channel openings were elicited by application of 2μM CCh.

The left-hand panel shows a plot of single channel current measured at holding potentials from -110 to -50 mV. Data points represent the peak of the Gaussian curve fitted to an amplitude frequency distribution drawn using 8 point Patlak averaging. Values given for conductance and reversal potential were calculated assuming linearity.

The right-hand panel shows currents recorded from this cell at -60, -80 and -100 mV holding potential. Openings are downward deflections in the current trace, reflecting inward current.

The lower left hand panel shows power spectra calculated from current fluctuations in response to 10 μM ACh and 10 μM CCh applied sequentially to the same cell. The corner frequencies indicated correspond to time constants of 6.1ms (ACh) and 5.2ms (CCh). Holding potential -80mV.

The lower right hand panel illustrates the subconductance level, recorded in whole cell mode. The histogram is a Patlak average and clearly shows two peaks corresponding to channel openings to the sub (mean 3.02 pA) and full (mean 4.84 pA) conductance level. Above are shown examples of each type of opening. Holding potential -100mV.

* This method (Patlak (1988)) improves the resolution of the current amplitude histogram. The mean and variance of n adjacent sample points is calculated, stepping through the record point by point. The amplitude histogram is compiled from those n point means whose variance does not exceed a preset level (≈ the variance of baseline current). Thus the histogram is effectively compiled from stable sections of the record and transitions between states are excluded.

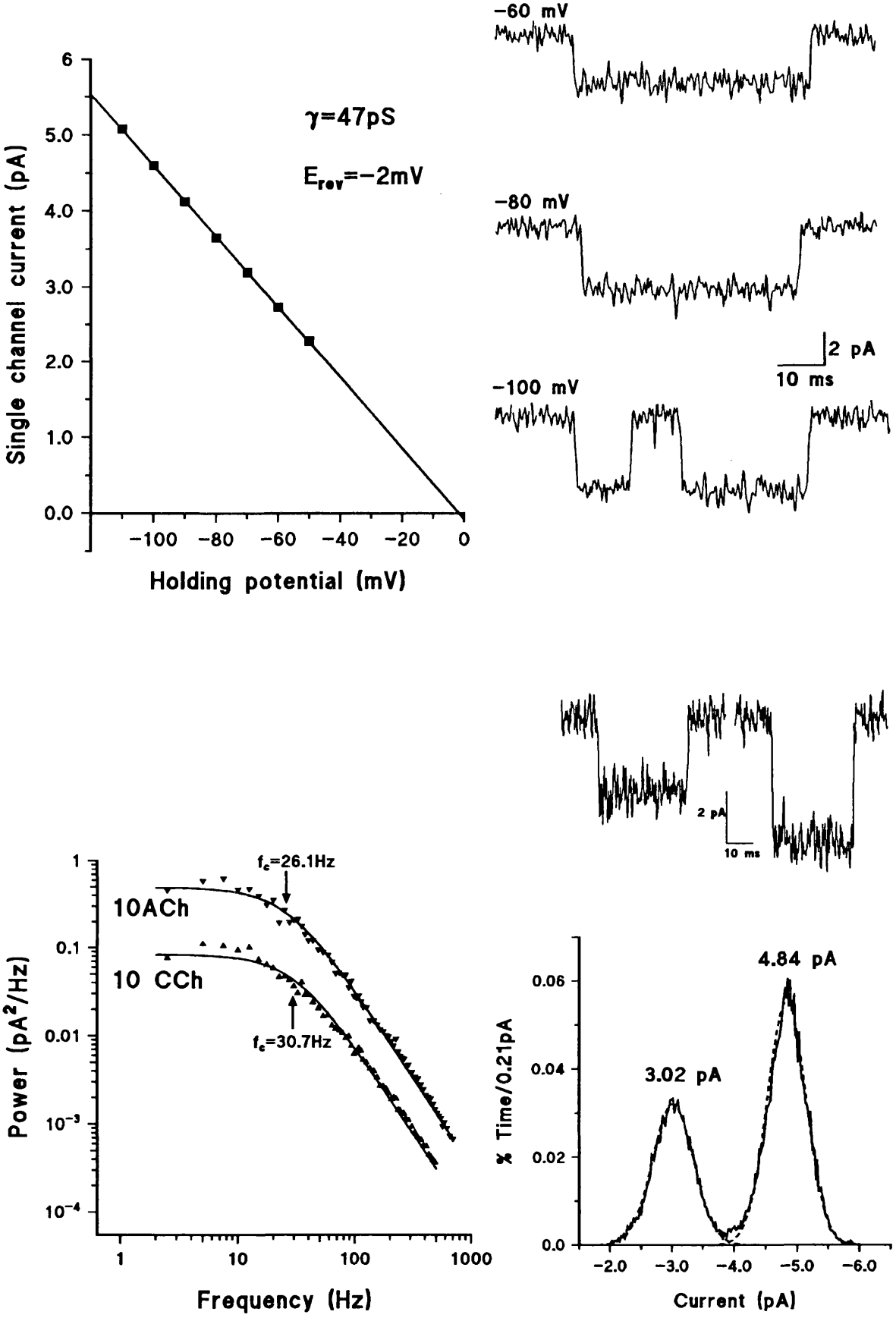
γ=47pS
E_rev=−2mV
Single channel current (pA)
Holding potential (mV)
−60 mV
−80 mV
−100 mV
2 pA
10 ms
10ACh
10 CCh
f_c=26.1Hz
f_c=30.7Hz
Power (pA²/Hz)
Frequency (Hz)
2 pA
10 ms
4.84 pA
3.02 pA
% Time/0.21pA
Current (pA)

3.2 Modulation of nicotinic channels by procaine

With a holding potential of -80 mV the steady-state inward current evoked by 10 μM carbachol had a mean value of 1.58 ± 0.22 pA. Co-application of 20 μM procaine with 10 μM carbachol reduced the inward current to 0.66 ± 0.12 pA (seven cells). When expressed as a percentage of the paired control the inward current was inhibited by 56 ± 6 % (n=7). In two cells 50 μM procaine reduced the steady-state inward current by 80%.

3.2a Noise analysis

At a holding potential of -80 mV spectral analysis of the noise induced by 10 μM carbachol yielded a frequency distribution that was adequately fitted by a single Lorentzian function with a corner frequency of 15.6 ± 1.1 Hz (n=7), corresponding to a time constant for channel closure of 10.2 ms. The single channel conductance estimated from the noise spectra and the mean inward current was 32 ± 1.5 pS (n=7).

In addition to its depressant action on inward current, procaine caused a second, higher frequency, component to appear prominently in the noise spectrum. With a holding potential of -80mV co-application of 10μM carbachol and 20 μM procaine gave noise spectra that were best fitted by the sum of two Lorentzians with corner frequencies of 22.5 ± 1.2 Hz and 122 ± 6 Hz (n=7) corresponding to time constants of 7.1 and 1.3 ms respectively. The S(0) intercept of the low frequency component was on average 2.4 times that of the high frequency component when the holding potential was -80 mV. A similar pattern is seen at other holding potentials (see Fig. 3.2.1). In two cells, application of 50 μM procaine plus 10 μM carbachol increased the corner frequencies further to 36 Hz and 280 Hz (corresponding to time constants of 4.4 and 0.6 ms). At this concentration of procaine the relative amplitude of the S(0) value of the high frequency component was also increased.

Procaine had no effect on the apparent single channel conductance calculated from the noise spectra. The conductance was 32.6±1.3 pS (n=7) in 20 μM procaine and 36 and 35 pS for two determinations in 50 μM procaine.

3.2b Voltage-dependence of procaine action

The voltage dependence of the noise spectra was examined in seven cells. In the absence of procaine the corner frequency showed no consistent change as the holding potential was varied between -100 mV and -50 mV. In the presence of 20 μM procaine neither the corner frequency of the low frequency component nor that of the high frequency component showed any statistically significant trend with membrane potential. In contrast, the S(0) intercept of the high frequency component increased approximately linearly with increasing hyperpolarisation showing an e-fold increase for a 55 mV hyperpolarisation (Fig. 3.2.1). At a holding potential of -100mV the S(0) values for both components were almost equal. Fig. 3.2.2 shows a typical example of the increase in power of the high frequency component with increasing membrane potential.

Figure 3.2.1

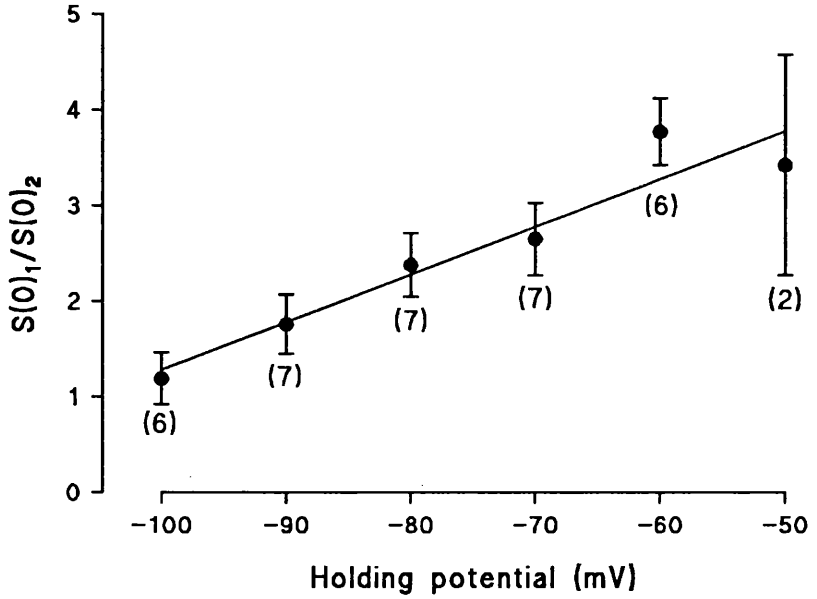

3.2c Single channel studies.

The following studies were performed in order to directly determine the influence of procaine on the kinetic gating parameters of the nicotinic acetylcholine receptor.

3.2c(i) Cell Attached patches

With the cell attached configuration, Cch (10μM) was always present in the patch pipette to activate the channels. In this configuration, application of procaine to the region outside the patch was ineffective in modifying the kinetics of channel opening so, where appropriate, procaine was included in the solution within the patch pipette at 2-50μM.

When activated by Cch alone, the channel openings were seen as inward currents of approximately 2pA (Fig. 3.2.3). The individual channel openings were usually single events and were not interrupted by brief closures (see below). Sub-conductance states were excluded from the formal analysis (see Methods).

The amplitude of the channel openings was unchanged by 2 and 10 μM procaine but 50 μM caused a statistically significant reduction in amplitude when assessed by the t-test ($p<0.05$; see Table 3.2.1). At this concentration, however, the channel openings are very brief with an open time distribution time constant of approximately 0.8 ms (see below). About two thirds of these fast openings will be shorter than 0.8ms and will be attenuated by the low-pass filter (-3dB at 1KHz). In addition, when channel openings are very brief, it is not easy to distinguish substates from attenuated full openings. This apparent reduction in channel conductance can, therefore, be fully explained by the filter characteristics of the recording system.

In the absence of procaine the duration of channel open times was best fitted by the sum of two exponentials with time constants of 1.07ms and 6.94ms. The combined data for seven

separate patches are shown in Fig. 3.2.3. The probability of the channel being in the open state (P_{open}) was low with a mean value of 0.0068 (Table 3.2.1).

Addition of procaine (2-50 μM) to the patch pipettes reduced the number of long duration openings and shifted the distribution of open times progressively to shorter intervals as the concentration of procaine increased (see Fig. 3.2.3). At the highest concentration tested, the open time distribution could be fitted by a single exponential with a time constant of 0.78 ms. The open time distributions of fig. 3.2.3 represent the combined data of between five and seven separate patches. The mean open time of the channels progressively decreased as the concentration of procaine increased as predicted by the sequential blocking model. The channel blocking rate constant was estimated* from these data as 2×10^7 M^{-1} s^{-1}. This decrease in mean channel open time was associated with marked flickering of the open state which increased in frequency with increasing concentrations of procaine (Fig. 3.2.3). The open state probability was not significantly different from control for 2 and 10 μM procaine but was reduced in the presence of 50 μM procaine (see Table 3.2.1).

The closed times were distributed in a biphasic manner with a high incidence of brief closures (<2ms) and a broad distribution of longer closed times which could be fitted with a time constant of about 500 ms. Application of procaine (2-50 μM) caused a progressive increase in the proportion of brief closures and their distribution was then best fitted by two exponentials (Fig. 3.2.4 and Table 3.2.1). As the time constant for the distribution of the long closures reflects the gap between bursts and as the number of channels in a patch is not known, the long time constants are difficult to interpret and have therefore been ignored in the analysis.

* From a fit of $1/(\alpha+f.c)$ to the plot of mean open time vs. [procaine].

Effects of procaine on bursting behaviour

In the absence of procaine, the channel open times were exponentially distributed and there were few short channel closures. The distribution of burst length was therefore very similar to the distribution of channel open time. In the presence of procaine, channel openings were more frequently interrupted by brief closures so giving a characteristic pattern which is typical of burst behaviour (see introduction). Nevertheless, even in the presence of 50 μM procaine the majority of channel openings were single events. For the experiments described here the classification of groups of openings as bursts was determined according to the criteria given by Clapham & Neher (1984b)(see Methods). In the absence of procaine the distribution of burst length could be described adequately by the sum of two exponentials but as the concentration of procaine increased the time constants of the distributions became shorter and mean burst length decreased e.g. from 7.94 ms in control to 5.21 ms in 2 μM and 2.91 ms in 50 μM procaine.

As the distribution of closed times progressively changed with increasing procaine concentration (see Fig. 3.2.4 and Table 3.2.1) the t_{crit} for calculating burst characteristics also changed. This will bias the calculation of mean blocked time. To compensate for this the data was also analysed with a fixed value for t_{crit} of 8 ms which is the value appropriate for 50 μM procaine. Although this reanalysis gives different mean values for burst length and blocked time at other concentrations of procaine (e.g. 8.4 ms burst length in control compared to 7.94 ms with a t_{crit} of 5ms), the tendency for burst length to decrease and blocked time to increase with increasing procaine concentration remains (Table 3.2.1., and see section 3.6a) Overall, increasing concentrations of procaine caused an increase in the number of gaps per burst and an increase in the mean blocked time but a reduction in mean burst length (Fig. 3.2.4).

3.2c(ii) Excised outside out patches

To gain better control of the membrane potential during drug application and to permit acquisition of data from the same channels in the presence and absence of anaesthetic, the effect of procaine was examined in three excised outside-out patches. With a holding potential of -70mV the channel openings are seen as inward current movements of 2.72±0.098 pA amplitude. As with the cell attached patches, the distribution of channel open times was best fitted by the sum of two exponentials with time constants of 0.47 ms and 6.7 ms (combined data from three patches). Application of procaine (50μM) reduced the amplitude of single channel events to 2.52±0.071 pA, abolished long duration openings and shifted the open time distribution curve to the left. As for the studies with cell attached patches, the distribution of channel open times in the presence of 50μM procaine was best fitted by a single exponential which, in this case, had a time constant of 1.33 ms.

As for channels activated by 10μM CCh in cell attached patches, the distribution of channel closed times was skewed with a large number of brief closures (< 2ms) and a broad distribution of longer closed times with a time constant of 500 ms. The distribution of brief closures could be fitted by the sum of two exponentials with time constants of 0.65 ms and 17 ms. Application of procaine caused a higher incidence of brief closures (from 12.5% of closures of 2 ms or less in control to 26% of closures of 2ms or less duration when 50 μM procaine was applied). The distribution of brief closures during application of procaine was best fitted by exponentials with time constants of 0.71 ms and 4.37 ms. In the absence of procaine, the distribution of burst length was well fitted by the sum of two exponentials which had time constants of 0.9 ms and 14.6 ms. In agreement with the studies in cell-attached patches, procaine decreased mean burst length from 7.34 ms to 4.31 ms, this decrease being evident in each of the patches studied. The data are summarised in Table 3.2.2.

Table 3.2.1

Procaine modulation of the kinetic constants of currents induced by 10 μM carbachol in cell-attached patches.

The time constants for closed times were calculated for closures of less than 50 ms using a bin width of 1 ms. The burst characteristics were calculated assuming a t_{crit} of 8 ms. Combined data from 5-7 patches with means $\pm$ s.e.m where appropriate. The time constants are given together with the standard error of the estimate. F_{open} is frequency of opening. (* denotes $p<0.05$ for the difference between control patches and those exposed to 50 μM procaine).

TABLE 3.2.1

Procaine modulation of the kinetic constants of currents induced by 10μM CCh in cell attached patches

parameter	CONTROL	2 μM PROCAINE	10 μM PROCAINE	50 μM PROCAINE
OPEN STATE				
Unit current (pA)	2.35±.09	2.29±0.12	2.28±0.10	1.98±0.072*
τ_{fast} (ms)	1.07±0.11	0.36±0.03	0.27±0.04	-
τ_{slow} (ms)	6.94±0.68	3.64±0.09	2.63±0.06	0.79±0.01
$Area_f/Area_s$	0.54	0.35	0.73	-
mean open time (ms)	7.32±1.56	4.26±0.45	2.67±0.33	1.07±0.10*
P_{open} (%)	0.68±0.07	0.70±0.15	1.1±0.04	0.21±0.08*
F_{open} (s^{-1})	1.05±0.31	1.83±0.47	4.06±1.42	2.16±0.63
CLOSED STATE				
τ_{fast} (ms)	0.75±0.03	0.50±0.03	0.96±0.03	0.85±0.27
τ_{slow} (ms)	-	13±4	11±3	8.8±2.6
$Area_f/Area_s$	-	1.89	2.65	1.09
BURST PARAMETERS				
Burst length (ms)	8.4±1.78	5.62±0.49	5.13±1.47	2.91±0.53*
mean blocked time (ms)	0.81±0.12	1.11±0.12	1.21±0.15	1.82±0.13*
gaps/burst	0.18±0.10	0.33±0.11	0.63±0.5	0.75±0.37*
τ_{fast} (ms)	2.08±0.13	1.04±0.10	1.39±0.05	0.84±0.02
τ_{slow} (ms)	10.57±1.03	5.58±0.34	9.18±0.51	10.22±0.76
$Area_f/Area_s$	0.87	0.52	1.02	2.63

Table 3.2.2

Effect of procaine on the kinetic properties of currents induced by 10 μM CCh recorded from outside-out patches

The time constants for closed times were calculated for closures of less than 50 ms using a bin width of 1 ms. The burst characteristics were calculated assuming a t_{crit} of 8 ms. Combined data from 3 patches (holding potential -70 mV) with means ± s.e.m where appropriate. The time constants are given together with the standard error of the estimate.
* denotes statistical significance at the 95% confidence level.

TABLE 3.2.2

Effect of procaine on the kinetic properties of currents induced by 10 μM CCh recorded from outside-out patches

	CONTROL	50 μM PROCAINE
OPEN STATE		
Unit current (pA)	2.72±0.098	2.52±0.071*
τ_f (ms)	0.47±0.05	-
τ_s (ms)	6.70±0.11	1.33±0.07*
$Area_f/Area_s$	1.61	-
Mean open time (ms)	5.8±2.2	1.44±0.26*
CLOSED STATE		
τ_f (ms)	0.65±0.04	0.71±0.12
τ_s (ms)	17±12	4.37±0.67
$Area_f/Area_s$	1.58	0.58
BURST PARAMETERS		
Burst length (ms)	7.34±3.1	4.31±2.5
mean blocked time (ms)	1.07±0.1	1.8±0.25*
gaps/burst	0.18±.03	0.73±0.52
τ_f (ms)	0.88±0.04	0.92±0.05
τ_s (ms)	14.6±4.8	11.7±4.6
$Area_f/Area_s$	2.14	2.59

Figure 3.2.2

Spectral analysis of current noise induced by 10μM CCh in the presence and absence of 20μM procaine. The left hand panels show the control spectra for holding potentials of -60mV (top), -80mV (middle) and -100mV (bottom). The right hand panels show the spectra for the same holding potentials in the presence of procaine. The corner frequency (ies) in control and in 20μM procaine are independent of voltage. In the presence of procaine however, the relative magnitude of the high frequency component rises with increasing hyperpolarisation. All data are from a single chromaffin cell. Note the difference in Y-axis range for control compared to procaine.

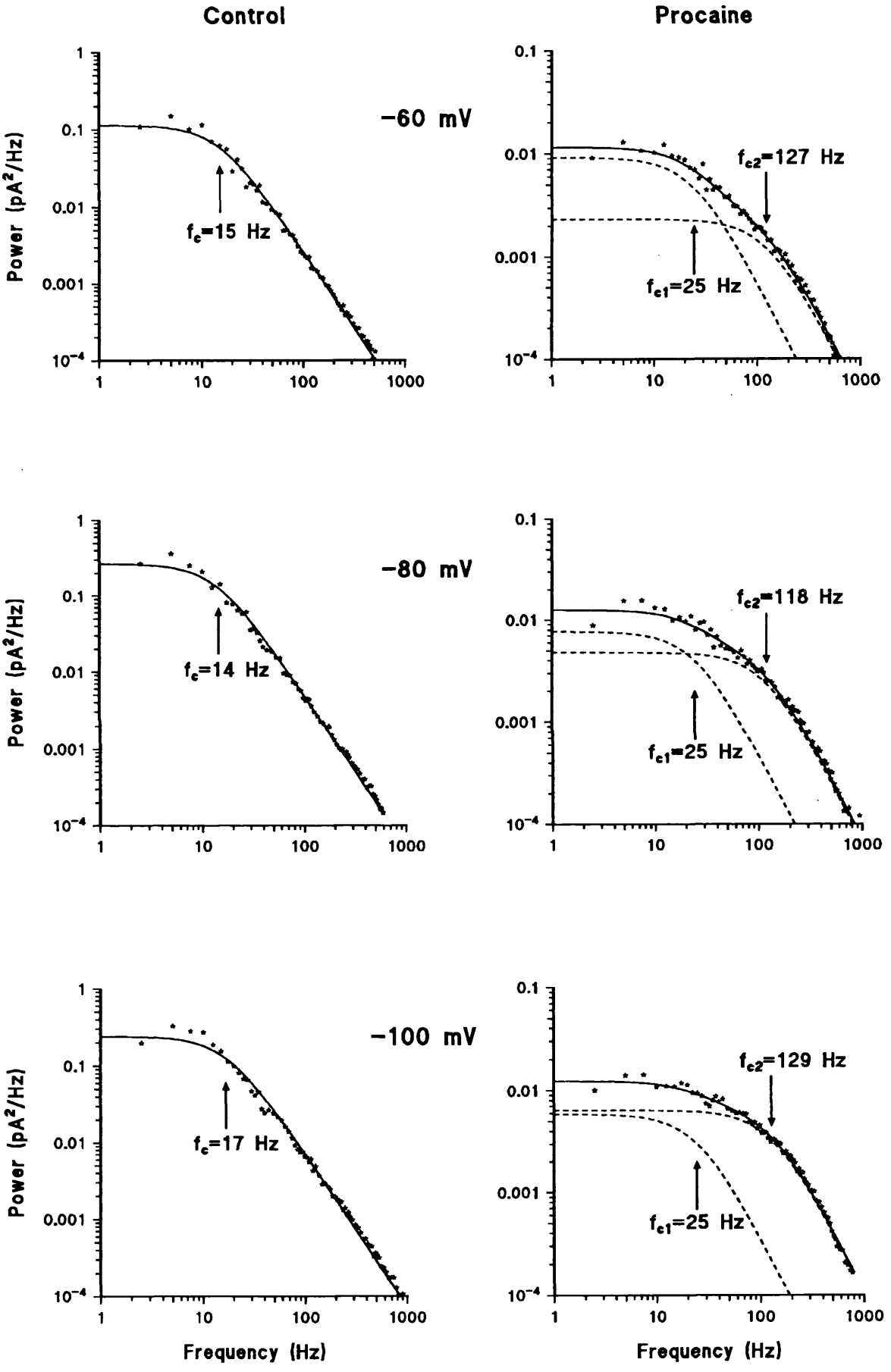
Control
Procaine
−60 mV
−80 mV
−100 mV
f_c=15 Hz
f_c=14 Hz
f_c=17 Hz
f_{c2}=127 Hz
f_{c1}=25 Hz
f_{c2}=118 Hz
f_{c1}=25 Hz
f_{c2}=129 Hz
f_{c1}=25 Hz
Power (pA²/Hz)
Frequency (Hz)
1
0.1
0.01
0.001
10⁻⁴
10
100
1000

Figure 3.2.3

The effect of increasing concentrations of procaine on the distribution of the open times of the channels activated by 10 μM carbachol. Each panel shows combined data from 5-7 cell-attached patches. The pipette potential was 0 mV. The smooth curves are the calculated exponential functions fitted to the frequency distribution. The parameters of the curve fits are shown in table 3.2.1. The inset records show examples of channel openings (downward deflections in the current trace). The calibration bars in the top left panel apply to all records and are 1 pA (vertical) and 10 ms (horizontal).

Top left panel: Control - 10 μM CCh alone (n=7)

Top right panel: 2 μM procaine + 10 μM CCh (n=6)

Bottom left panel: 10 μM procaine + 10 μM CCh (n=6)

Bottom right panel: 50 μM procaine + 10 μM CCh (n=5)

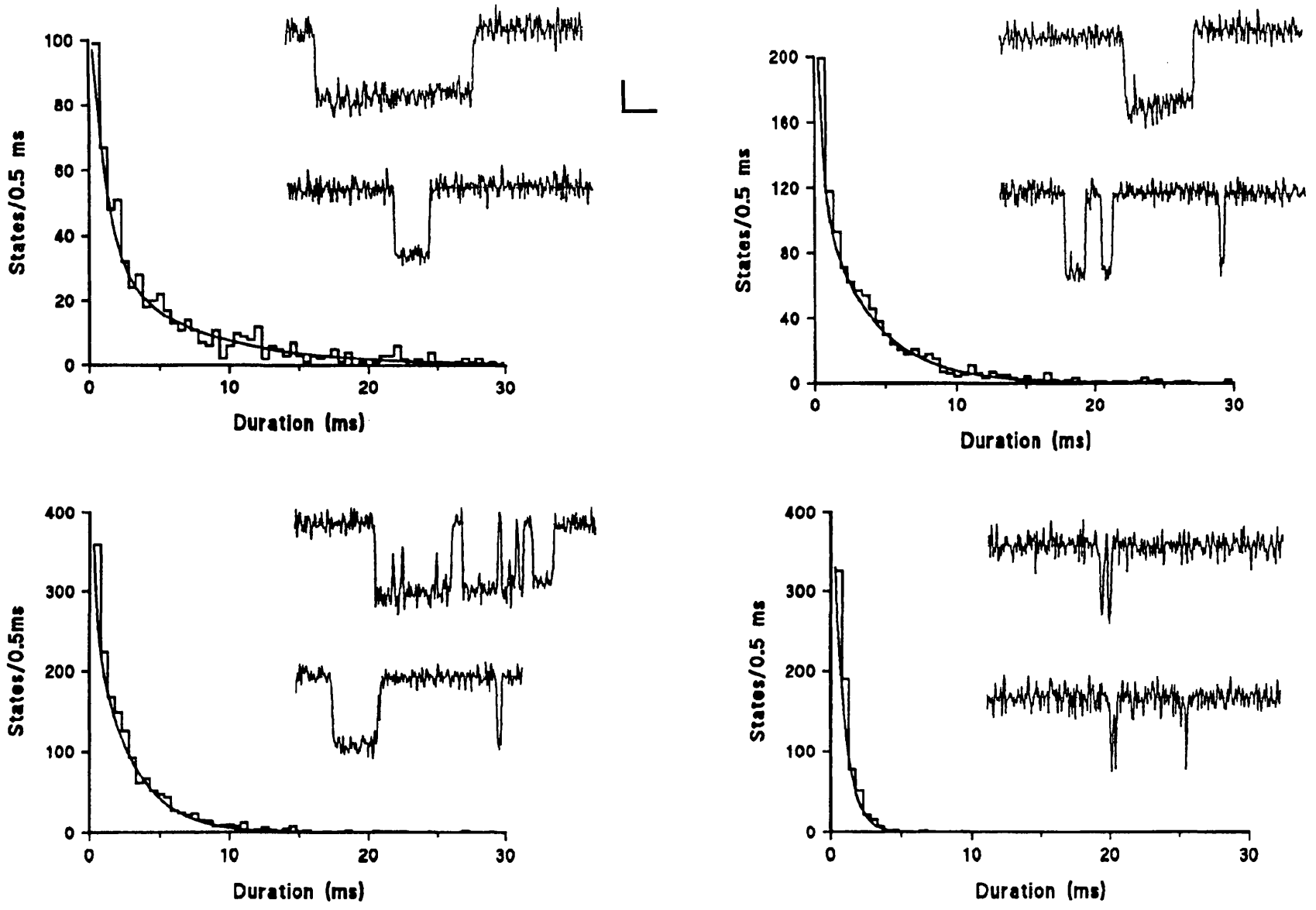
States/0.5 ms
Duration (ms)
States/0.5 ms
Duration (ms)
States/0.5ms
Duration (ms)
States/0.5 ms
Duration (ms)

Figure 3.2.4

The effect of 50 μM procaine on the frequency distribution of burst length (upper panels) and closed times (middle panels). In each case the ordinate is expressed as the a percentage of the total number of events. Combined data from 7 (control) and 5 (50 μM procaine) cell attached patches are shown. The smooth curves are the calculated double exponential functions fitted to the frequency distribution. The parameters of the curve fits are shown in table 3.2.1.
The total number of bursts was 578 (control), 524 (50 μM procaine). The total number of closures was 668 (control), 914 (50 μM procaine).

The lower left panel shows a plot of mean burst length against procaine concentration and the lower right hand panel a plot of mean blocked time against procaine concentration. Error bars represent the standard error of the mean.

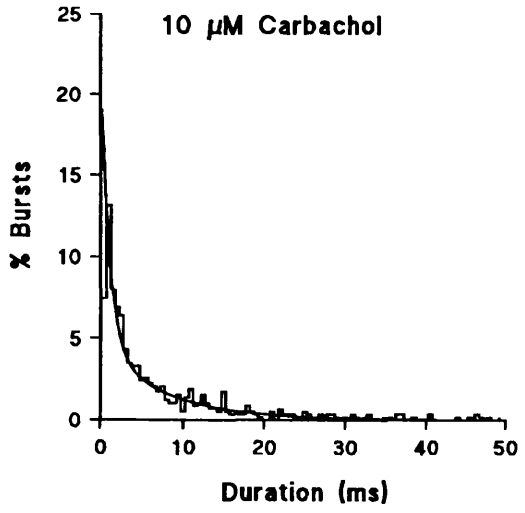
10 μM Carbachol
% Bursts
Duration (ms)

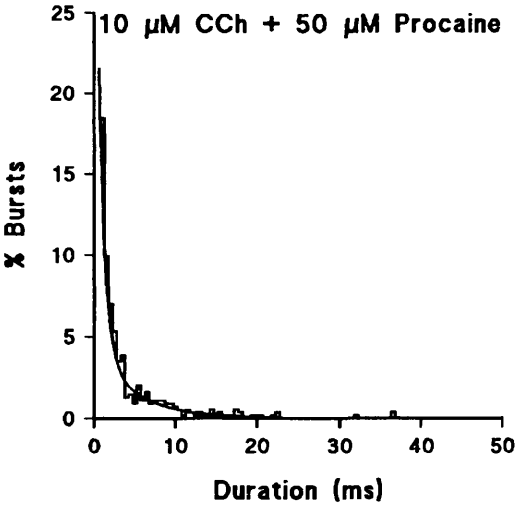
10 μM CCh + 50 μM Procaine
% Bursts
Duration (ms)

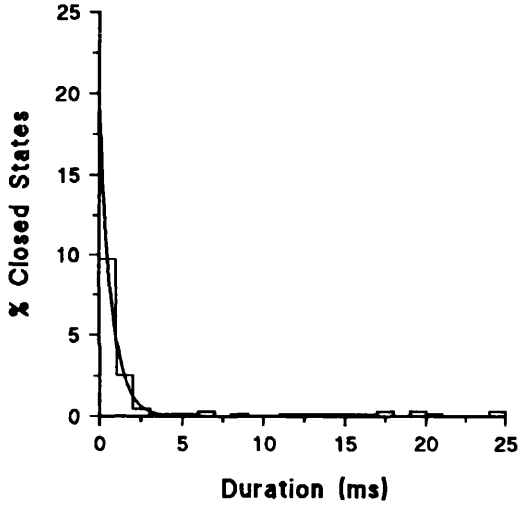
% Closed States
Duration (ms)

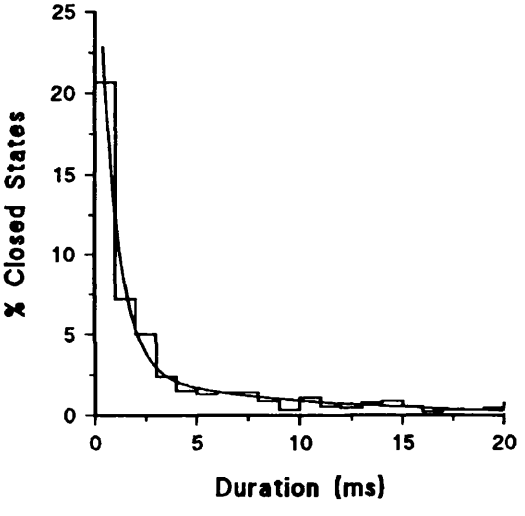
% Closed States
Duration (ms)

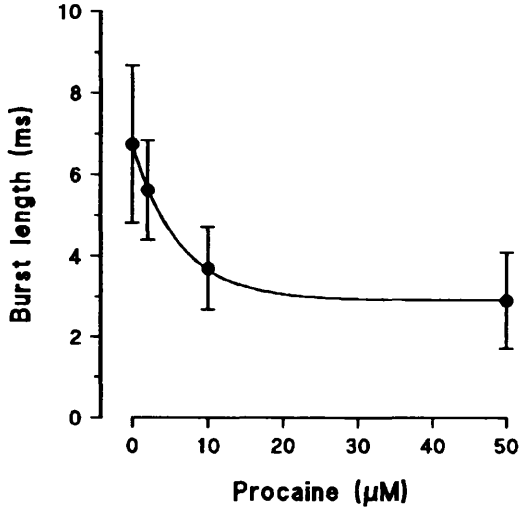
Burst length (ms)
Procaine (μM)

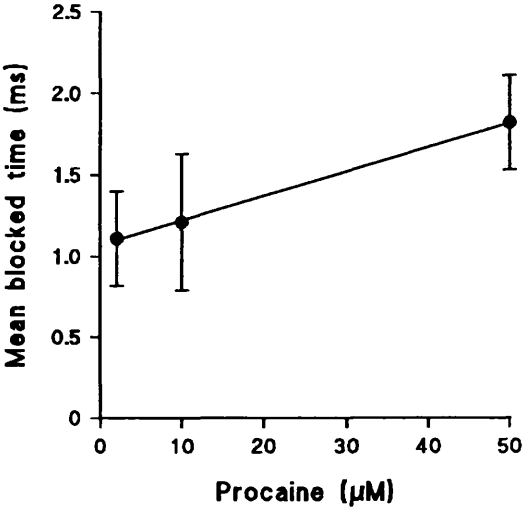
Mean blocked time (ms)
Procaine (μM)

3.3 Modulation of nAChR by Methoxyflurane

3.3a Noise Analysis

The effect of methoxyflurane on whole cell current noise evoked by 25 μM carbachol was studied in 7 cells. Power spectra were calculated from 30s stretches of record obtained during application of carbachol alone, or carbachol plus methoxyflurane (100-500 μM). In the control, and in the presence of all concentrations of methoxyflurane, spectra were well fitted by a single Lorentzian function. The corner frequency of the fitted curve increased with increasing methoxyflurane concentration, revealing a dose-dependent reduction in the time constant for channel closure. At -80 mV, corner frequency increased from 18.1 $\pm$ 3.1 Hz (τ=8.8ms) in control to 21.1 $\pm$ 2.2 Hz (τ=7.5ms) with 100 μM methoxyflurane, to 30.9 $\pm$ 4.6 Hz (τ=5.2ms) with 250 μM methoxyflurane, to 63.8 $\pm$ 0.2 Hz (τ=2.5ms) with 500 μM methoxyflurane. Methoxyflurane had no effect on the single channel conductance calculated from the parameters of the fitted Lorentzian curves.(36.1 pS for control, 35.8 for 500 μM methoxyflurane). Fig. 3.3.1 shows power spectra calculated for a typical cell.

3.3b Single channel studies

3.3b(i) Whole cell recording

Small chromaffin cells (3-5pF; 9-13 μM) were selected for whole cell patch clamp recording. With pipette and bath solutions described in the methods, there was no detectable channel activity at potentials below -60 mV and baseline current noise was low (standard deviation of Gaussian curve fit 0.4-0.45 pA). Perfusion with methoxyflurane alone (250 μM) had no detectable effect on the recorded current.

Application of low concentrations of carbachol (1-2 μM) evoked nAChR channel openings at a low frequency (0.5-13 Hz; P_{open} 0.004-0.066 in control). At the holding potential of -100 mV used for these experiments, the signal to noise ratio, coupled to the low channel open probability, allowed detection of single channel openings as described in Methods.

Under these conditions, stable levels of channel activity could be recorded for long periods, allowing the sequential application to individual cells, of carbachol, and carbachol plus varying concentrations of methoxyflurane (100-500 μM), followed by a return to carbachol alone. Typically, cells were perfused with test solution for 5-10 minutes, with 3-4 minutes between successive applications. Segments of record were filtered at 1KHz and digitised at 5KHz prior to analysis.

Visual inspection of records revealed that the predominant effect of methoxyflurane was to reduce the duration of individual channel openings, an effect which became more marked with increasing anaesthetic concentration. This is shown in the open state duration histograms (fig. 3.3.2); increasing concentrations of methoxyflurane progressively shift the distribution to shorter intervals.

Methoxyflurane, at any concentration studied, did not appear to induce brief closures within openings, characteristic of agents such as procaine. Despite the apparent lack of any burst behaviour records were subjected to burst analysis using a fixed t_{crit} of 10ms (see section 3.6.1). This was done both to confirm the absence of an anaesthetic related increase in brief channel closures and to allow formal comparison with other agents. Fig. 3.3.3 shows that mean open time and mean burst length, expressed as a percentage of control values, have the same relationship to methoxyflurane concentration. Furthermore, the mean number of brief (<10ms) closures per opening did not change significantly ($p<0.05$) with increasing concentrations of methoxyflurane (see table 3.3.1).

Single channel amplitude (the mean of the Gaussian curve fitted to a histogram of open state amplitudes) was unaffected by all concentrations of methoxyflurane.

3.3b(ii) Cell attached patches

The effect of methoxyflurane on nAChR channels was studied in four cell-attached patches. In these experiments, CCh (20 μM) was present in the patch pipette to activate channels and the cell perfused with methoxyflurane (100-500 μM). Applied in this way, methoxyflurane produced rapid effects on channel gating kinetics (c.f procaine), the magnitude of which were similar to those observed in the whole cell experiments described above. Expressed as a percentage of control values, 250 μM methoxyflurane reduced mean open time to 51.0 ± 11.0 %, channel open probability to 36.2 ± 9.9 % and opening frequency to 69.5 ± 2.9 %.

The essential features of the action of methoxyflurane on the nAChR can be summarised as follows:

1.) Methoxyflurane causes a dose dependent decrease in mean open time. The IC_{50} for this parameter is about 400 μM.

2.) After a small rise at 100 μM methoxyflurane, the frequency of channel opening falls at higher concentrations. The IC_{50} estimated by extrapolation is 600 μM.

3.) The channel open probability falls in a dose dependent manner, due to a combination of the above effects, but predominantly the reduction in channel open lifetime. The IC_{50} for this action of methoxyflurane is 250 μM.

4.) Bursts of channel openings are not seen at any concentration of methoxyflurane.

The implications of these findings are discussed at the end of this section together with further quantitative analysis

Table 3.3.1

Modulation by methoxyflurane of the kinetic constants of nAChR channel openings evoked by 1-2 μM CCh in small whole cells.

Errors shown are standard error of the mean or, for curve fit parameters, the 95 % confidence limits.

Table 3.3.1

Methoxyflurane modulation of the kinetic constants of nAChR channel openings evoked by 1-2 μM CCh in small whole cells .

	Control	100 μM methoxyflurane	250 μM methoxyflurane	500 μM methoxyflurane
Open state	(11)	(9)	(8)	(5)
τ_f (ms)	0.89 ± 0.09	0.75 ± 0.14	0.80 ± 0.16	0.78 ± 0.19
τ_s (ms)	8.13 ± 0.56	5.03 ± 0.48	4.53 ± 0.26	3.95 ± 0.39
$Area_f/Area_s$	1.37	1.12	1.26	1.86
mean open time (ms)	5.26 ± 0.33	3.62 ± 0.18	2.84 ± 0.18	2.25 ± 0.19
P_{open} (%)	2.15 ± 0.53	1.79 ± 0.44	0.82 ± 0.30	0.64 ± 0.25
F_{open} (Hz)	4.36 ± 1.06	4.96 ± 1.27	2.61 ± 0.81	2.19 ± 0.76
Closed state				
τ_f (ms)	0.69 ± 0.17	0.59 ± 0.13	0.67 ± 0.14	0.44 ± 0.23
τ_f (ms)	99.5 ± 17.3	111.8 ± 23.8	220.0 ± 158.1	209.8 ± 171.5
$Area_f/Area_s$	0.072	0.100	0.095	0.090

Figure 3.3.1

Spectral analysis of current noise evoked by 25μM CCh alone (top left), and in the presence of 100μM (top right), 250μM (bottom left) and 500μM (bottom right) methoxyflurane. The corner frequency increases and Y-axis intercept decreases with rising methoxyflurane concentration. Holding potential -80mV. All data from a single chromaffin cell. Corner frequencies for this cell correspond to time constants of 10.9ms (control), 8.7ms (100μM MF), 6.3ms (250μM MF) and 2.5ms (500μM MF).

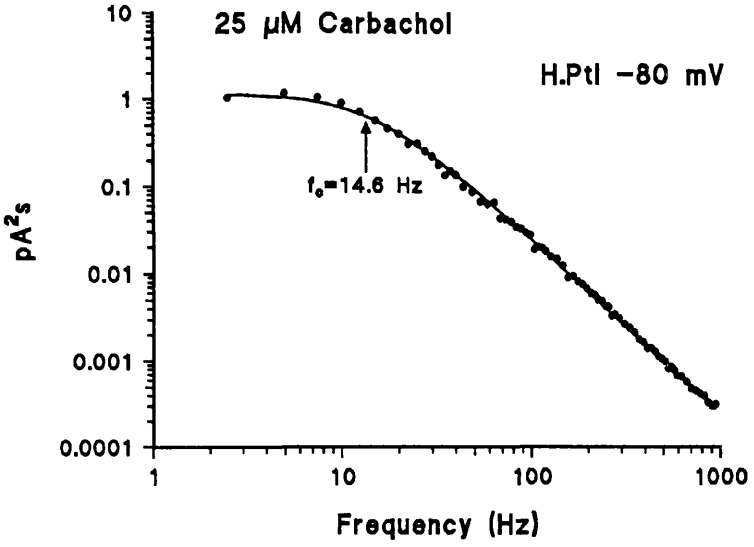
25 μM Carbachol
H.Ptl −80 mV
f_c=14.6 Hz
10
1
0.1
0.01
0.001
0.0001
pA²s
1
10
100
1000
Frequency (Hz)

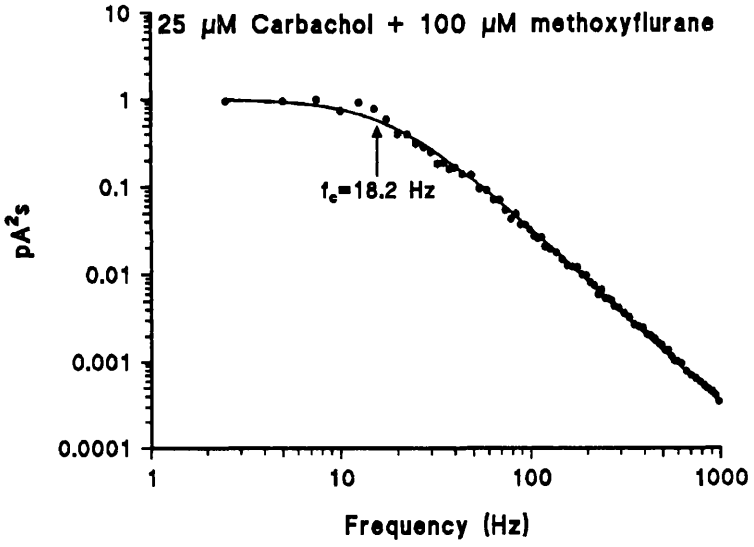
25 μM Carbachol + 100 μM methoxyflurane
f_c=18.2 Hz
10
1
0.1
0.01
0.001
0.0001
pA²s
1
10
100
1000
Frequency (Hz)

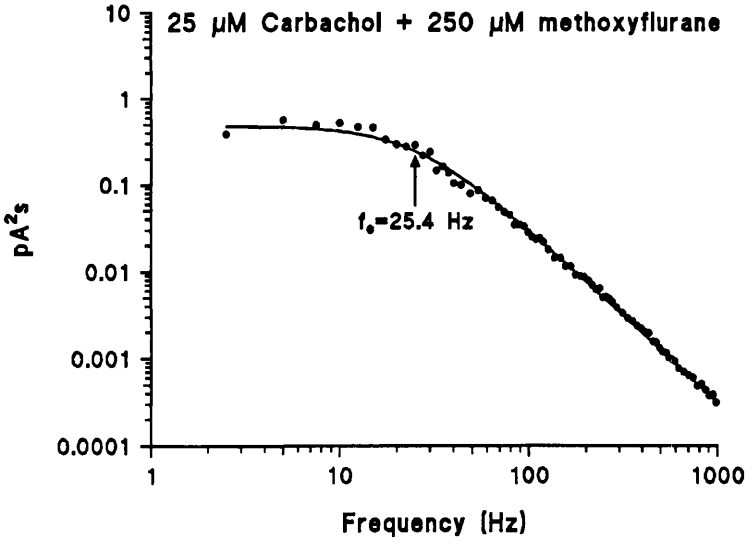
25 μM Carbachol + 250 μM methoxyflurane
f_c=25.4 Hz
10
1
0.1
0.01
0.001
0.0001
pA²s
1
10
100
1000
Frequency (Hz)

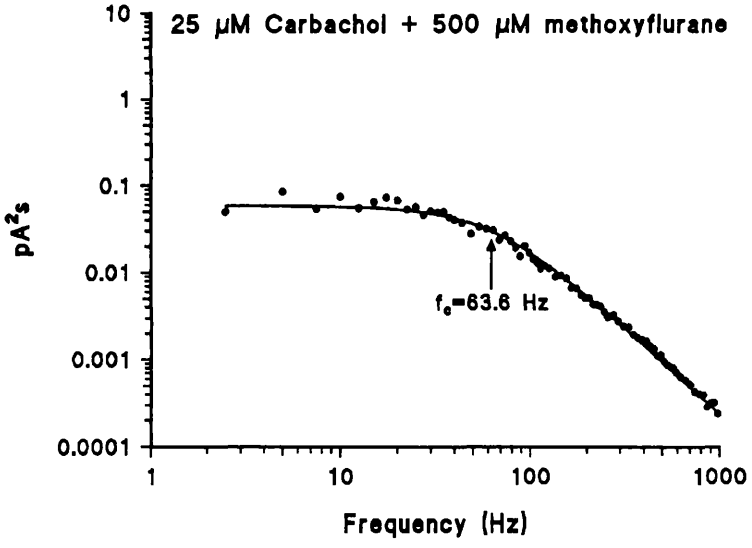
25 μM Carbachol + 500 μM methoxyflurane
f_c=63.6 Hz
10
1
0.1
0.01
0.001
0.0001
pA²s
1
10
100
1000
Frequency (Hz)

Figure 3.3.2

The effect of increasing concentrations of methoxyflurane on the distribution of the open times of nAChR channels activated by 1-2μM CCh in the whole cell recording configuration. Each panel shows combined data for 5-11 cells (control: 11 cells and 4116 openings; 100μM MF: 9 cells, 3302 events; 250μM MF: 8 cells, 1953 events; 500μM MF: 5 cells, 1383 events). Holding potential was -100mV throughout and glutamate recording solution was used. The smooth curves are the calculated double exponential functions fitted to the frequency distribution. The parameters of the curve fits are given in table 3.3.1.

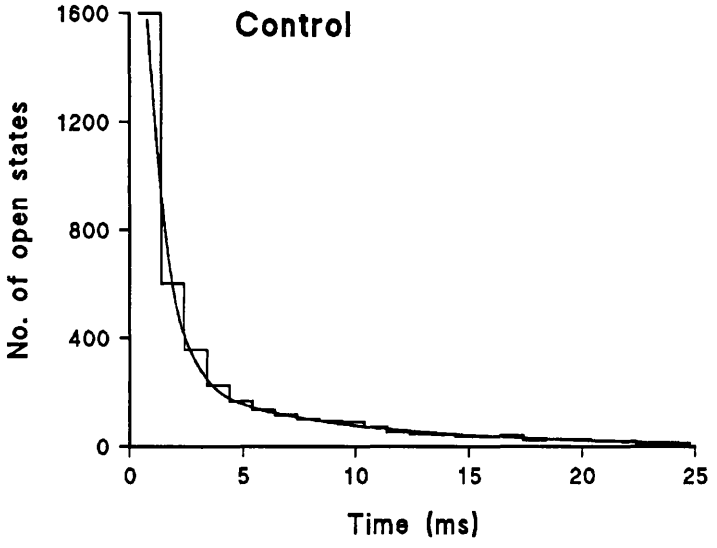
Control
No. of open states
1600
1200
800
400
0
0
5
10
15
20
25
Time (ms)

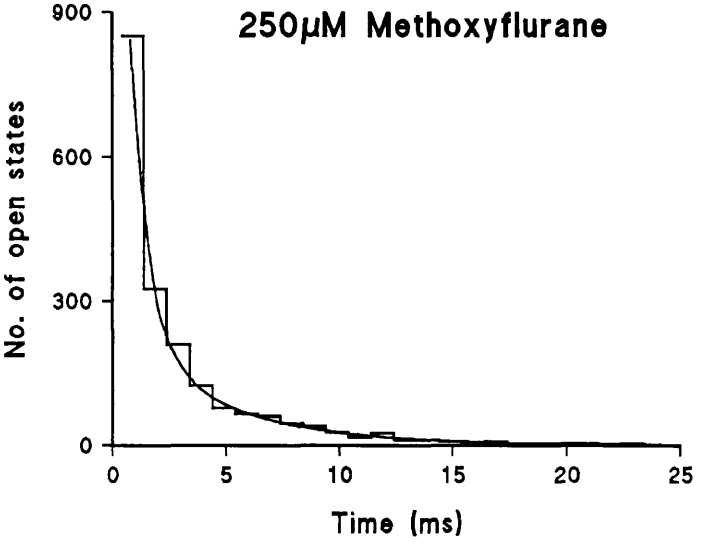
250μM Methoxyflurane
No. of open states
900
600
300
0
0
5
10
15
20
25
Time (ms)

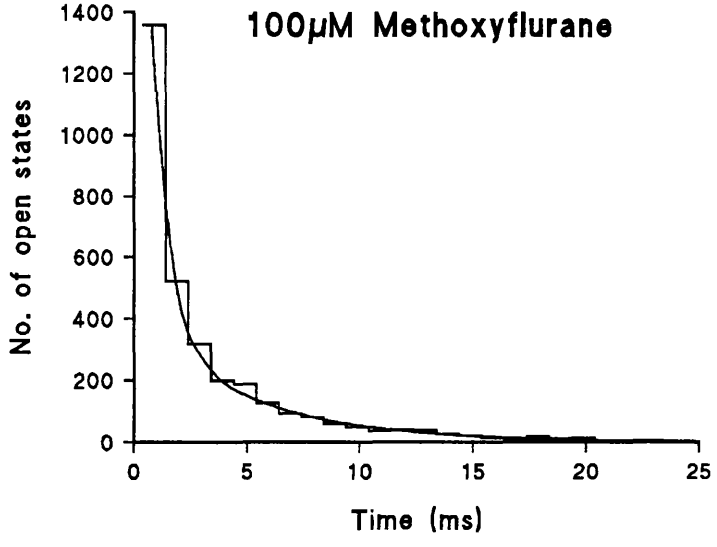
100μM Methoxyflurane
No. of open states
1400
1200
1000
800
600
400
200
0
0
5
10
15
20
25
Time (ms)

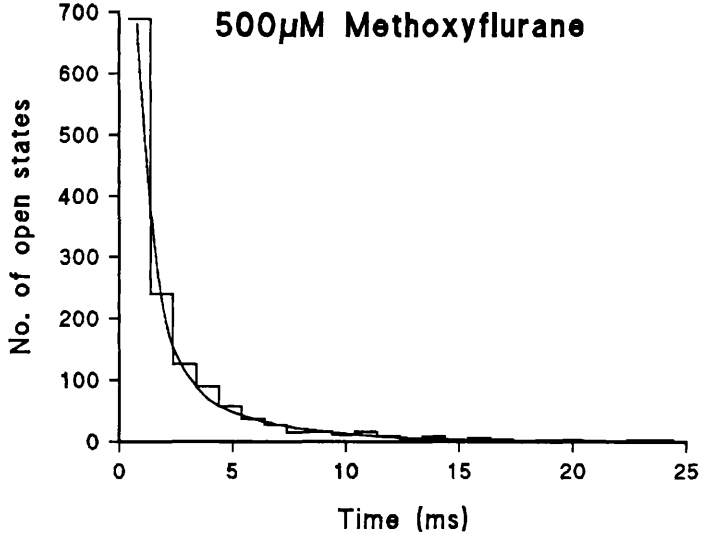
500μM Methoxyflurane
No. of open states
700
600
500
400
300
200
100
0
0
5
10
15
20
25
Time (ms)

Figure 3.3.3

Summary of the effects of methoxyflurane on the single channel properties of nAChR. Data from small whole cell experiments. The effect of 100-500μM methoxyflurane on mean burst length and mean open time (top panel), and burst frequency and open probability (lower panel). Values were first calculated for individual cells and these values were then averaged to give the plotted data points. Error bars represent the standard error of the mean. Number of cells are shown next to the data points in the top panel.
* denotes statistical significance at the 95% confidence level.

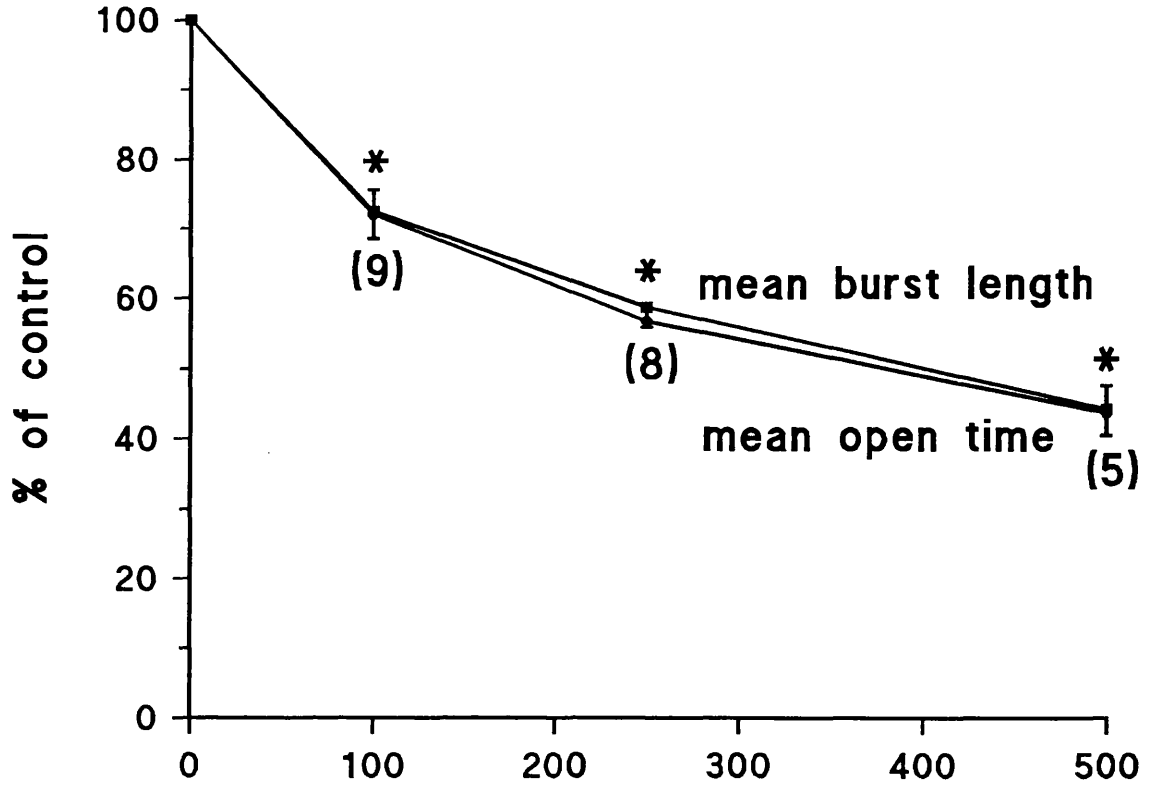
100
80
60
40
20
0
% of control
*
(9)
*
(8)
*
(5)
mean burst length
mean open time
0
100
200
300
400
500

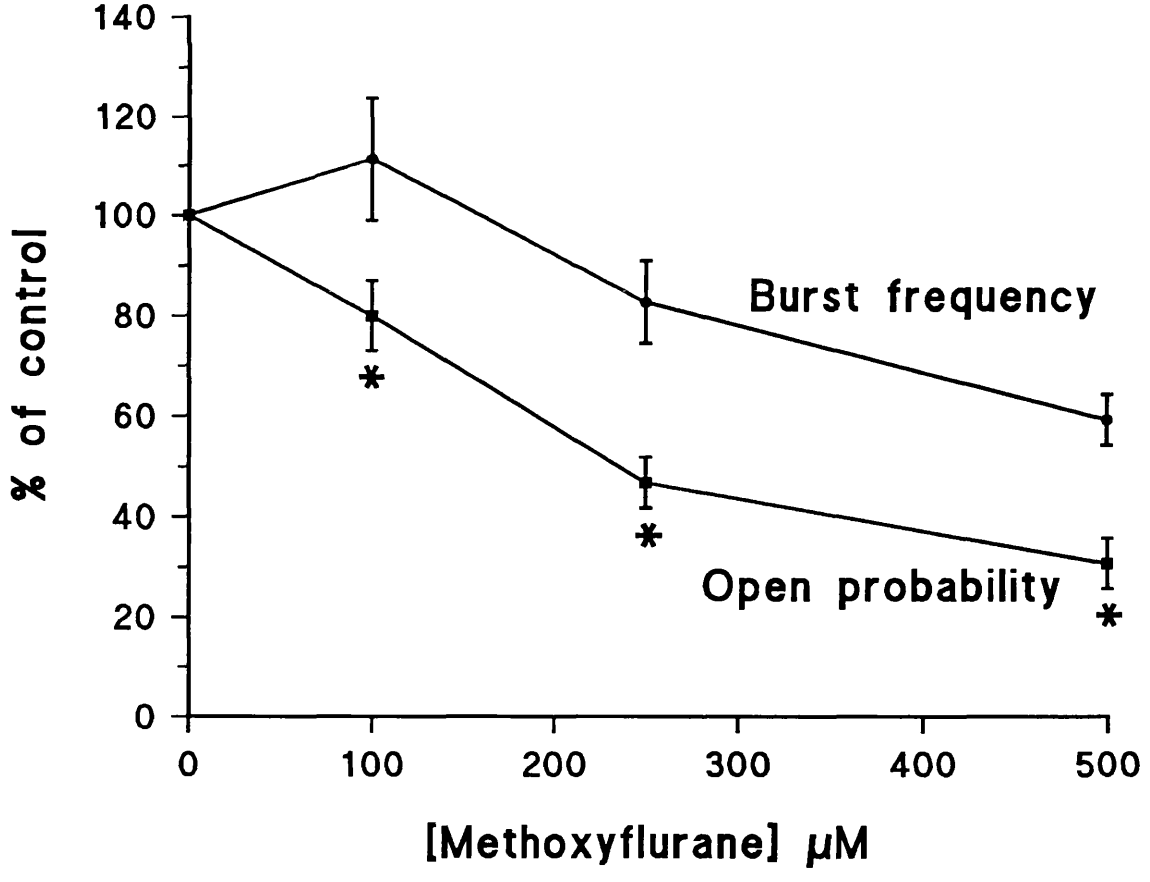
140
120
100
80
60
40
20
0
% of control
Burst frequency
*
*
Open probability
*
0
100
200
300
400
500
[Methoxyflurane] μM

3.4 Modulation of nAChR by Methohexitone

3.4a Currents activated by methohexitone alone

Methohexitone (50 μM) was found to evoke an inward current in whole cell recordings in which chloride internal recording medium was used (E_{Cl}=-1mV, see methods). The magnitude of this current was highly variable but was substantial in a few cells. Barbiturates have been reported to activate $GABA_A$ receptor gated chloride channels directly (see Jacobson et al 1991, Peters et al 1988). It seemed likely therefore that the inward current observed in response to methohexitone was due to an outward movement of chloride ions through $GABA_A$ channels. This was supported by the finding that 10 μM bicuculline largely blocked the current evoked by 50 μM methohexitone in a cell which showed a strong response to methohexitone alone. Application of 10 μM GABA to the same cell elicited a current of similar magnitude to that evoked by 50 μM methohexitone. Histograms of current amplitudes did not reveal any clear peaks suggesting a variety of channel conductances.

In order to avoid the possibility of nicotinic currents being contaminated by chloride currents activated by methohexitone, an internal recording solution in which glutamate replaced 96% of chloride was used for all experiments examining the effect of methohexitone on the nAChR channel. This recording medium established an E_{Cl} of -86 mV relative to Locke's solution externally (see methods). Thus, at holding potentials of -80 or -100 mV used in these experiments any chloride conductance activated would be of very low amplitude.(The largest reported $GABA_A$ chloride channel conductance (45 pS, Bormann & Clapham 1985) would give rise to + 0.27 pA amplitude openings at -80mV and -0.63 pA openings at -100mV.)

3.4b Noise Analysis

The effect of methohexitone (20-100 μM) on whole cell current noise evoked by 25 μM CCh was studied in three cells. Power spectra were calculated from 30 s stretches of steady-state current evoked by sequential application of carbachol alone or carbachol plus methohexitone (20,50 or 100 μM), followed by a further application of CCh alone. Spectra obtained under all conditions were well fitted by a single Lorentzian function. The corner frequency of the fitted curve increased with increasing methohexitone concentration. At -80 mV holding potential the corner frequencies and corresponding time constants of channel closure were: control 20.3 ± 4.5 Hz (τ=7.8ms); 20 μM methohexitone 31.0 ± 6.4 Hz (τ=5.1 ms); 50 μM methohexitone 46.6 ± 7.0 Hz (τ=3.4ms); 100 μM methohexitone 77.7 ± 12.0 Hz (τ=2.0ms); recovery after application of all three methohexitone concentrations 18.3 ± 5.5 Hz (τ=8.7ms). The open state lifetime of the channel is thus reduced in a dose dependent and reversible manner by methohexitone, as was the mean inward current. This was 4.43 ± 1.3 pA in control falling to 2.67 ± 0.64 pA, 1.66 ± 0.54 pA and 0.84 ± 0.41 pA in the presence of 20, 50 and 100 μM methohexitone respectively. Mean inward current recovered to 2.95 ± 0.99 pA after washing. Examples of power spectra calculated for a single cell under each recording condition are shown in fig. 3.4.1.

Methohexitone did not significantly alter the single channel conductance calculated from the parameters of the Lorentzian curves.

3.4c Single channel studies

Currents amenable to single channel analysis were obtained from whole cell recordings of small chromaffin cells (4.1-5.7 pF), as described previously. All recordings were made with glutamate recording solution (see above and methods). At the holding potentials used for these experiments (-80mV for 2

cells and -100 mV for 9 cells) there was no detectable resting channel activity. Under these conditions, methohexitone alone did not elicit resolvable channel activity.

A similar protocol was used for these experiments as described previously. Cells were sequentially perfused with carbachol (2 μM throughout these experiments), or carbachol plus 10, 20 ,50 or 100 μM methohexitone. Records were filtered at 1 KHz and digitised at 5 Khz prior to analysis.

At increasing concentrations of methohexitone individual channel openings became progressively shorter. Open state duration frequency histograms show a corresponding leftward shift with increasing methohexitone concentration. This is shown in fig. 3.4.2.

An increasing number of brief closures within channel openings were also observed, although the majority of openings were uninterrupted under all recording conditions. Burst analysis, performed using a fixed t_{crit} of 10 ms, confirmed that a small but significant* rise in the number of brief channel closures was induced in a dose dependent manner by methohexitone (see table 3.4.1 and fig. 3.4.3). Fig. 3.4.4 shows that both burst length and open time, expressed as a percentage of control, differ significantly in the presence of methohexitone.

In summary, the action of methohexitone on nicotinic receptor channels of bovine chromaffin cells is as follows:

1) Mean open time is reduced progressively by increasing methohexitone concentration. The IC_{50} for this effect is ~40 μM.

---

* $p<0.025$ for all concentrations of methohexitone.

2) Mean burst length is significantly higher than mean open time in the presence of methohexitone and falls less steeply as a function of methohexitone concentration. The IC_{50} for burst length reduction is >100 μM.

3) The frequency of channel activations (bursts) increases, being almost double the control value at 100 μM methohexitone.

4) Open probability has a relatively weak dependence on methohexitone concentration, as a result of the opposing influences of effects 1 & 3. The mean inward current evoked by 25 μM CCh is however reduced with an IC_{50} of about 30 μM. This may suggest that the action of methohexitone is dependent on the agonist concentration.

Table 3.4.1

Modulation by methohexitone of the kinetic constants of nAChR channel openings evoked by 2 μM CCh in small whole cells.

Errors shown are standard error of the mean or, for curve fit parameters, the 95 % confidence limits.

Table 3.4.1

Methohexitone modulation of the kinetic constants of nAChR channel openings evoked by 2 μM CCh in small whole cells .

	Control	10 μM methohexitone	20 μM methohexitone	50 μM methohexitone
Open state				
τ_f (ms)	1.06 ± 0.11	0.90 ± 0.18	0.54 ± 0.23	1.20 ± 0.28
τ_s (ms)	10.06 ± 0.81	6.09 ± 0.59	4.13 ± 0.29	2.97 ± 0.37
$Area_f/Area_s$	1.41	0.82	0.49	0.93
mean open time (ms)	6.02 ± 0.33	4.29 ± 0.28	3.55 ± 0.16	2.32 ± 0.11
P_{open} (%)	2.89 ± 0.44	3.34 ± 0.73	3.58 ± 0.90	2.43 ± 0.58
F_{open} (Hz)	4.78 ± 0.63	7.54 ± 1.30	9.60 ± 2.15	10.25 ± 2.22
Closed State				
τ_f (ms)	0.71 ± 0.30	1.81 ± 0.41	2.45 ± 0.39	1.80 ± 0.19
τ_s (ms)	191.4 ± 66.4	84.81 ± 19.7	57.05 ± 8.47	51.93 ± 4.51
$Area_f/Area_s$	0.028	0.106	0.171	0.151
Burst parameters				
τ_f (ms)	1.03 ± .12	0.89 ± 0.17	0.89 ± 0.18	1.15 ± 0.15
τ_s (ms)	10.58 ± 1.03	8.22 ± 0.79	7.49 ± 0.65	6.10 ± 0.52
$Area_f/Area_s$	1.19	0.88	0.76	1.09
Mean burst length (ms)	6.78 ± 0.38	5.74 ± 0.46	5.43 ± 0.49	3.82 ± 0.31
gaps/burst	0.08 ± 0.01	0.17 ± 0.02	0.25 ± 0.04	0.25 ± 0.03
blocked time (ms)	3.52 ± 0.26	3.82 ± 0.18	3.79 ± 0.09	3.37 ± 0.11

Figure 3.4.1

Spectral analysis of current noise evoked by 25 μM CCh alone (top left), and in the presence of 20 μM (top right), 50 μM (bottom left) and 100 μM (bottom right) methohexitone. The corner frequency increases and Y-axis intercept decreases with rising methohexitone concentration. Holding potential -80 mV. All data from a single chromaffin cell. Corner frequencies for this cell correspond to time constants of 8.7 ms (control), 5.5 ms (20μM MH), 3.4 ms (50μM MH) and 2.0 ms (100μM MH).

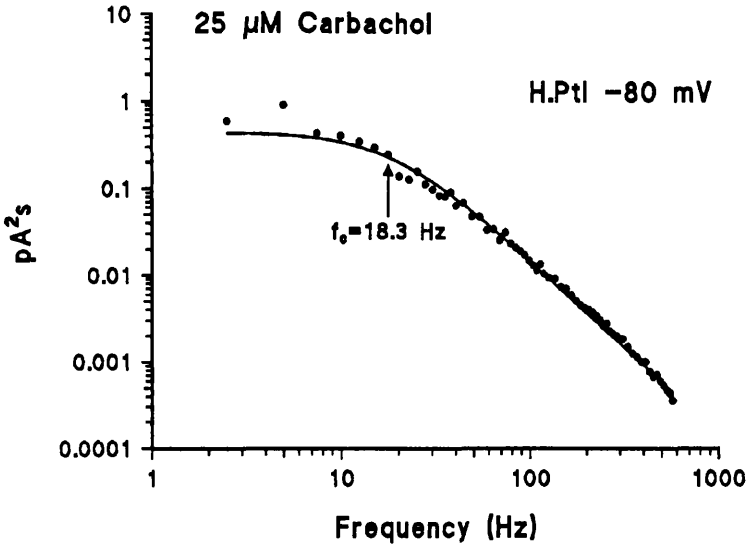
25 μM Carbachol
H.Ptl −80 mV
f_c=18.3 Hz
pA²s
Frequency (Hz)
10
1
0.1
0.01
0.001
0.0001
1
10
100
1000

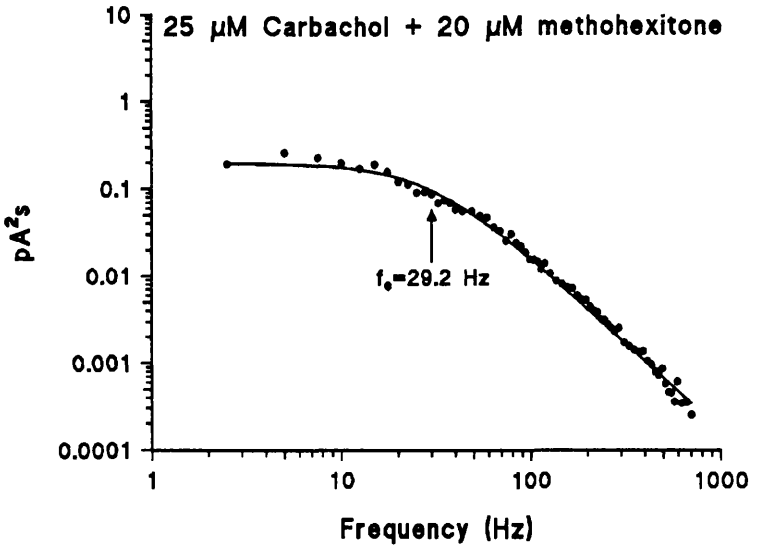
25 μM Carbachol + 20 μM methohexitone
f_c=29.2 Hz
pA²s
Frequency (Hz)
10
1
0.1
0.01
0.001
0.0001
1
10
100
1000

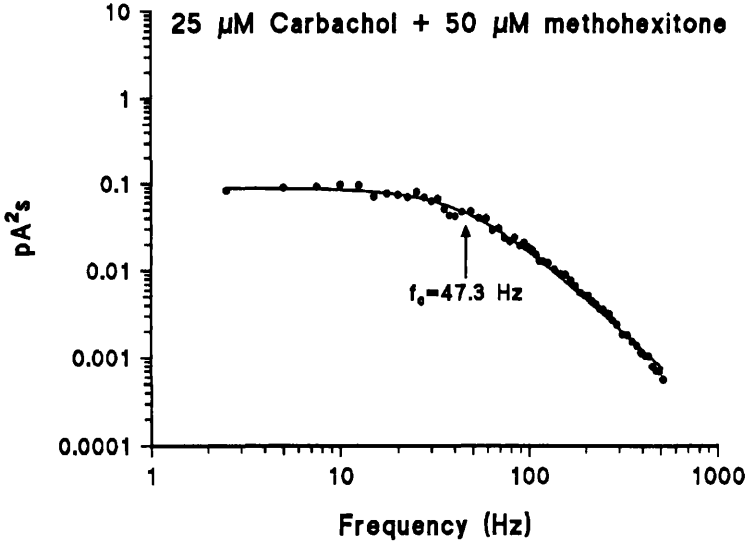
25 μM Carbachol + 50 μM methohexitone
f_c=47.3 Hz
pA²s
Frequency (Hz)
10
1
0.1
0.01
0.001
0.0001
1
10
100
1000

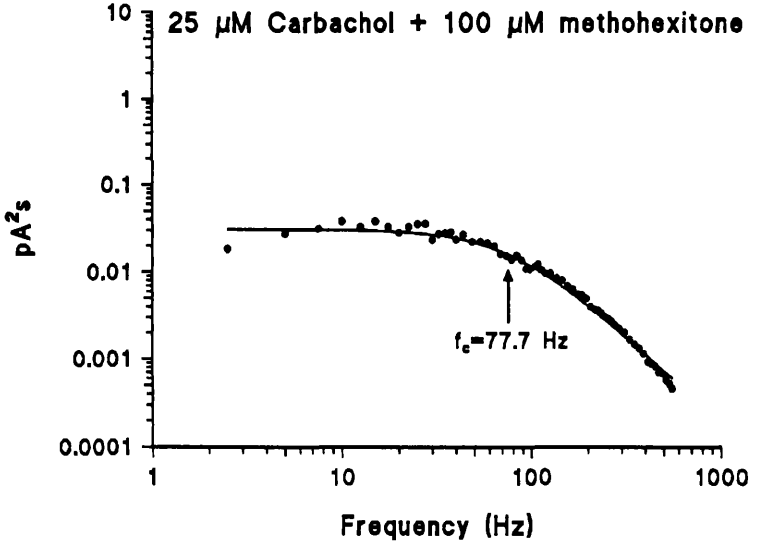
25 μM Carbachol + 100 μM methohexitone
f_c=77.7 Hz
pA²s
Frequency (Hz)
10
1
0.1
0.01
0.001
0.0001
1
10
100
1000

Figure 3.4.2

The effect of increasing concentrations of methohexitone on the distribution of the open times of nAChR channels activated by 2μM CCh in the whole cell recording configuration. Each panel shows combined data for 3-8 cells (control: 8 cells and 3440 openings; 10 μM MH: 3 cells, 2171 openings; 20 μM MH: 6 cells, 3606 openings; 50 μM MH: 7 cells, 4244 openings). Holding potential was -100mV throughout and glutamate recording solution was used. The smooth curves are the calculated double exponential functions fitted to the frequency distribution. The parameters of the curve fits are given in table 3.4.1.

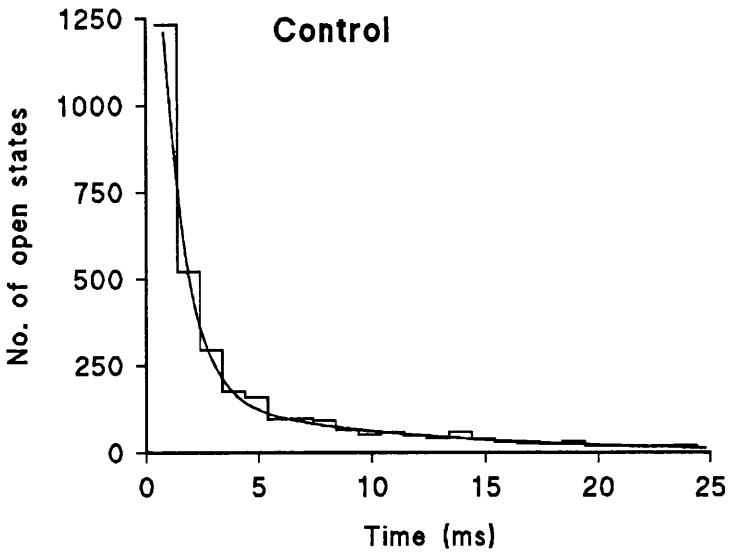
Control
No. of open states
1250
1000
750
500
250
0
0
5
10
15
20
25
Time (ms)

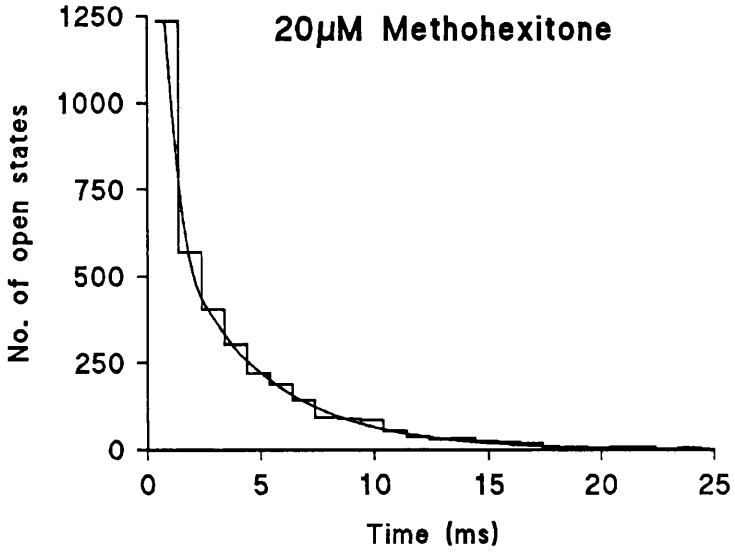
20μM Methohexitone
No. of open states
1250
1000
750
500
250
0
0
5
10
15
20
25
Time (ms)

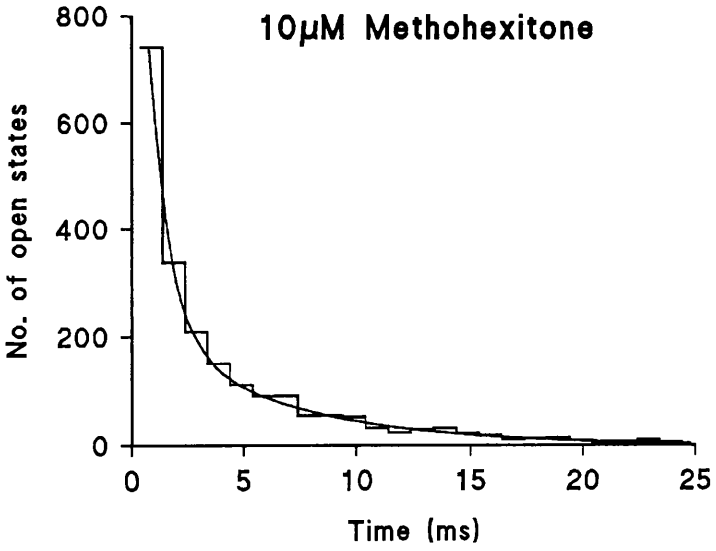
10μM Methohexitone
No. of open states
800
600
400
200
0
0
5
10
15
20
25
Time (ms)

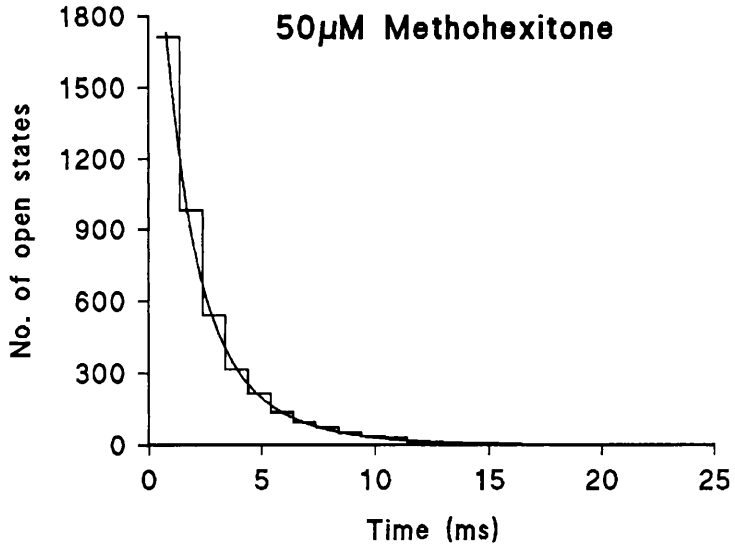
50μM Methohexitone
No. of open states
1800
1500
1200
900
600
300
0
0
5
10
15
20
25
Time (ms)

Figure 3.4.3

The effect of 50 μM methohexitone on the frequency distribution of closed times (left-hand panels) and of burst lengths (right-hand panels) compared to control (upper panels). The smooth curves are the calculated double exponential functions fitted to the frequency distributions. Parameters of the fitted curves are shown in table 3.4.1.

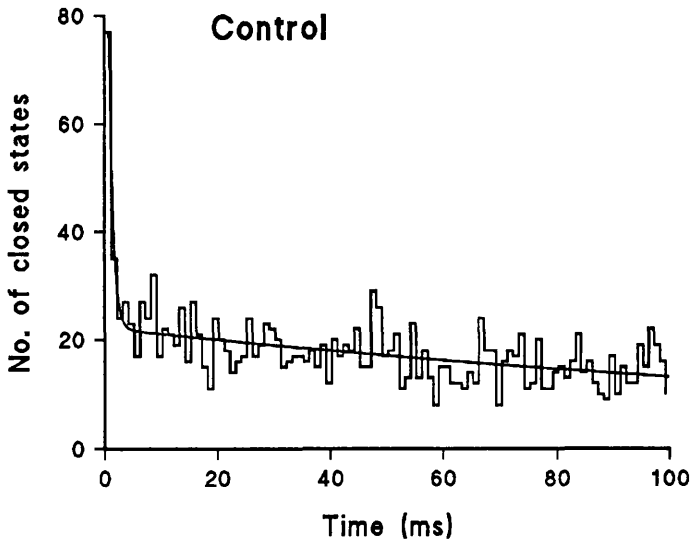
Control
No. of closed states
Time (ms)
0
20
40
60
80
100

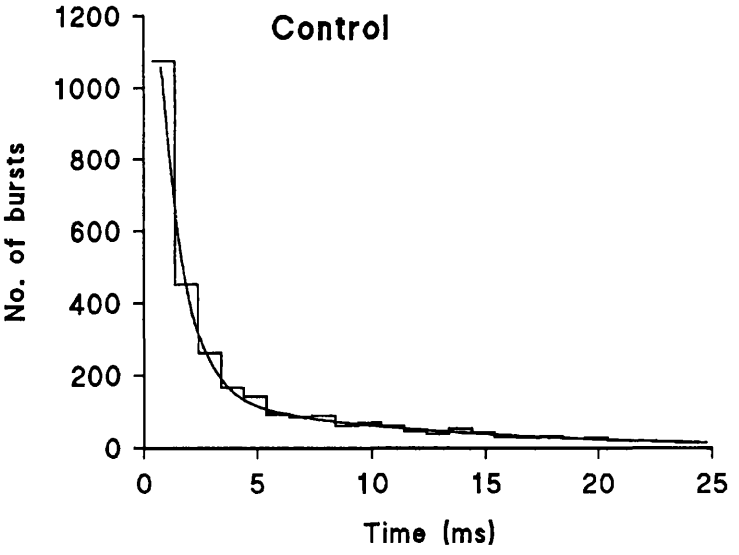
Control
No. of bursts
Time (ms)
0
200
400
600
800
1000
1200
0
5
10
15
20
25

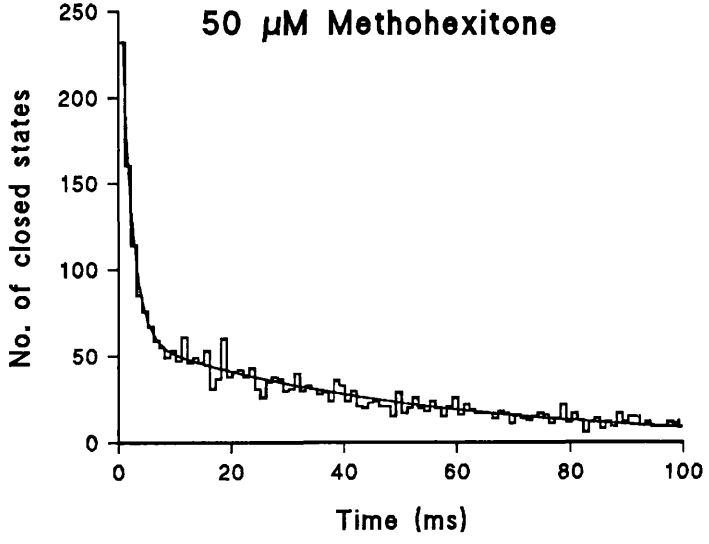
50 μM Methohexitone
No. of closed states
Time (ms)
0
50
100
150
200
250
0
20
40
60
80
100

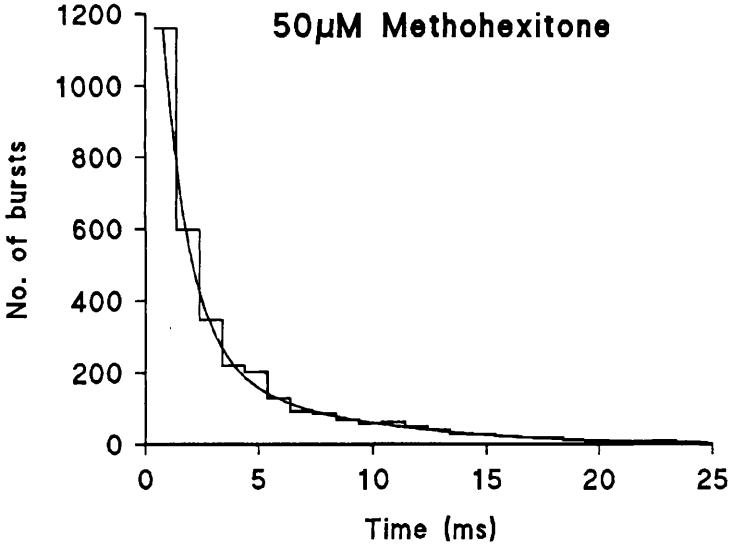
50μM Methohexitone
No. of bursts
Time (ms)
0
200
400
600
800
1000
1200
0
5
10
15
20
25

Figure 3.4.4

Summary of the effects of methohexitone on the single channel properties of nAChR. The effect of 10-100μM methohexitone on mean burst length and mean open time (top panel), and burst frequency and open probability (lower panel). Values were calculated as described previously (see fig 3.3.3). Error bars represent the standard error of the mean. Number of cells are shown next to the data points in the top panel. * denotes statistical significance at the 95% confidence level.

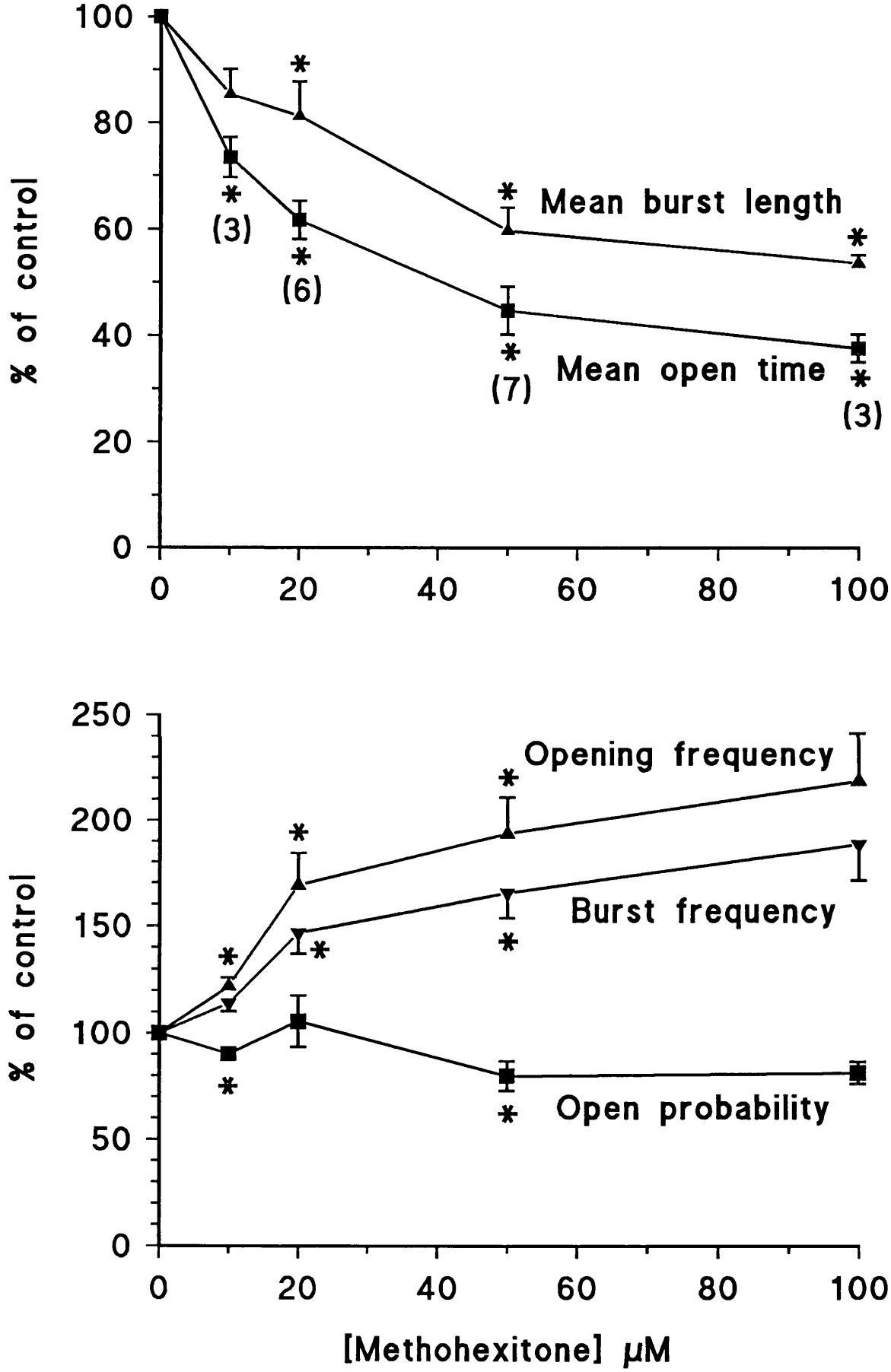
100
80
60
40
20
0
% of control
0
20
40
60
80
100
Mean burst length
Mean open time
(3)
(6)
(7)
(3)
250
200
150
100
50
0
% of control
Opening frequency
Burst frequency
Open probability
[Methohexitone] μM

3.5 Modulation of nAChR by Etomidate

3.5a Noise Analysis

The effect of etomidate on whole cell current noise evoked by 25 μM CCh was studied in three cells. Currents were recorded in the presence of carbachol or carbachol plus etomidate (10-50 μM) and background-subtracted power spectra calculated as before. All spectra obtained were well fitted by a single Lorentzian function, the corner frequency of which increased with increasing etomidate concentration. At -80 mV holding potential the values of f_c and corresponding τ for channel closure were: control, 20.3 ± 2.7 Hz (τ=7.8 ms); 10 μM etomidate, 31.4 ± 6.0 Hz (τ=5.1 ms); 25 μM etomidate, 40.1 ± 2.8 Hz (τ=4.0ms); 50 μM etomidate 42.7 ± 5.2 Hz (τ=3.7ms). Mean inward current also fell with rising etomidate concentration: 2.91 ± 0.59 pA (control), 2.92 ± 0.34 pA (10 μM etomidate), 1.83 ± 0.10 pA (25μM etomidate), 1.30 ± 0.07 pA (50 μM etomidate) and 1.51 ± 0.35 pA (recovery). Fig. 3.5.1 shows examples of power spectra calculated for each condition for a single cell.

Etomidate did not significantly change the calculated single channel conductance (33.6 pS in control, 32.9 pS at 50 μM etomidate).

3.5b Single Channel Studies

Records suitable for single channel analysis were obtained from whole cell recordings of small cells, as previously described. Glutamate recording solution was used to avoid contamination by etomidate activated chloride currents. nAChR channel openings were evoked by 1 μM CCh, and records were filtered at 1 KHz and digitised at 5 KHz prior to analysis as before.

The duration of individual channel openings was reduced in a dose dependent manner by etomidate (10-50 μM). Figure 3.5.2 shows this as a progressive leftward shift in the channel open time frequency distribution with increasing etomidate concentration. The distributions were fitted with a double exponential function, except that for 50 μM etomidate which was fitted with a single exponential.

The reduction in channel open lifetime with increasing etomidate concentration is accompanied by a modest, but significant*, rise in the number of brief channel closures. As a result, burst length (defined with a t_{crit} of 10 ms) falls less steeply than open time as a function of etomidate concentration (see figure 3.5.3 and table 3.5.1).

Table 3.5.1 and figure 3.5.4 describe the main features of the single channel analysis with this agent.

In summary the action of etomidate on the nAChR is as follows:

1) Etomidate causes a concentration dependent reduction in mean open time with IC_{50} 25 μM.

2) Mean burst length also falls with increasing etomidate concentration (IC_{50} 50 μM) , but at each concentration > 10 μM it is higher than mean open time.

3) Burst frequency rises initially and then falls with increasing etomidate concentration, although at 50 μM etomidate it is still higher than in control.

4) Open probability is reduced, after a small rise at low (10 μM) etomidate concentration. IC_{50} 50 μM.

---

* $p<0.025$ for all concentrations of etomidate.

Table 3.5.1

Modulation by etomidate of the kinetic constants of nAChR channel openings evoked by 1 μM CCh in small whole cells.

Errors shown are standard error of the mean or, for curve fit parameters, the 95 % confidence limits.

Table 3.5.1

Etomidate modulation of the kinetic constants of nAChR channel openings evoked by 1 μM CCh in small whole cells .

	Control	10 μM Etomidate	25 μM Etomidate	50 μM Etomidate
Open state	(6)	(5)	(5)	(4)
τ_f (ms)	1.23 ± 0.20	0.97 ± 0.30	0.94 ± 0.34	----
τ_s (ms)	8.70 ± 0.82	5.67 ± 0.65	3.56 ± 0.47	2.03 ± 0.16
$Area_f/Area_s$	0.86	0.63	0.63	----
mean open time (ms)	6.44 ± 0.58	4.44 ± 0.22	2.92 ± 0.11	2.16 ± 0.11
P_{open} (%)	1.41 ± 0.36	1.33 ± 0.43	0.96 ± 0.20	0.37 ± 0.12
F_{open} (Hz)	2.33 ± 0.60	2.92 ± 0.89	3.29 ± 0.66	3.61 ± 1.43
Closed State				
τ_f (ms)	0.62 ± 0.11	1.54 ± 0.14	1.55 ± 0.10	1.38 ± 0.14
τ_s (ms)	130.1 ± 55.8	48.66 ± 15.8	67.42 ± 21.9	38.77 ± 10.4
$Area_f/Area_s$	0.183	0.708	0.697	0.632
Burst parameters				
τ_f (ms)	1.17 ± 0.19	1.24 ± 0.20	0.96 ± 0.26	1.29 ± 0.26
τ_s (ms)	9.59 ± 0.95	9.58 ± 1.00	5.75 ± 0.76	5.84 ± 0.92
$Area_f/Area_s$	0.87	1.03	0.89	1.25
Mean burst length (ms)	7.32 ± 0.70	6.30 ± 0.37	4.53 ± 0.23	3.48 ± 0.36
gaps/burst	0.10 ± 0.02	0.26 ± 0.02	0.30 ± 0.03	0.28 ± 0.05
blocked time (ms)	1.79 ± 0.26	2.37 ± 0.15	2.35 ± 0.08	2.37 ± 0.16

Figure 3.5.1

Spectral analysis of current noise evoked by 25 μM CCh alone (top left), and in the presence of 10 μM (top right), 25 μM (bottom left) and 50 μM (bottom right) etomidate. The corner frequency increases and Y-axis intercept decreases with rising etomidate concentration. Holding potential -80 mV. All data from a single chromaffin cell. Corner frequencies for this cell correspond to time constants of 8.0 ms (control), 6.3 ms (10 μM etomidate), 4.3 ms (25 μM etomidate) and 3.4 ms (50 μM etomidate).

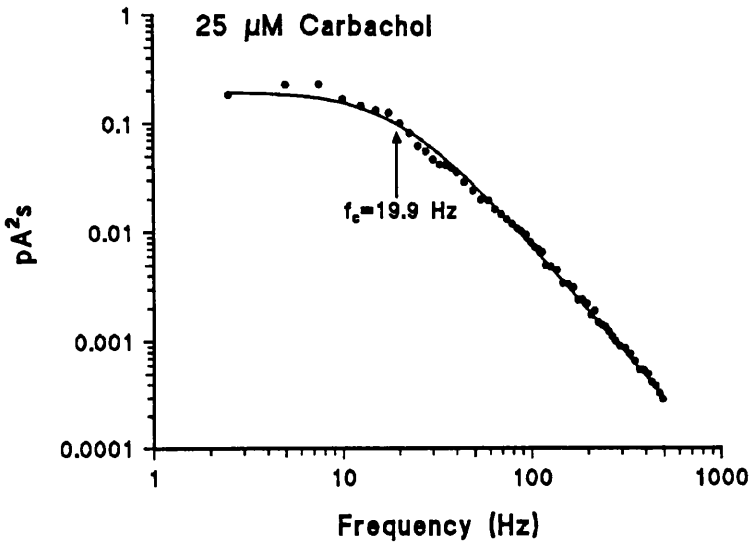
25 μM Carbachol
f_c=19.9 Hz
pA²s
Frequency (Hz)
1
0.1
0.01
0.001
0.0001
1
10
100
1000

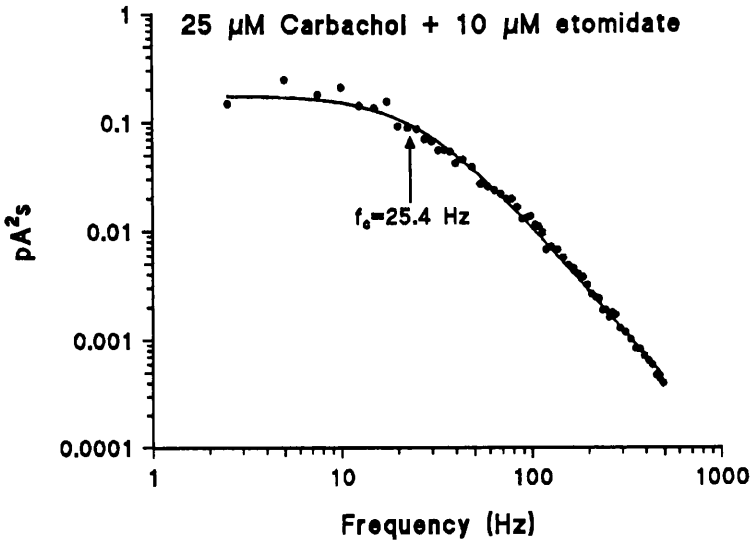
25 μM Carbachol + 10 μM etomidate
f_c=25.4 Hz
pA²s
Frequency (Hz)
1
0.1
0.01
0.001
0.0001
1
10
100
1000

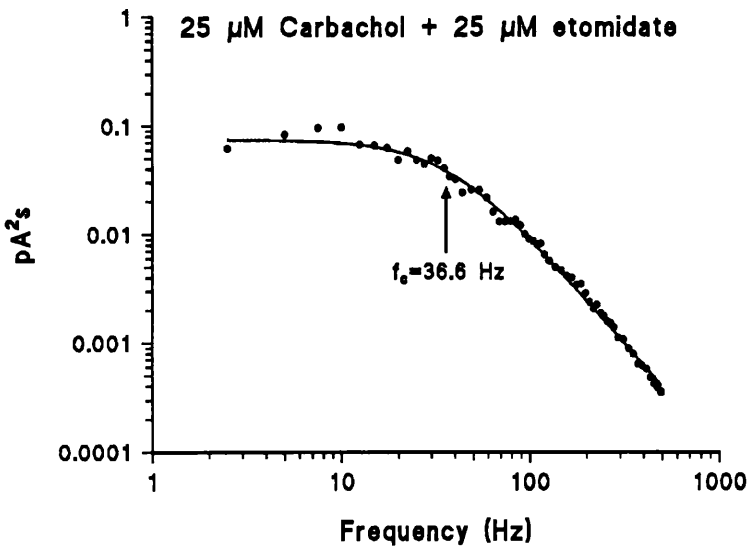
25 μM Carbachol + 25 μM etomidate
f_c=36.6 Hz
pA²s
Frequency (Hz)
1
0.1
0.01
0.001
0.0001
1
10
100
1000

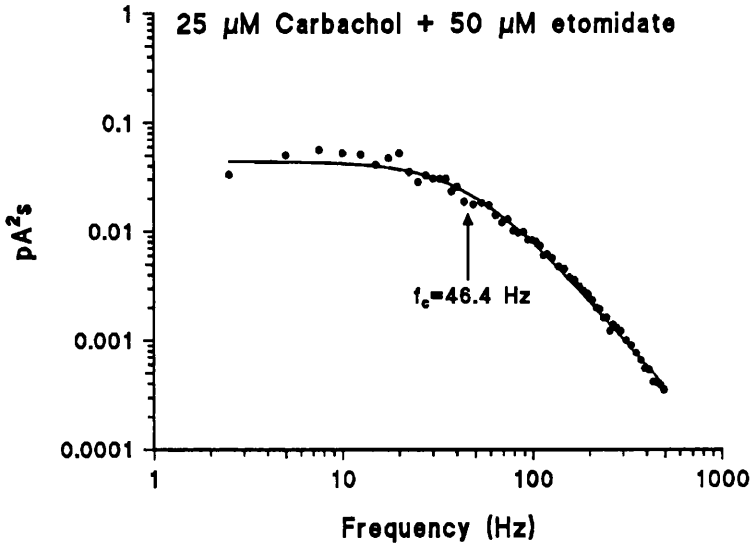
25 μM Carbachol + 50 μM etomidate
f_c=46.4 Hz
pA²s
Frequency (Hz)
1
0.1
0.01
0.001
0.0001
1
10
100
1000

Figure 3.5.2

The effect of increasing concentrations of etomidate on the distribution of the open times of nAChR channels activated by 1 μM CCh in the whole cell recording configuration. Each panel shows combined data for 4-7 cells (control: 7 cells and 1809 openings; 10 μM etomidate: 5 cells, 1786 events; 25 μM etomidate: 5 cells, 1985 events; 50 μM etomidate: 4 cells, 1126 events). Holding potential was -100mV throughout and glutamate recording solution was used. The smooth curves are the calculated double exponential functions fitted to the frequency distribution. The parameters of the curve fits are given in table 3.5.1.

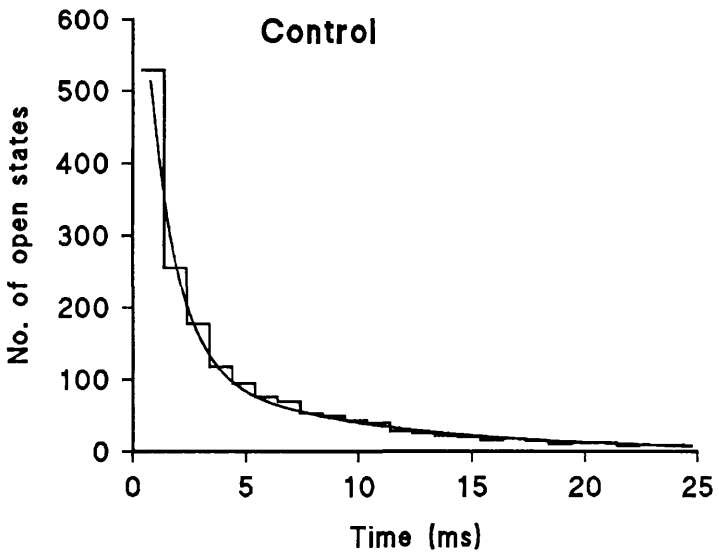
Control
No. of open states
Time (ms)
0
100
200
300
400
500
600
0
5
10
15
20
25

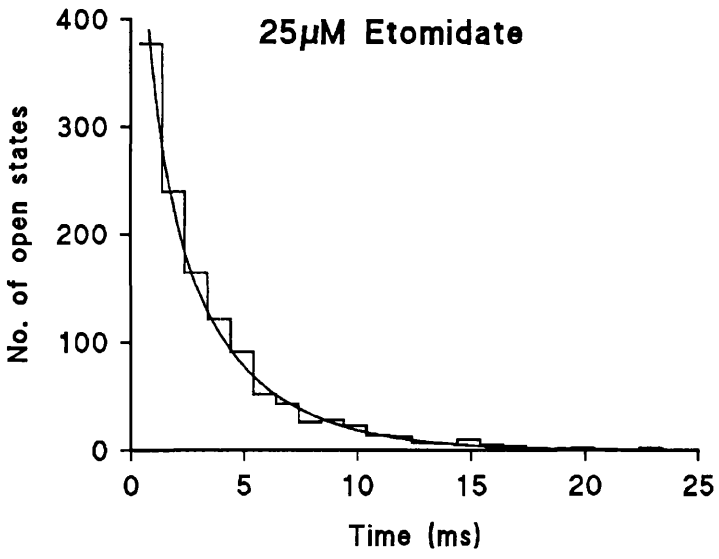
25μM Etomidate
No. of open states
Time (ms)
0
100
200
300
400
0
5
10
15
20
25

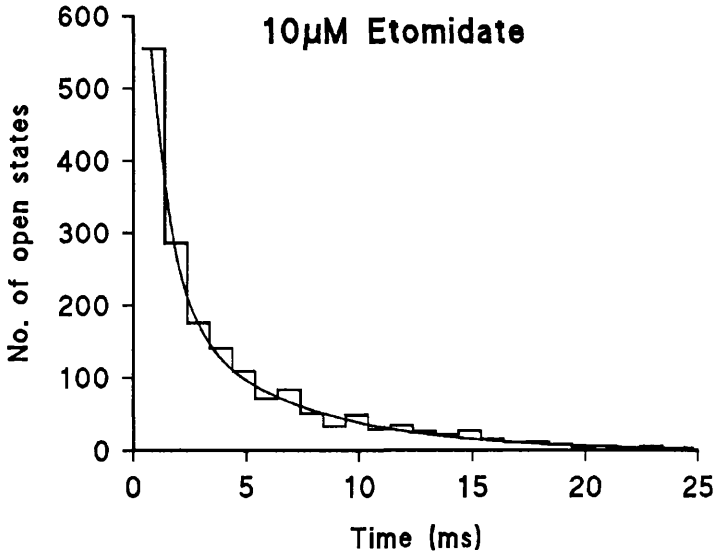
10μM Etomidate
No. of open states
Time (ms)
0
100
200
300
400
500
600
0
5
10
15
20
25

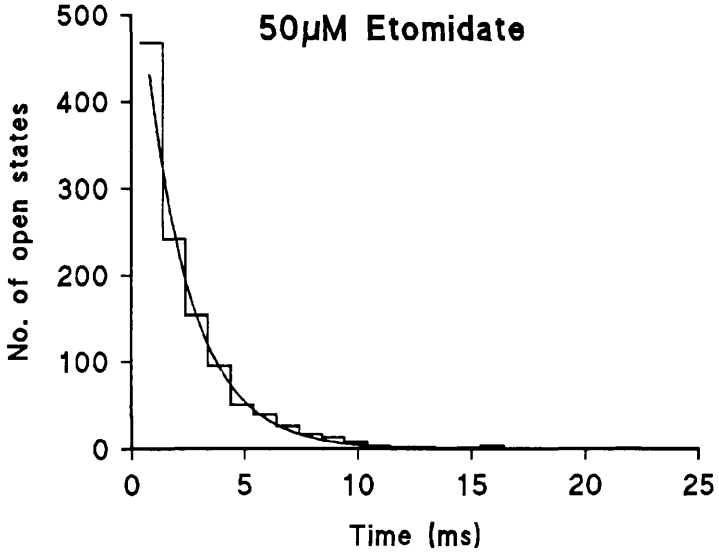
50μM Etomidate
No. of open states
Time (ms)
0
100
200
300
400
500
0
5
10
15
20
25

Figure 3.5.3

The effect of 50 μM etomidate on the frequency distribution of closed times (left-hand panels) and of burst lengths (right-hand panels) compared to control (upper panels). The smooth curves are the calculated double exponential functions fitted to the frequency distributions. Parameters of the fitted curves are shown in table 3.5.1.

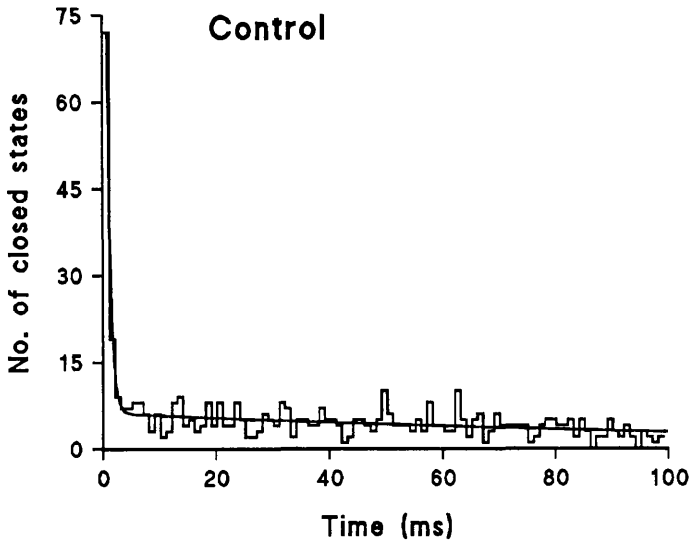
Control
No. of closed states
75
60
45
30
15
0
0
20
40
60
80
100
Time (ms)

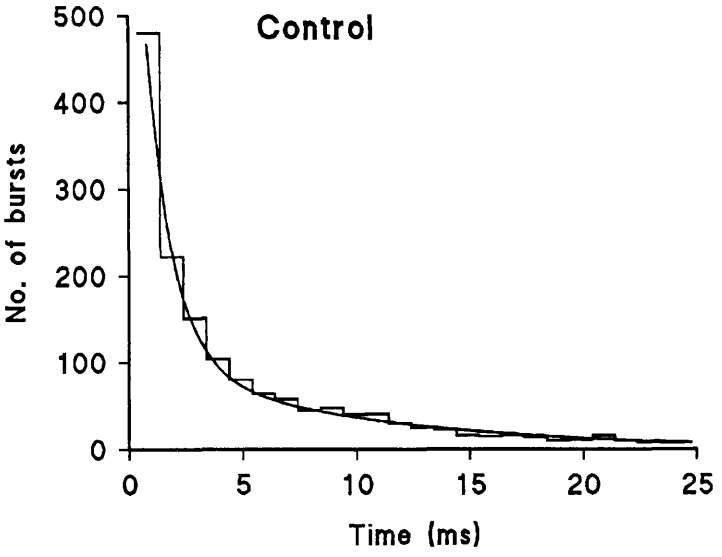
Control
No. of bursts
500
400
300
200
100
0
0
5
10
15
20
25
Time (ms)

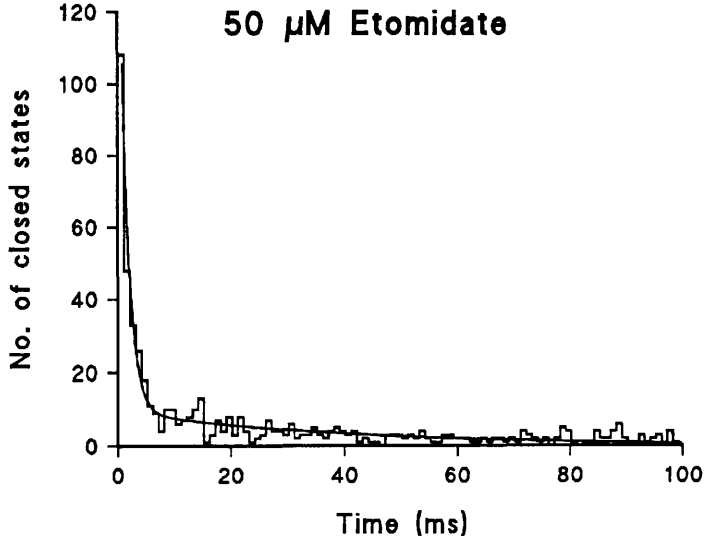
50 μM Etomidate
No. of closed states
120
100
80
60
40
20
0
0
20
40
60
80
100
Time (ms)

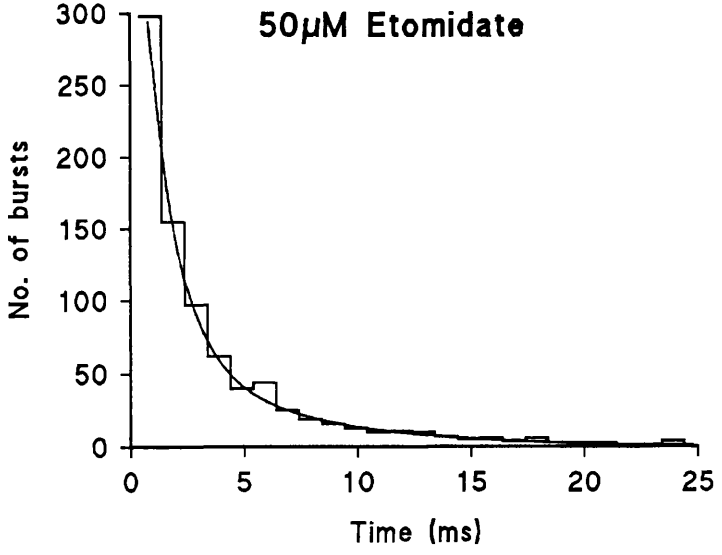
50μM Etomidate
No. of bursts
300
250
200
150
100
50
0
0
5
10
15
20
25
Time (ms)

Figure 3.5.4

Summary of the effects of etomidate on the single channel properties of nAChR. The effect of 10-50 μM etomidate on mean burst length and mean open time (top panel), and burst frequency and open probability (lower panel). Values were calculated as described previously (see fig 3.3.3). Error bars represent the standard error of the mean. Number of cells are shown next to the data points in the top panel.
* denotes statistical significance at the 95% confidence level.

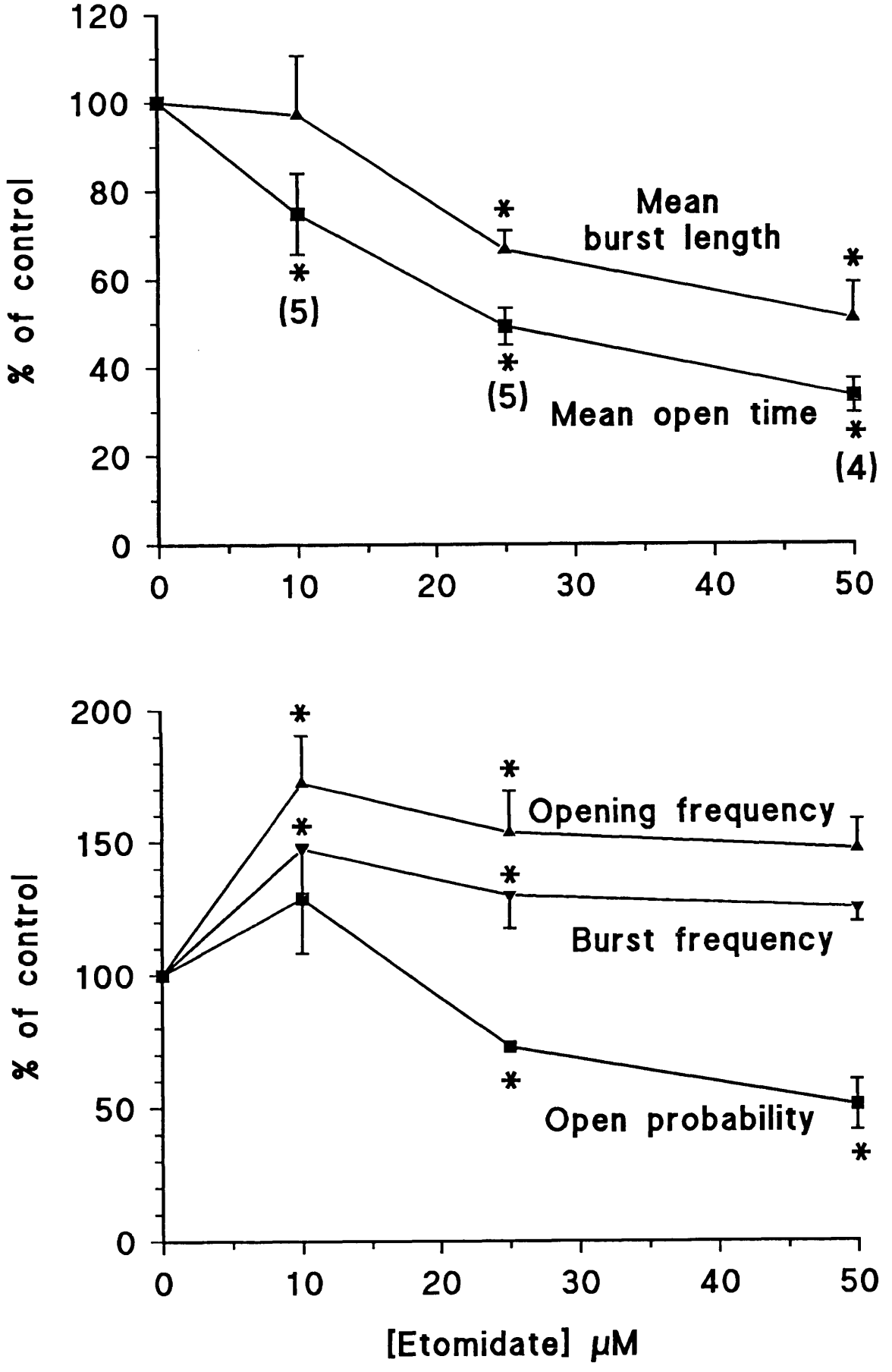
120
100
80
60
40
20
0
% of control
Mean
burst length
Mean open time
(5)
(5)
(4)
0
10
20
30
40
50
200
150
100
50
0
% of control
Opening frequency
Burst frequency
Open probability
0
10
20
30
40
50
[Etomidate] μM

3.6 Modelling of nAChR/Anaesthetic Interactions

In the introduction, sequential blocking models were reviewed which have provided (partially) successful explanations of the interaction of anaesthetics with nAChR. (Neher and Steinbach 1978, Dilger and Brett 1991b). These models make specific predictions for the dependence of various channel gating parameters on anaesthetic concentration, against which the data presented in the previous chapter may be tested. The predictions can be summarised as follows:

$$C \underset{\alpha}{\overset{\beta}{\rightleftharpoons}} O^* \underset{b}{\overset{f.c}{\rightleftharpoons}} O\text{-}B \; (\dashrightarrow C\text{-}B) \qquad \alpha'$$

(Definition of constants as in equations in section 1.3.)

Mean open time (i) $1/\alpha+f.c$

(ii) " "

Mean burst length (i) $(1+f.c/b)/\alpha$

(ii) $1+f.c.b/(b+\alpha')^2/(\alpha+f.c.\alpha'/(b+\alpha'))$

Mean blocked time (i) $1/b$

(ii) $1/b+\alpha'$

Open time per burst (i) $1/\alpha$

(ii) $1/\alpha+(f.c.\alpha'/(b+\alpha'))$

Equations are for (i) the simple sequential blocking model

(ii) the extended blocking model (Dilger & Brett 1991b) See appendix 1

Both models predict the same relationship between mean open time and concentration of anaesthetic, and the data for all four agents fitted this equation well with values of f, the forward blocking rate constant, shown in table 3.6.1. Figure 3.6.1 shows the linear relationship between inverse mean open time and the anaesthetic concentration seen for each agent.

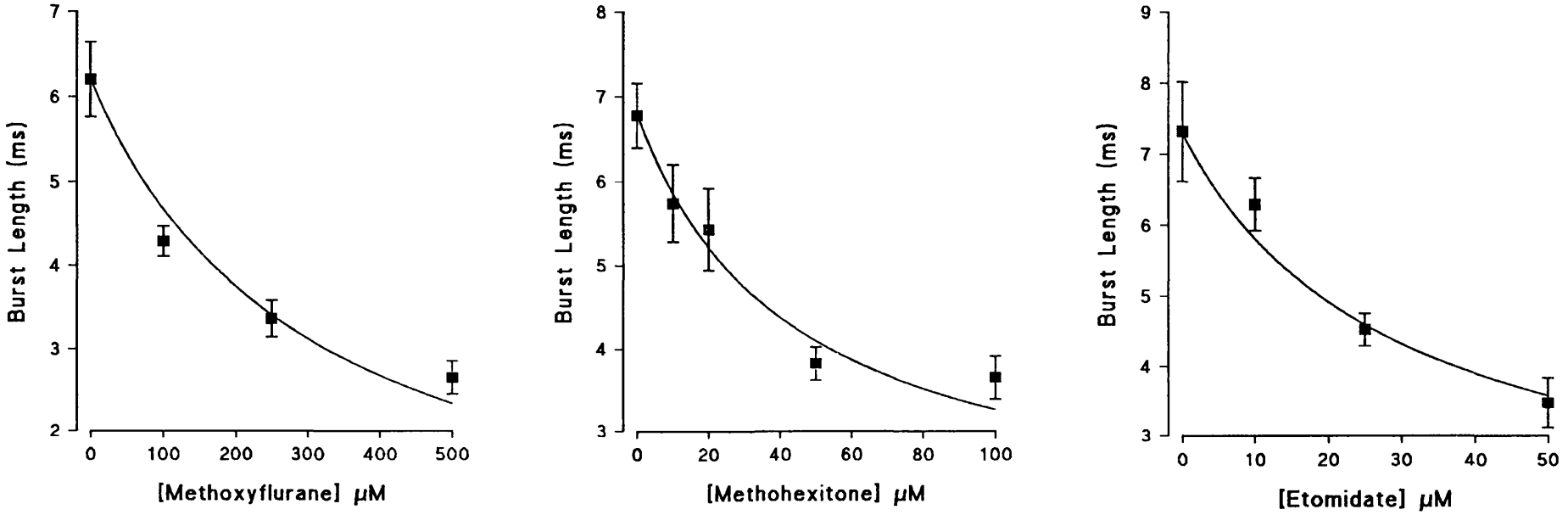

Figure 3.6.1a

The relationship between mean burst length and anaesthetic concentration for methoxyflurane, methohexitone and etomidate. In each case the solid line represents the curve fitted to the data points according to the equation predicted from the extended blocking model (see p.91).

It is clear that none of the agents tested will satisfy the prediction of the simple model that burst length rises with anaesthetic concentration. Data for mean burst length were therefore fitted to the equation derived from the extended model, according to which burst length may fall with rising concentration of anaesthetic due to the curtailment of bursts by entry into a long-lived closed state. A reasonable fit was obtained for each agent and the parameters yielded are shown in table 3.6.1. The curve fits are shown in fig.3.6.1a.

Table 3.6.1

Parameters of the extended channel blocking model

	f ($\mu M.s^{-1}$)	b (s^{-1})	α' (s^{-1})	b/α' --	b/f (μM)
Procaine	21.2	250	299	0.84	11.8
Methoxyflurane	0.51	40	331	0.12	77.6
Methohexitone	5.37	141	230	0.62	26.3
Etomidate	6.83	130	241	0.54	19.0

(Values for procaine calculated from data for 50μM. Values for others assume a mean blocked time ($=1/b + \alpha'$) of 2.69ms for all conditions. This was the mean value of the mean blocked time for all small whole cell experiments).

The rate of blocked channel closure (α') differs relatively little between agents, while b varies markedly. The value of b/α' determines the relative propensity of blocked channels either to re-open or to close and hence the degree to which individual activations of the channel appear as bursts i.e. the degree of 'flicker'. This correlates with the observed effect - the degree of flicker decreases in the order procaine $>$ methohexitone $\approx$ etomidate $>>$ methoxyflurane.

3.6a The analysis of bursts of openings

An inherent assumption underlying the analysis of bursts is that brief closures within bursts of openings form a single population distinct from closed periods between separate activations of receptor/channels. However, mean blocked time was found to rise with increasing procaine concentration, contrary to the predictions of both models outlined above. Therefore, in order to test the predictions of these models an approximation had to be made which was known to be invalid, namely that there was a *constant* closed time interval, below which closures were drug-induced blockages, and above which they reflected the resting channel state.

Given this complication, the procaine data were analysed using t_{crit} calculated in three ways.(i) The value appropriate for each patch was calculated, according to the criteria of Clapham & Neher (1984b); (ii) the average value for each procaine concentration was calculated from these values, and (iii) a fixed value was used for all conditions (as the models predict should be the case). Absolute values of mean burst length for each condition varied slightly with different t_{crit}, and the tendency for burst length to decrease with increasing procaine concentration remained. This was also true for the rise in mean blocked time, but in this case values varied more as different values of t_{crit} were used. For purposes of comparison, it was considered to be least biased to use a fixed value of t_{crit} for all patches and conditions.

For single channel data derived from whole cell recordings a fixed value of t_{crit} of 10 ms was used to analyse bursts throughout.

Analysis of closed times in general is complex, especially in situations where there are multiple active channels. This was obviously the case for whole cell recordings, but was probably also true for most patches. The limitations imposed by the analytical method used are discussed further in section 5.5.

Figure 3.6.1

Plots of the reciprocal of the mean open time against anaesthetic concentration, for procaine (top left), methoxyflurane (top right), methohexitone (bottom left) and etomidate (bottom right). In each case points are fitted to a regression line, the slope of which is equal to the forward rate constant of channel block (f). This value is shown in each panel.

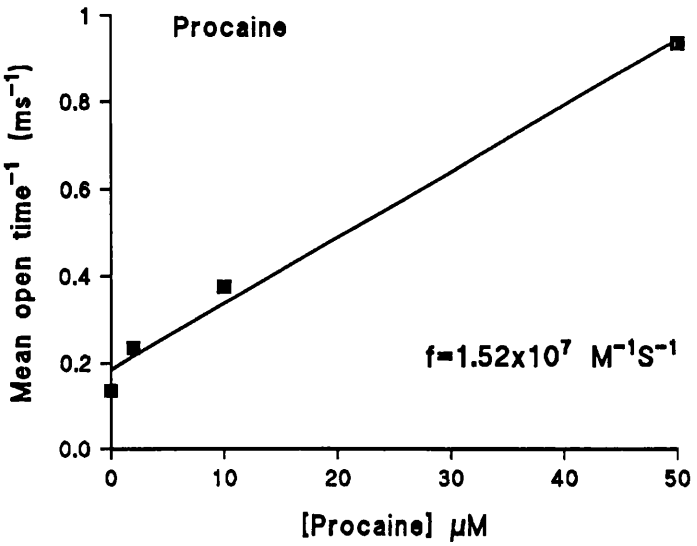
Procaine
Mean open time^{-1} (ms^{-1})
[Procaine] μM
f=1.52x10^{7} M^{-1}S^{-1}
0.0
0.2
0.4
0.6
0.8
1
0
10
20
30
40
50

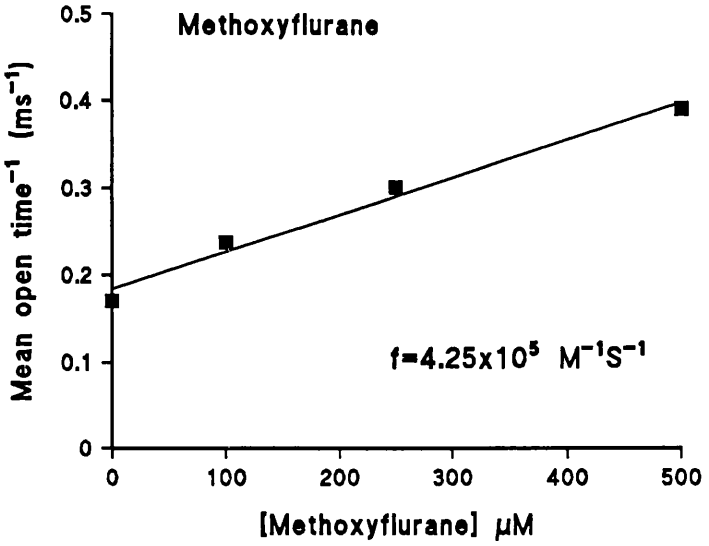
Methoxyflurane
Mean open time^{-1} (ms^{-1})
[Methoxyflurane] μM
f=4.25x10^{5} M^{-1}S^{-1}
0
0.1
0.2
0.3
0.4
0.5
0
100
200
300
400
500

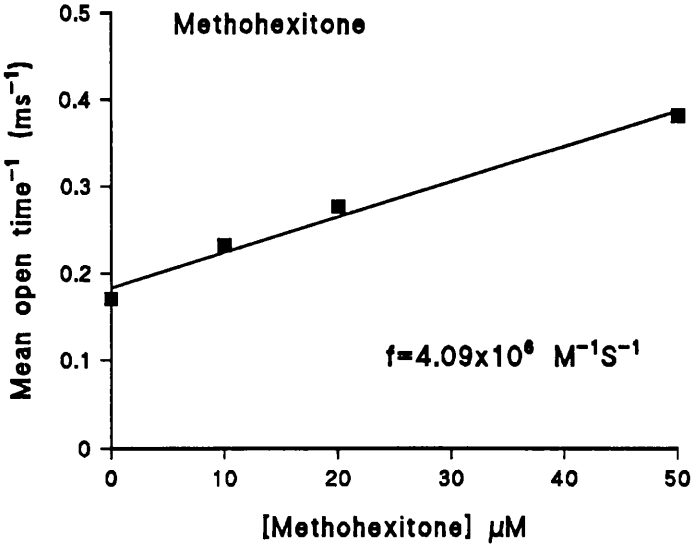
Methohexitone
Mean open time^{-1} (ms^{-1})
[Methohexitone] μM
f=4.09x10^{6} M^{-1}S^{-1}
0
0.1
0.2
0.3
0.4
0.5
0
10
20
30
40
50

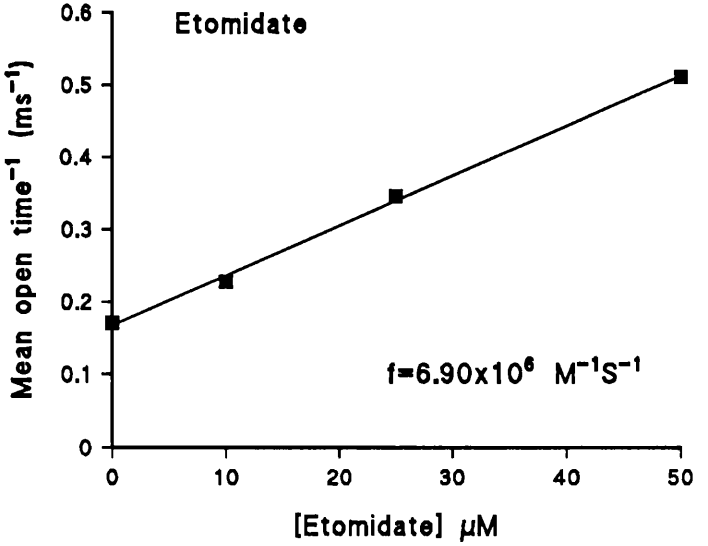
Etomidate
Mean open time^{-1} (ms^{-1})
[Etomidate] μM
f=6.90x10^{6} M^{-1}S^{-1}
0
0.1
0.2
0.3
0.4
0.5
0.6
0
10
20
30
40
50

4. Voltage-gated Calcium Currents And Their Modulation By Anaesthetics

4.1 Characteristics of Voltage-gated Calcium Currents

4.1a Introduction

Voltage dependent calcium channel currents in bovine adrenal chromaffin cells have been described in a number of studies (Fenwick et al 1982b, Hoshi et al 1984 & 1987, Hans et al 1990, Artalejo et al 1990, 1991 a&b, Bossu et al 1991 a&b, Charlesworth et al 1991).

Fenwick et al showed that the current (5mM Ca_{ext}) had a high activation threshold (-35mV), peak current was evoked by steps to +5mV, with a sharp rise in the I-V relationship around the half activation potential, and reversed at about +60mV. These characteristics of the current-voltage relationship have been replicated, with minor differences, by all subsequent patch-clamp investigations.

Whole cell calcium currents were found to run down irreversibly over periods of tens of minutes, and this process was accelerated by frequent stimulation or by raising Ca_i. While currents decreased in size during rundown, the shape of the current-voltage relation was unchanged. Stimulus-dependent inactivation, i.e the decay of current during a voltage step, was observed but the proportion of inactivating current varied greatly from cell to cell and was sometimes absent. Double pulse experiments showed that pre-pulses to potentials greater than -10mV caused a small enhancement of currents elicited by subsequent test-pulses to potentials less than the peak current potential, but caused a reduction in currents evoked by steps greater than the peak potential. The authors concluded that this behaviour was best explained by a small ($\sim$1mV) leftward shift in the I-V plot being caused by the pre-pulse.

Bossu et al (1991a&b) also found wide cell to cell variability of stimulus dependent inactivation, the magnitude of the current which decayed over a 350ms test pulse varied from 0 to 40% of the peak calcium current. It was found that the transient and sustained current components had markedly different sensitivities to holding potential, being half-inactivated at -52mV and -17mV respectively. This suggested that the current was carried by two distinct channel types, supported by the finding that the two current components differed in their pharmacological sensitivity: the sustained component being blocked by dihydropyridine antagonists (and the transient component being inhibited by ω-conotoxin). These properties are very similar to those of currents carried by L (slowly decaying, DHP sensitive) and N (inactivated at depolarised holding potential, transient) type channels as described by Nowycky et al (1985) (and see Fox et al 1987 a&b, Miller et al 1987). No evidence of a low threshold transient T type current was seen, consistent with the findings of all other groups.

Similar findings were reported by Hans et al (1990): a decaying component seen in currents evoked from a holding potential of -90mV was absent when cells were held at -40mV, while 50% of cells tested only had a sustained current component. ω-conotoxin (1-25μM) maximally blocked 40-50% of the current, consistent with the presence of sensitive and insensitive channels. However, the kinetics and holding potential sensitivity of the currents were essentially unaltered by ω-conotoxin. This suggests that both kinetic components of the current are themselves composed of two elements with different ω-CTX sensitivity.

The findings of Artalejo et al (1991a&b) are fundamentally different in many respects from those of Bossu et al and Hans et al. Single test pulses elicited sustained currents, termed 'standard', the magnitude and kinetics of which were unaltered by varying holding potential in the range -60 to -100mV. Strong depolarising pre-pulses increased the current recorded

during a subsequent test pulse by an average of 60%. The current component recruited by pre-pulses, termed the 'facilitation' current showed a similar test potential-current relation as the standard current. It could also be activated by repetitive depolarisations to the peak current potential at high frequency (1Hz). DHP antagonists blocked the facilitation current but did not affect the standard current. Hoshi et al (1984) also demonstrated calcium current facilitation in bovine adrenal chromaffin cells, induced both by strong pre-depolarisations and by repetitive stimuli, though the magnitude of the enhancement was smaller (25-35 %). At present there appears to be no explanation for the major differences in current characteristics observed.

4.1b Results

Voltage-gated calcium channel currents of adrenal chromaffin cells were recorded using the whole cell patch clamp technique, as described in the Methods. Under these conditions, depolarising voltage steps elicit inward currents attributable to the movement of Ba^{++} ions through calcium channels (see Fox et al 1987a). This is supported by the following observations (see Fig. 4.1.1):

i) Currents recorded using barium as the charge carrying ion have essentially the same characteristics as those recorded with calcium.

ii) Inward currents are blocked by 50 μM cadmium ions, leaving small outward leak currents.

iii) Inward currents are reversibly eliminated upon exchange with a zero barium bathing solution. Under these conditions, a larger outward current than can be accounted for by leak current is seen. This is probably due to Cs^{+} ions leaving the cell, unopposed by Ba^{++} ions moving in.

iv) Voltage activated sodium currents were completely blocked by 1μM TTX. 1-10 μM TTX was used throughout these experiments.

For convenience the voltage activated currents will be referred to as calcium currents, although the charge carrying ion is barium.

channel

4.1b(i) Activation and inactivation of calcium currents

From holding potentials in the range -100 to -40 mV the threshold for eliciting inward calcium currents was about -30mV. Current amplitude increased steeply with depolarisations of increasing magnitude until a maximal current was elicited at a test potential of 0mV. Currents reversed at potentials greater than +50mV; outward current observed above this test potential were probably due to the outward movement of Cs^+ ions (see Fenwick et al 1982b).

Fig. 4.1.2 shows the current voltage relationship and examples of current records for a typical cell. This figure shows that the inactivating current component has a similar current voltage relationship to the peak and sustained (late) current components and that there is no low threshold inactivating current. These features suggest the presence of L and N-type channels, but not T-type channels in these cells.

Exponential curves were fitted to currents in order to quantify the decay characteristics. Most currents were accurately fitted by the sum of two exponentials. However, since the time constant of the slowly decaying component was much greater than the longest pulse durations used (300 ms), currents could generally be well fitted by a single exponential plus residual component. This fitting procedure was used routinely, as it allows comparison between experiments.

The inactivating and non-inactivating current components show a marked difference in sensitivity to varying holding

potential, as shown in fig. 4.1.3. The inactivating and sustained components were half-inactivated at holding potentials of -75 mV and -40 mV respectively.

The proportion of peak current which inactivated during a step depolarisation varied substantially between cells. For 100ms pulses from -80mV to 0mV it varied in the range 0-45 % of peak current (mean 28.0% ± 10.0% s.d ; n=54).

4.1b(ii) Pharmacological sensitivity

The possibility of differential pharmacological sensitivity of the two current components was examined using the dihydropyridine calcium channel antagonist nicardipine and the snail toxin ω-conotoxin GVIA.

Nicardipine (2 μM) preferentially blocked the sustained current component, as shown in fig. 4.1.4. The nicardipine sensitive current component, obtained by subtraction (trace labelled C), shows no decay during the voltage pulse. The mean current remaining after nicardipine treatment showed a greater sensitivity to holding potential than the control current, consistent with an increased proportion of inactivating component. The effect of nicardipine was partially reversible. Higher concentrations (≥10 μM) blocked all currents.

ω-conotoxin (1 μM) irreversibly blocked ~50% of the calcium current, but apparently had no selective effect on the current components. Fig. 4.1.4 shows that currents decay with similar kinetics before and after ω-conotoxin treatment.

4.1b(iii) Run-down

The magnitude of inward calcium channel currents recorded in response to depolarising voltage pulses decreased during the course of experiments. The rate of this run down depended on the duration and frequency of voltage steps. The stimulation parameters used to test the effect of anaesthetics (100 ms pulses to 0 mV at 0.1 Hz) resulted in a modest current run

down, which was minimal in the best cases (see baseline prior to anaesthetic application in figs 4.3.1 and 4.4.1). Increasing rate or duration of stimulation enhanced run-down. This is in marked contrast to the findings of Artalejo et al (1991a), who found currents to be *enhanced* by increased stimulation frequency.

Facilitation of currents by applying strong depolarising pulses immediately prior to the test-pulse was also not observed.

4.1b(iv) Tail currents

Upon repolarisation to -80 mV following a test pulse (>-30 mV) a fast inward current was observed when the signal was sampled at a sufficiently high rate (see methods). The decay rate of this current reflects the rate at which open channels close on return to the holding potential (-80 mV).

Tail currents were fitted well by single exponential curves, extrapolated to the end of the voltage pulse (see control traces, figs 4.3.2 and 4.4.3). The decay time constant was independent of the test potential used to evoke currents: for currents following a test pulse to 0 mV it was 156 $\pm$ 5.0 µs. (143 $\pm$ 28.0 µs and 157 $\pm$ 7.7 µs for -25 mV and +25 mV test pulses respectively. All mean $\pm$ s.d, n=5).

The maximum amplitude (extrapolated to t=o) of the tail current is directly proportional to the fraction of channels activated by the test pulse. The results show that channel activation approaches a maximal value at test potentials of about +40 mV (see figs 4.3.2. & 4.4.3.). This is similar to the findings of Fenwick et al 1982b.

Figure 4.1.1

Features of voltage-gated currents in chromaffin cells.

The upper panel shows the current-voltage relationship for 20 ms depolarising pulses delivered from a holding potential of -80 mV, in the presence of various bathing media. Solutions were exchanged in the order: control - 50 μM Cd^{++} - control - 0 Ba^{++} . 0 Ba^{++} solution had the same composition as standard bathing medium for calcium current experiments, except 10 mM $BaCl_2$ was replaced by an extra 15 mM TEA-Cl.

The lower panel shows the whole cell current activated by a 25 ms step from -80 to 0 mV in the presence and absence of 5 μM tetrodotoxin. KCl recording solution (solution A - see methods) was used, rather than the TEA-Cl solution used for all other experiments presented in this chapter. Outward potassium currents therefore remain. The fast inward current, attributable to sodium channels, is clearly blocked by TTX.

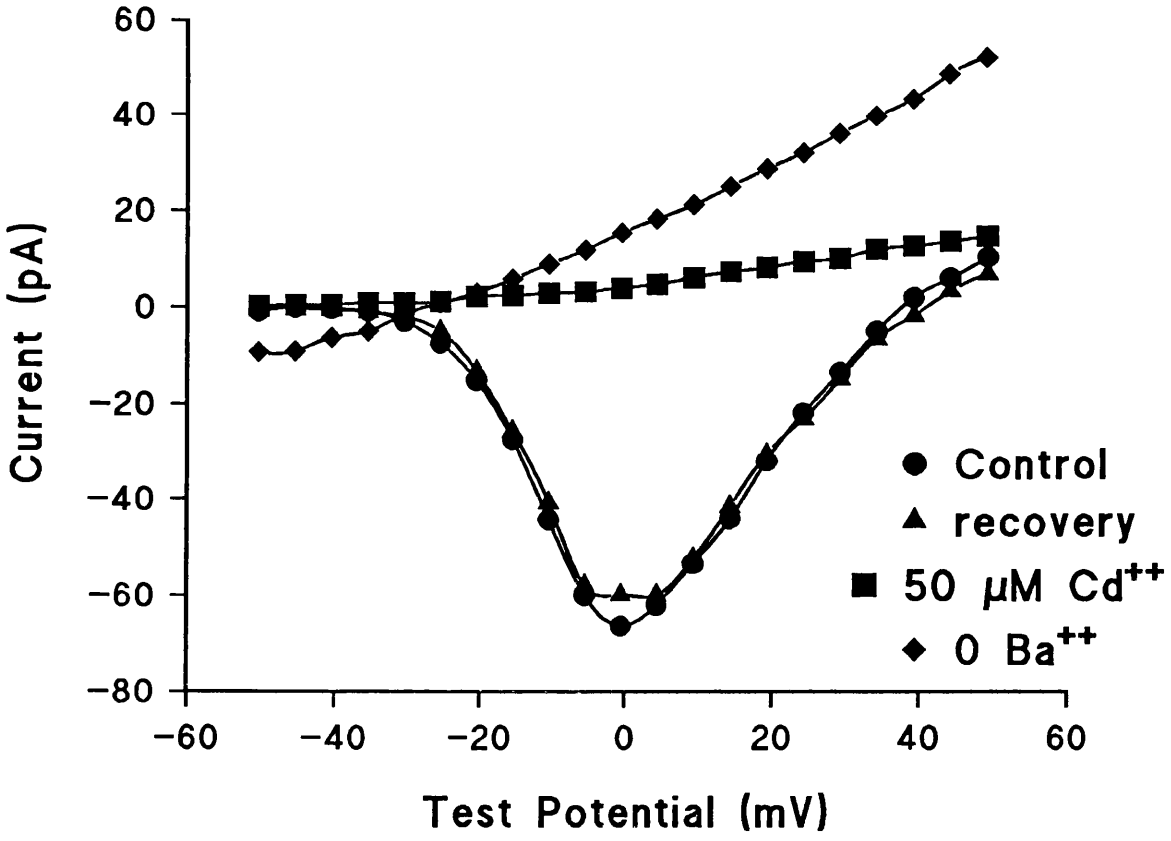
60
40
20
0
−20
−40
−60
−80
Current (pA)
−60
−40
−20
0
20
40
60
Test Potential (mV)
Control
recovery
50 μM Cd++
0 Ba++

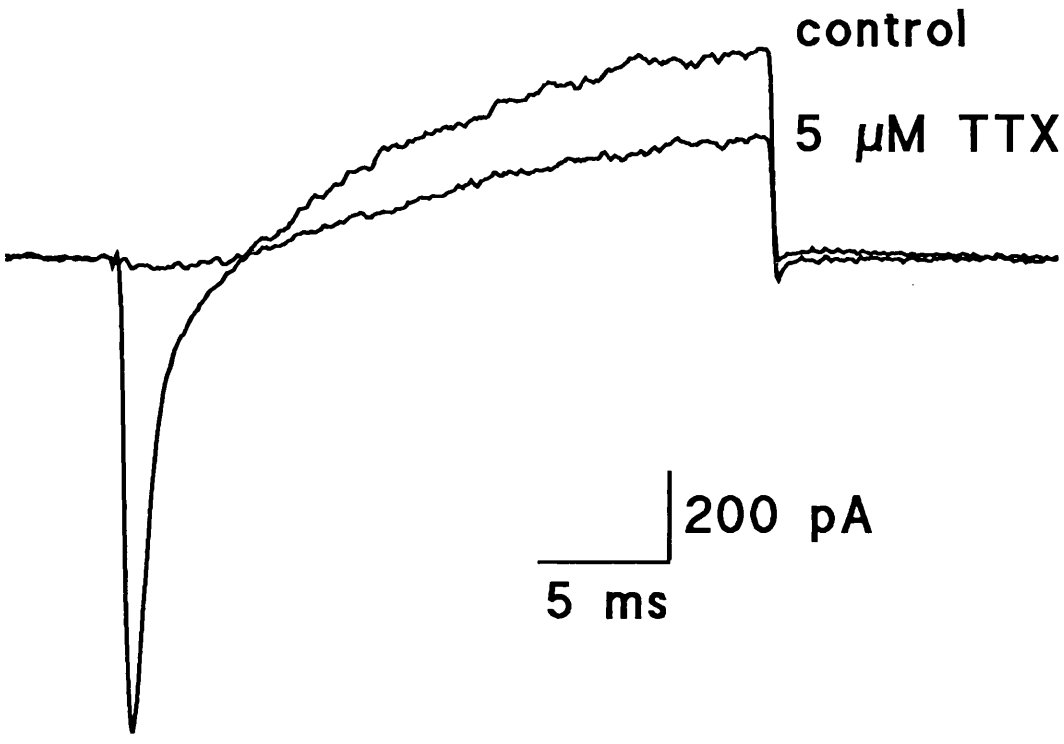
control
5 μM TTX
200 pA
5 ms

Figure 4.1.2

Voltage-gated calcium currents in a chromaffin cell.

The cell was held at -100 mV and 100 ms pulses to voltages between -40 and +50 mV with 5 mV increment were applied at a frequency of 0.2 Hz. The top panel shows the relationship between each of the measured components (see inset) of the calcium current and the test potential. The bottom panel shows the currents recorded for steps to -20, -10, 0, +10 and +30 mV. Each trace is a single response. Signals were digitised at 2.5 KHz and were not leak subtracted. 1-2 sample points were deleted at the start and end of the voltage pulse to eliminate residual uncancelled capacitative artefacts. All data from the same cell (4.2 pF, series resistance 11.6 MΩ).

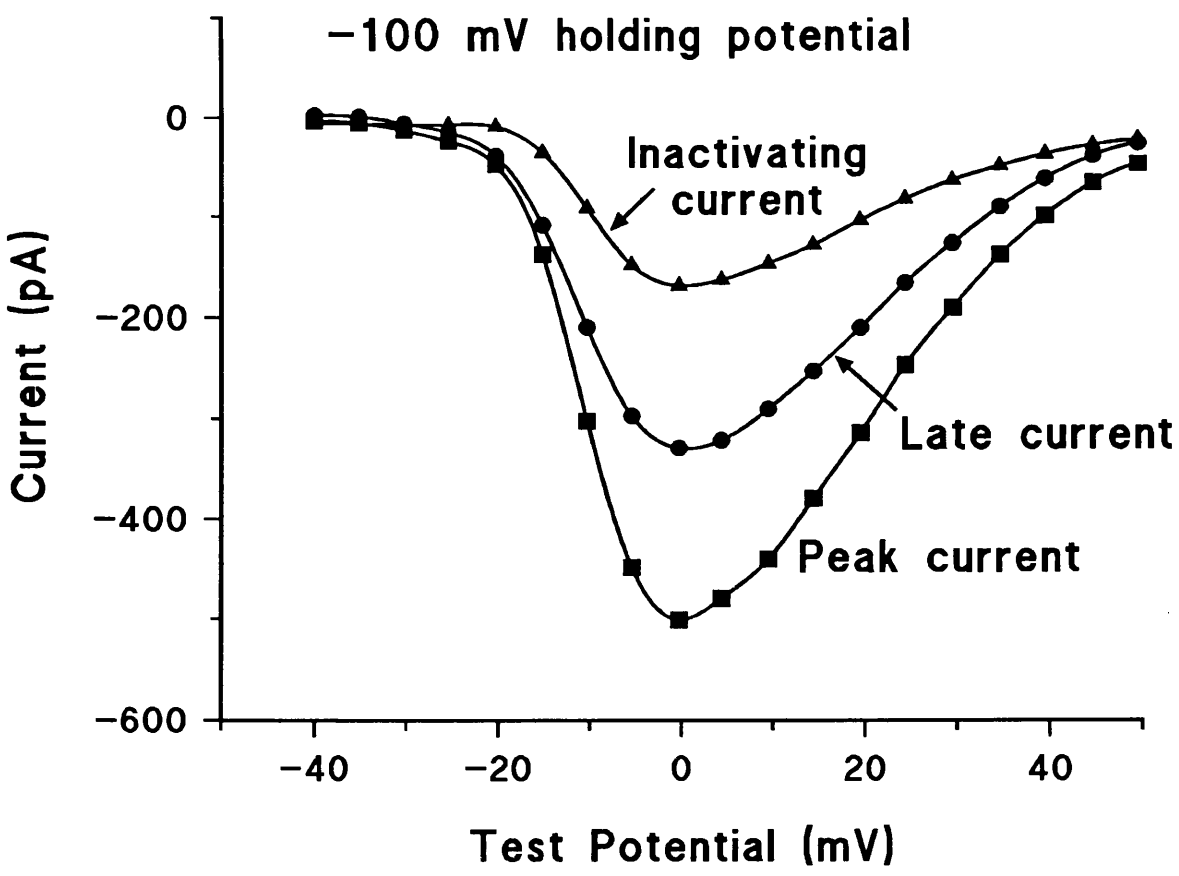
−100 mV holding potential
Inactivating current
Late current
Peak current
Current (pA)
0
−200
−400
−600
−40
−20
0
20
40
Test Potential (mV)

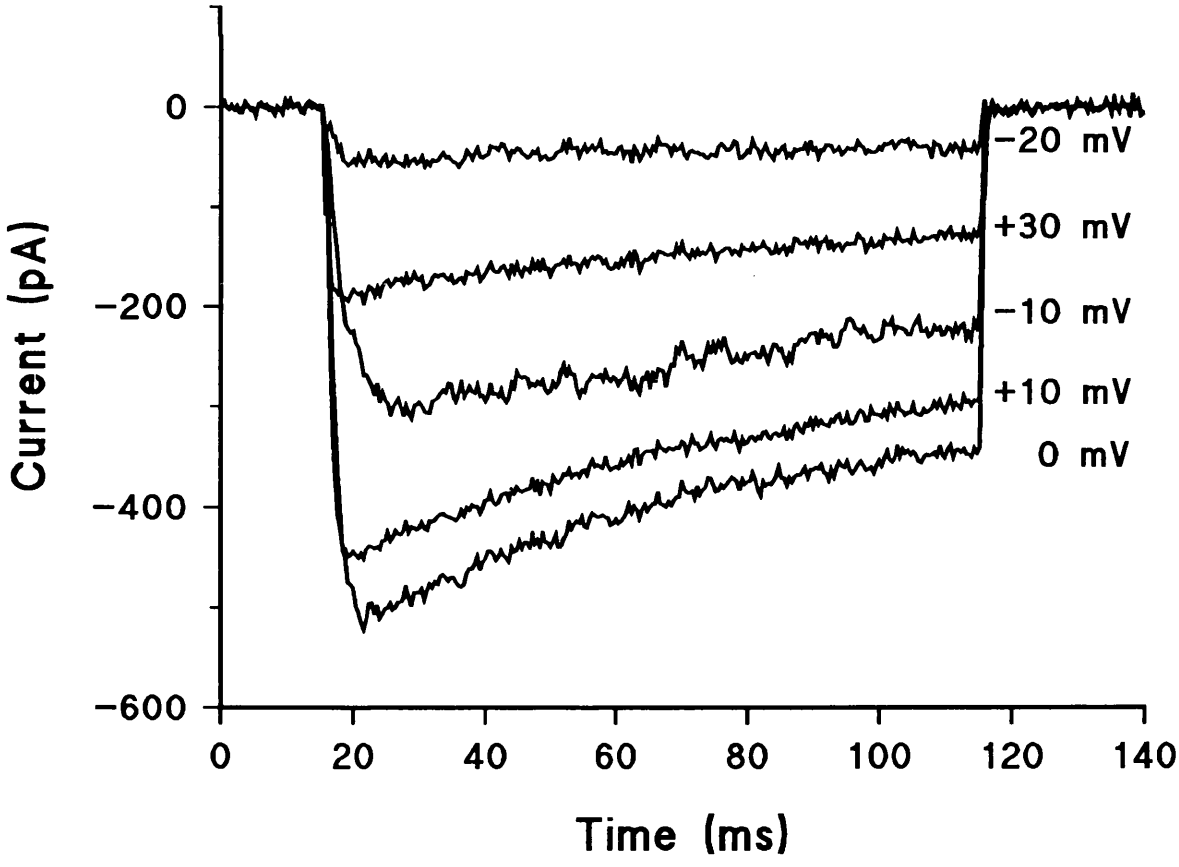
−20 mV
+30 mV
−10 mV
+10 mV
0 mV
Current (pA)
0
−200
−400
−600
0
20
40
60
80
100
120
140
Time (ms)

Figure 4.1.3

Steady-state inactivation of chromaffin cell calcium currents. Currents were evoked by 300 ms test pulses to 0 mV from varying holding potentials. The upper panel shows examples of currents recorded at holding potentials of -40, -60, -80 and -100 mV. Note the large increase in peak current, relative to sustained current, with hyperpolarisation.

The lower panel shows the relationship between holding potential and the relative magnitude of each current component. The dotted lines indicate half inactivation (-40 mV for the late current component and -75 mV for the inactivating component).

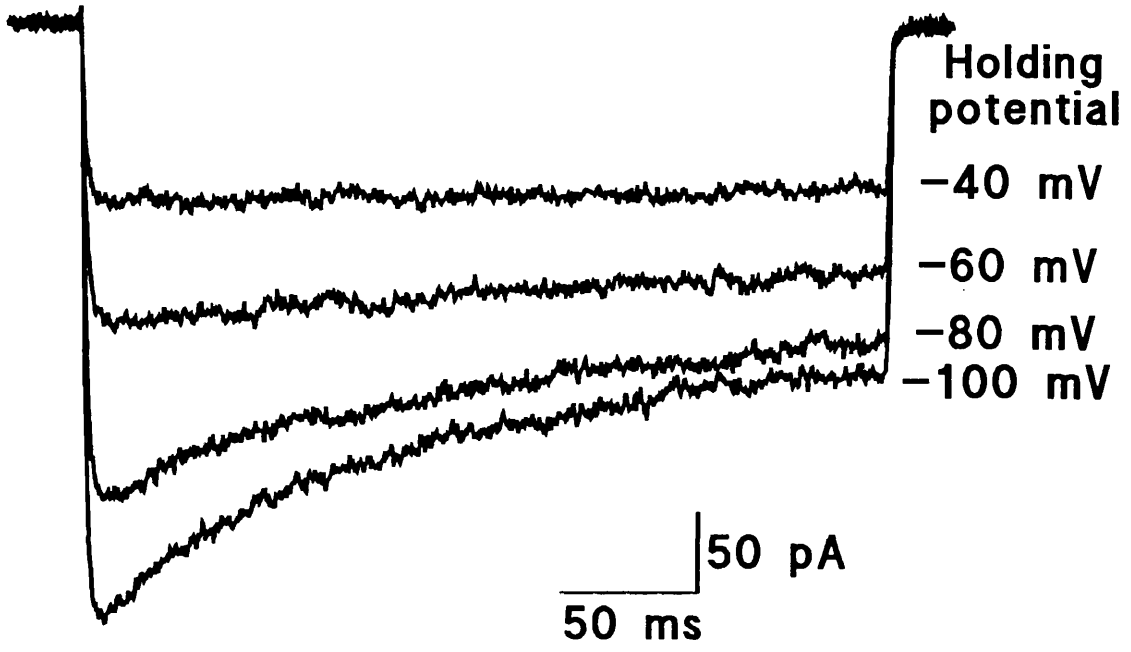
Holding
potential
−40 mV
−60 mV
−80 mV
−100 mV
50 pA
50 ms

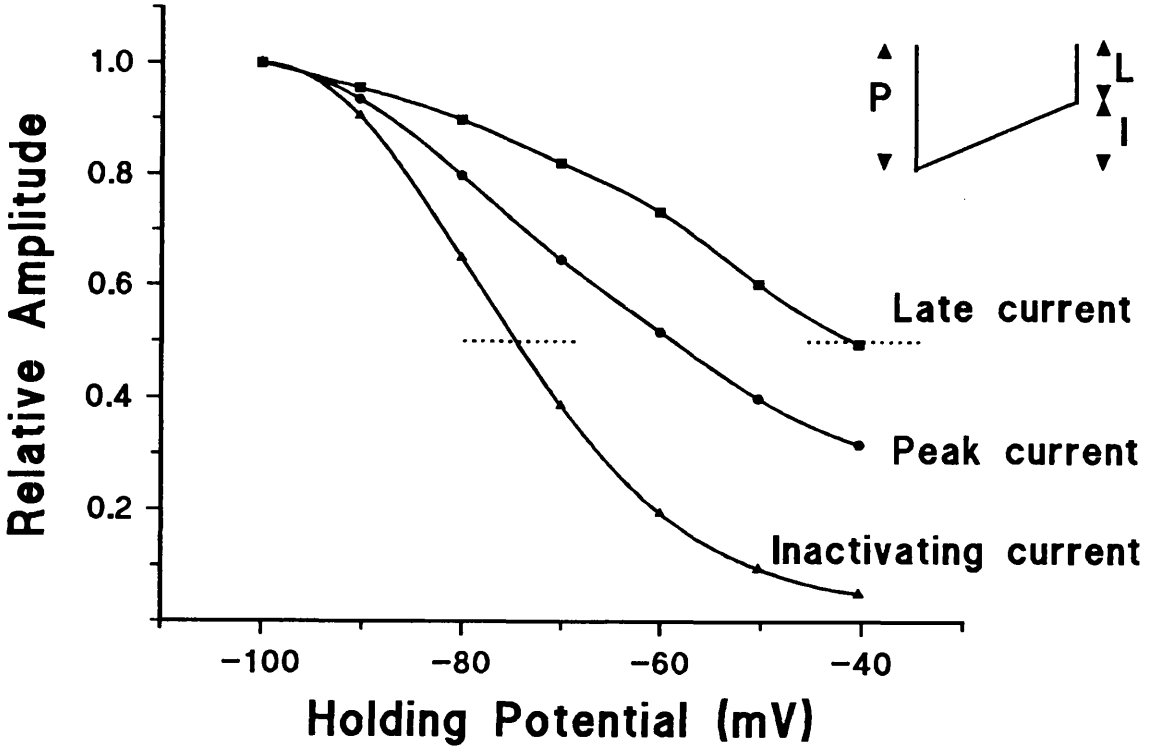
Relative Amplitude
1.0
0.8
0.6
0.4
0.2
P
L
I
Late current
Peak current
Inactivating current
−100
−80
−60
−40
Holding Potential (mV)

Figure 4.1.4

The effect of nicardipine and ω-conotoxin on voltage-gated calcium currents recorded from chromaffin cells. For all panels: A = Control current

B = Current during application of blocker

C = Current sensitive to blocker, obtained by subtracting trace B from trace A.

The left hand panels show the effect of 2 μM nicardipine. At -100 mV holding potential (top panel), the current displayed a significant inactivating component. Application of 2 μM nicardipine reduced the peak current but had little effect on the magnitude of the inactivating component. A similar effect is seen at -50 mV holding potential (lower panel), although the magnitude of the inactivating component in control is much reduced and the proportion of total current blocked by nicardipine is greater. At both holding potentials the nicardipine sensitive current (C traces) showed no stimulus dependent inactivation, typical of L-type current.

The right hand panels show the effect of 1 μM ω-conotoxin at -100 (upper panel) and -50 mV (lower panel) holding potential. In both cases the toxin blocked a similar proportion of the current and the sensitive current decayed with similar kinetics to the control current, indicating that both current components are equally sensitive to ω-conotoxin.

Effect of nicardipine

Test pulse from −100 mV to 0 mV

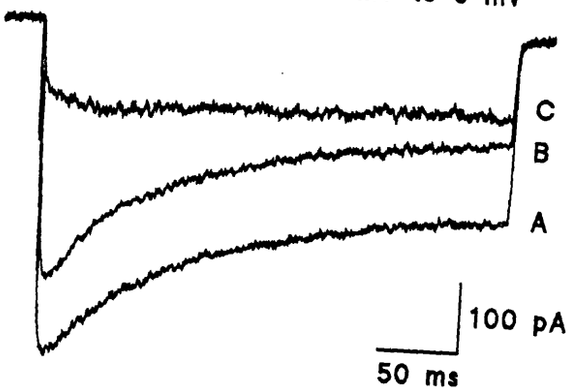

Effect of omega−conotoxin

Test pulse from −100 mV to 0 mV

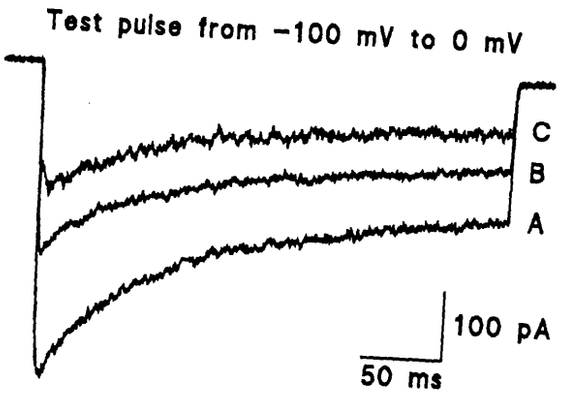

Test pulse from −50 mV to 0 mV

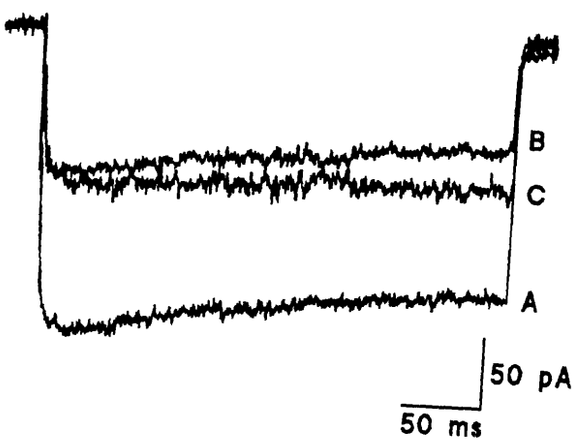

Test pulse from −50 mV to 0 mV

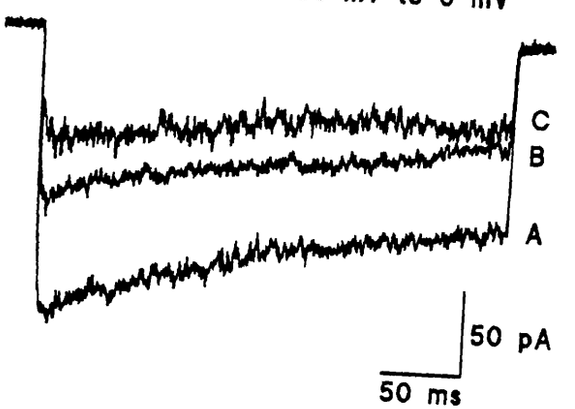

Anaesthetic Modulation of Calcium Currents

Calcium currents were recorded under conditions described in the Methods. To determine the dose dependency of the modulation of calcium currents by anaesthetic agents, a simple protocol was employed. Currents were evoked by 100 ms depolarisations from a holding potential of -80 mV to a test potential of 0 mV at a frequency of 0.1 Hz. With these stimulation parameters, the run-down of current amplitude was minimised. Currents were recorded for 200-300 s to produce a stable control baseline before the first application of anaesthetic. Agents were dissolved in bathing medium and applied for 100 s periods using the U-tube microperfusion apparatus described in the Methods. Upon returning to control bathing solution 200 s was allowed for recovery of the currents before a further application of a second concentration. Averages of three consecutive currents recorded before, after, and at the peak of the anaesthetic response were analysed. When less than 50% of the anaesthetic effect on mean calcium current (reduction) was reversed upon washing, currents were not analysed further. The average recovery of anaesthetic effect on mean current for accepted records was 78.1% (48 applications). No correction was made for run down of the currents. The magnitude of the depression of currents caused by the agents studied will therefore be slightly overestimated and percentage recovery correspondingly underestimated.

4.2 Procaine

The effects of this agent were studied in 10 cells. Concentrations in the range 500-2000 μM were required to inhibit the currents, 200 μM procaine having a barely detectable effect (see fig.4.2.1). Analysis of currents shows that procaine affected both peak and late currents equally.

Figure 4.2.1

The effect of procaine on voltage-activated calcium currents. Currents were evoked by 100 ms depolarisations to 0 mV from a holding potential of -80 mV at a frequency of 0.1 Hz.

The upper panels show examples of currents recorded before, during, and after application of 500 μM (left) and 2000 μM (right) procaine. The lower left panel shows the time course of the action of 200, 500 and 2000 μM procaine on voltage-activated calcium currents. All data are from the same cell.

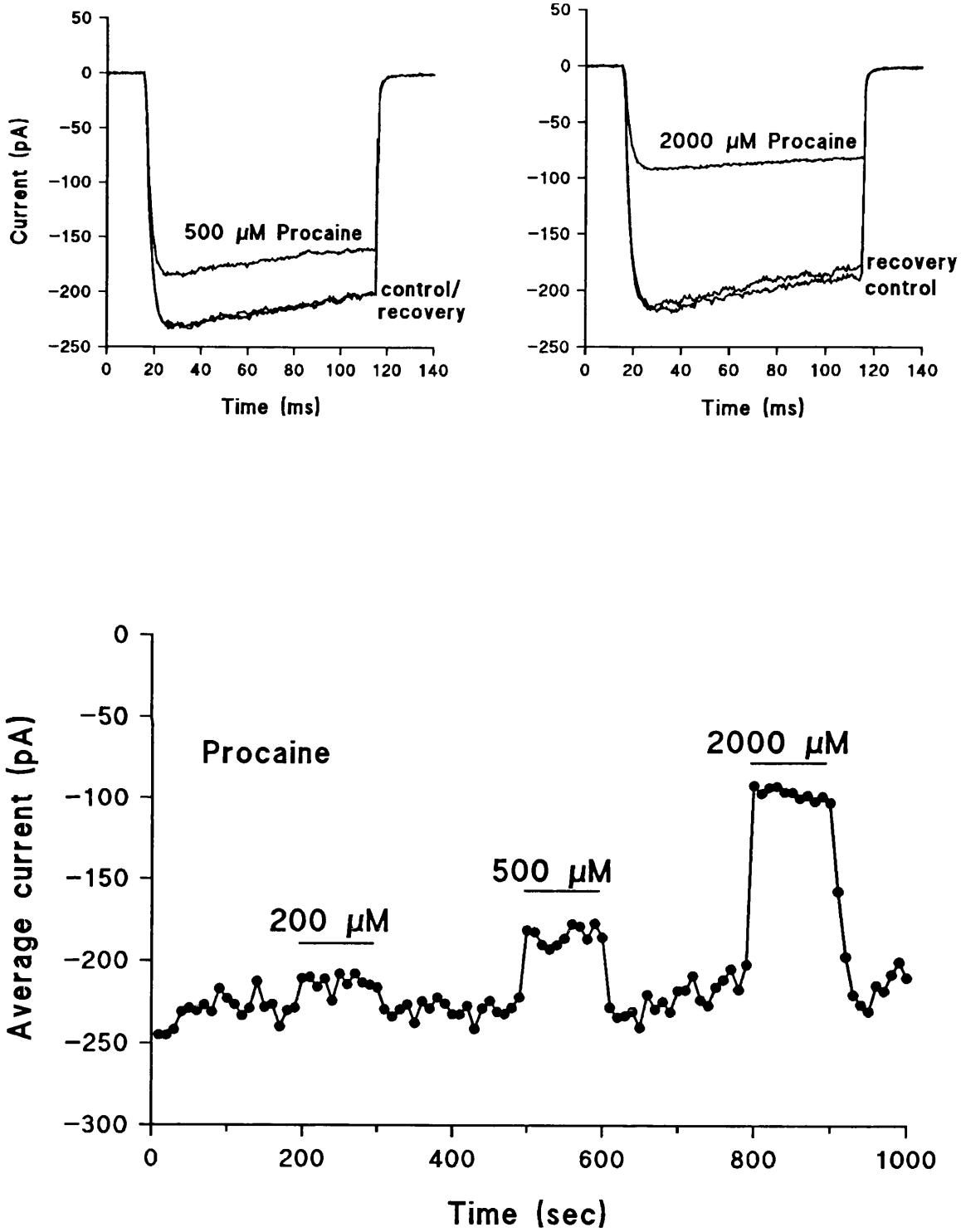
50
0
-50
-100
-150
-200
-250
Current (pA)
500 μM Procaine
control/
recovery
0 20 40 60 80 100 120 140
Time (ms)
2000 μM Procaine
recovery
control
Average current (pA)
Procaine
200 μM
500 μM
2000 μM
-300
0 200 400 600 800 1000
Time (sec)

4.3 Methoxyflurane

The effects of methoxyflurane (200-1600 μM) on the voltage-activated calcium channel currents were studied in 11 cells. The peak inward current was reduced in each case, the reduction being related to the concentration of anaesthetic applied. The apparent $I.C._{50}$ for reduction in total inward current was about 1300 μM (Fig.4.3.1). During application of methoxyflurane the mean latency to peak current was slightly shorter but this difference was not statistically significant (6.8 ± 1.03ms in control and 5.90 ± 1.18 ms in the presence of 1600 μM methoxyflurane). Moreover, not all cells showed a reduced latency to peak.

The time constant of the current decay decreased in a concentration-dependent manner e.g. from c.85 ms in the absence of anaesthetic to c. 40 ms in 1600 μM methoxyflurane (see Fig. 4.6.1). The fraction of the inward current that showed a stimulus-dependent inactivation progressively increased with increasing concentration of anaesthetic. When normalised to the peak inward current the inactivating current increased from 28.5 ± 13.6% in control to 40.6 ± 5.2% in 400 μM, 46 ± 3.5% in 800 μM and 56.2 ± 4.3% in 1600 μM methoxyflurane (all mean $\pm$ s.d.; see Fig. 4.6.1). The increase in the proportion of inactivating current was greater than could be explained by a selective depression of the non-inactivating component. Furthermore, two cells possessed currents with very long time constants (330ms and 660ms respectively) and there was little stimulus-dependent inactivation. Addition of anaesthetic (400 μM methoxyflurane) to these cells induced an inactivating component with time constants of 69ms and 67ms respectively.

The effects of the anaesthetic on the extent and rate of current decay were fully reversible while the current amplitude after washing out the anaesthetic recovered to a degree consistent with the extent of the time-dependent rundown.

The effect of 1 mM methoxyflurane on the amplitude and decay rate of tail currents was examined in two cells. Tail currents were elicited by repolarisation to -80 mV following a test depolarisation to -50 to +50 mV. In the presence and absence of methoxyflurane, tail currents were fitted well by single exponential functions. These curves were extrapolated back to the end of the test pulse in order to estimate the peak tail current amplitude. Fig. 4.3.2 shows the relationship between peak tail current and the test potential used to activate the channels. Methoxyflurane reduced tail current amplitude by about 50 %, but did not alter the shape of the activation curve: half-maximal activation of the channels occurred at -5 mV in the presence and absence of anaesthetic.

Methoxyflurane also had no apparent effect on the decay rate of tail currents (Fig. 4.3.2., lower panel). The time constants of fitted single exponential functions did not alter after exposure to 1mM methoxyflurane.

Figure 4.3.1

The effect of methoxyflurane on voltage-activated calcium currents. Currents were evoked by 100 ms depolarisations to 0 mV from a holding potential of -80 mV at a frequency of 0.1 Hz.

The upper panels show examples of currents recorded before, during, and after application of 800 μM (left) and 1600 μM (right) methoxyflurane. The lower left panel shows the time course of the action of methoxyflurane on voltage-activated calcium currents. All data from the same cell

The lower right panel shows the dose-response curve for the action of methoxyflurane on the total calcium current, expressed as a percentage of control. The figures in brackets indicate the number of cells and error bars represent the standard error of the mean. * denotes statistical significance at the 95% confidence level.

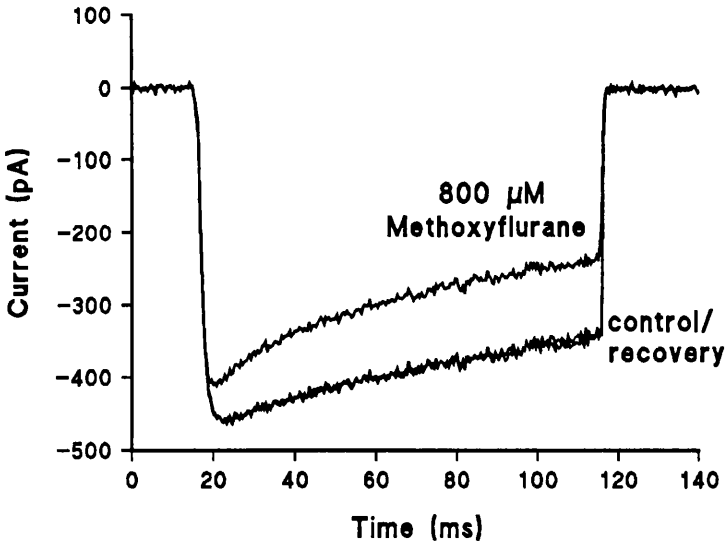
100
0
-100
-200
-300
-400
-500
Current (pA)
800 μM
Methoxyflurane
control/
recovery
0
20
40
60
80
100
120
140
Time (ms)

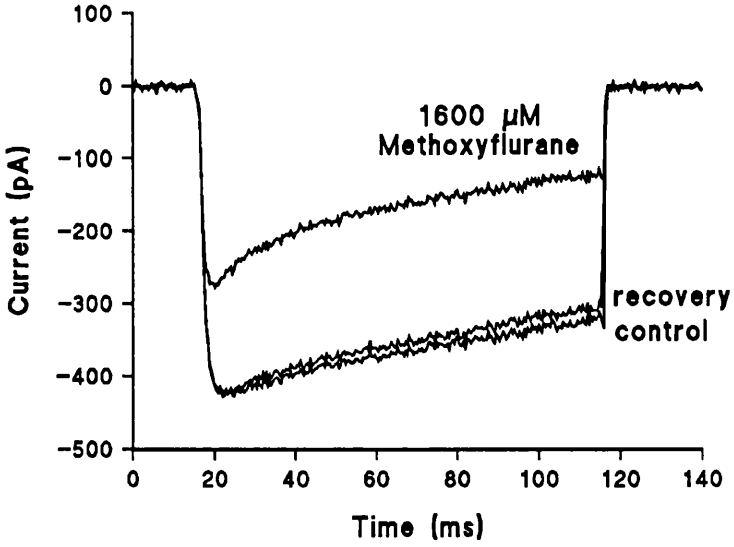
100
0
-100
-200
-300
-400
-500
Current (pA)
1600 μM
Methoxyflurane
recovery
control
0
20
40
60
80
100
120
140
Time (ms)

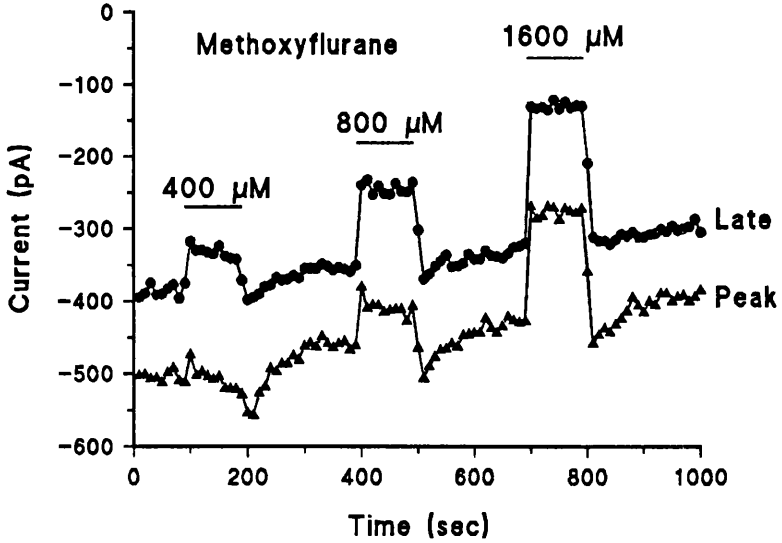
0
-100
-200
-300
-400
-500
-600
Current (pA)
Methoxyflurane
1600 μM
800 μM
400 μM
Late
Peak
0
200
400
600
800
1000
Time (sec)

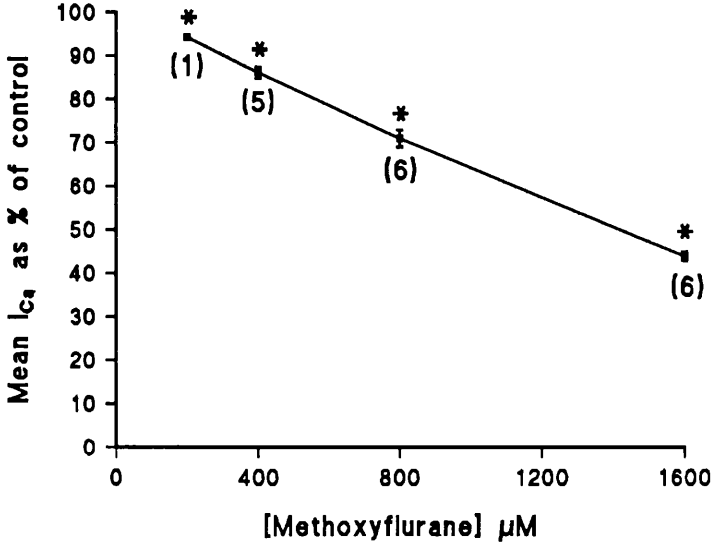
100
90
80
70
60
50
40
30
20
10
0
Mean I_{Ca} as % of control
(1)
(5)
(6)
(6)
0
400
800
1200
1600
[Methoxyflurane] μM

Figure 4.3.2

The effect of 1 mM methoxyflurane on calcium channel tail currents. Tail currents were evoked by repolarising to -80 mV from test potentials of -50 to +30 mV.

The upper panel shows a plot of peak tail current amplitude (estimated by extrapolation to the end of the test pulse) against test potential, in the presence and absence of 1 mM methoxyflurane. Methoxyflurane substantially reduces the amplitude of tail current, but does not alter the shape of the activation curve.

The lower panel shows tail currents recorded in the presence (smaller peak) and absence (larger peak) of 1 mM methoxyflurane. Also shown (dotted line) is the tail current recorded in the presence of methoxyflurane scaled to the height of the control peak. This shows that methoxyflurane does not alter the tail current decay rate, although peak amplitude is reduced by about 50 %.

The equation of the solid line fitted to the data is:

$$y = \frac{Max}{(1+((x/x_{50})^{-p}))}$$

The parameters of the curve fits are:

	Control	1 mM methoxyflurane
Max (pA)	7109	3511
x_{50} (mV)	75.6	77.8
p	9.06	8.77

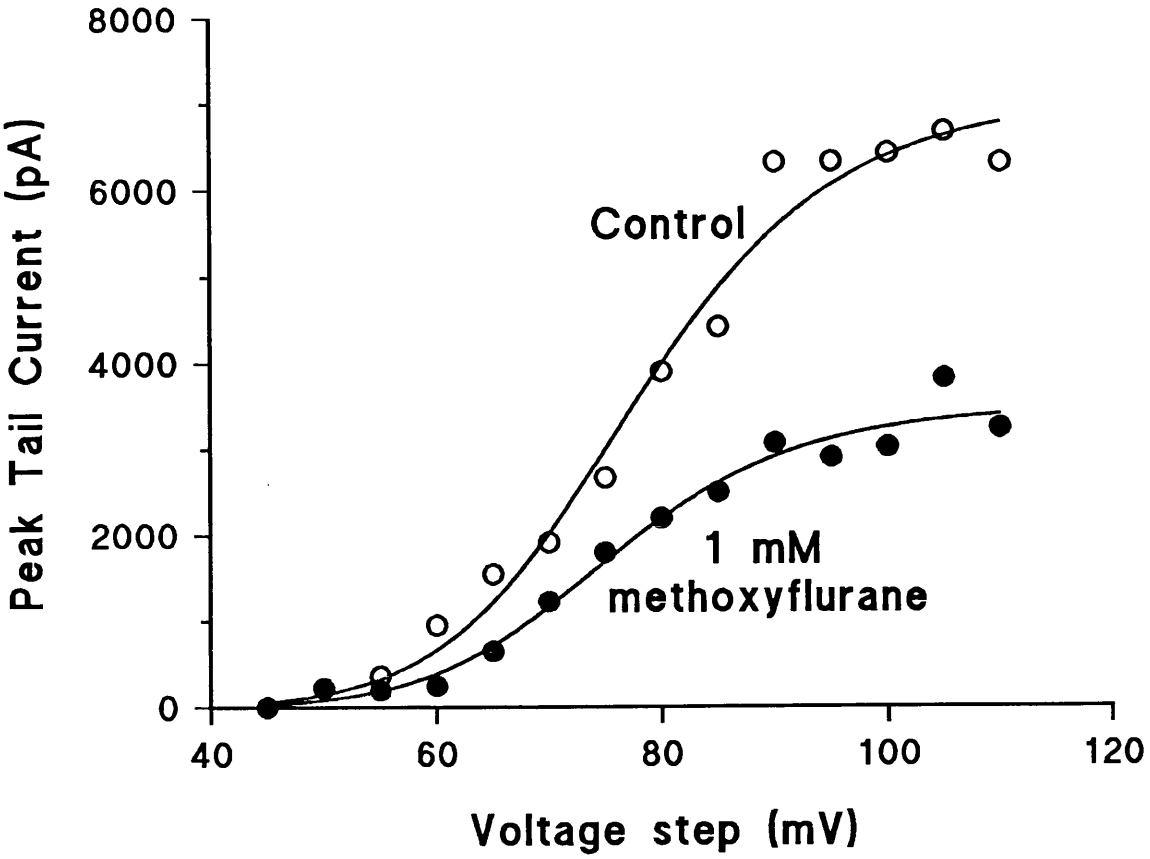
8000
6000
4000
2000
0
Peak Tail Current (pA)
Control
1 mM
methoxyflurane
40
60
80
100
120
Voltage step (mV)

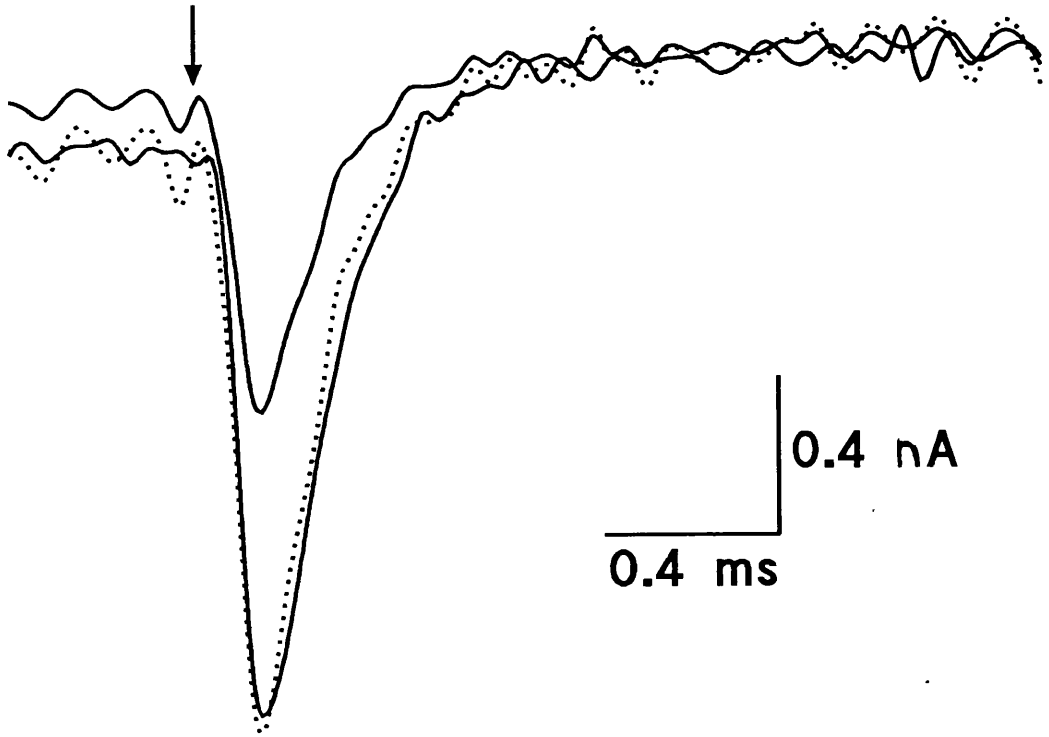
0.4 nA
0.4 ms

4.4 Methohexitone

The effects of methohexitone (20-500 μM) were studied in 13 cells. Concentrations in the range 50-500 μM both reduced the peak inward current and decreased the time constant for current decay. Both effects were related to the concentration of anaesthetic applied. The apparent $I.C._{50}$ for reduction in total inward current was approximately 150 μM (Fig. 4.4.1).

The latency to the peak of the inward current was reduced in all but one cell but the reduction was small ~ 1-1.2 ms and its magnitude did not increase progressively with increasing concentration of anaesthetic. For example in control the latency to peak was 6.54 ± 1.02 ms and in 50 μM methohexitone it was 5.33 ± 0.78 ms; when 500 μM methohexitone was applied the latency was 5.24 ± 0.73 ms and that of the paired controls was 6.28 ± 0.71ms. Nevertheless, the initial rate of growth of the current was unaltered by the anaesthetic.*

The effect on the time constant for current decay was similar to that observed with methoxyflurane except that methohexitone was more potent (Fig. 4.6.1). The time constant decreased from 80 ± 51ms in control (7 cells) to 55 ± 11ms in 50μM, 45 ± 5ms in 100μM and 25 ± 7ms in 500 μM methohexitone (Fig. 4.6.1). When normalised to the peak inward current the inactivating current increased from 29.9 ± 16.4% in control to 49.6 ± 15.5% in 50 μM, 60.3 ± 3.2% in 100 μM and 80.7 ± 10.6% in 500 μM methohexitone (all mean ± s.d.). In six cells the effects of 20 μM methohexitone were explored. At this concentration there was a small increase in the amplitude of the peak calcium current. This was partly offset by a slight reduction in the late current, consistent with the effects of higher concentrations on the time constant for current decay.

A notable feature of the action of methohexitone was the difference in the time taken for the peak and late currents to reach equilibrium after commencing perfusion with high

*The apparent reduction in latency is probably simply due to the reduction in peak current.

concentrations of methohexitone. In every case the late current was largely blocked within 10 seconds while the peak current decayed with a time constant in the range 20-30s (see Figure 4.4.2). After washout of 500 μM methohexitone the peak and late currents recovered with a similar time course.

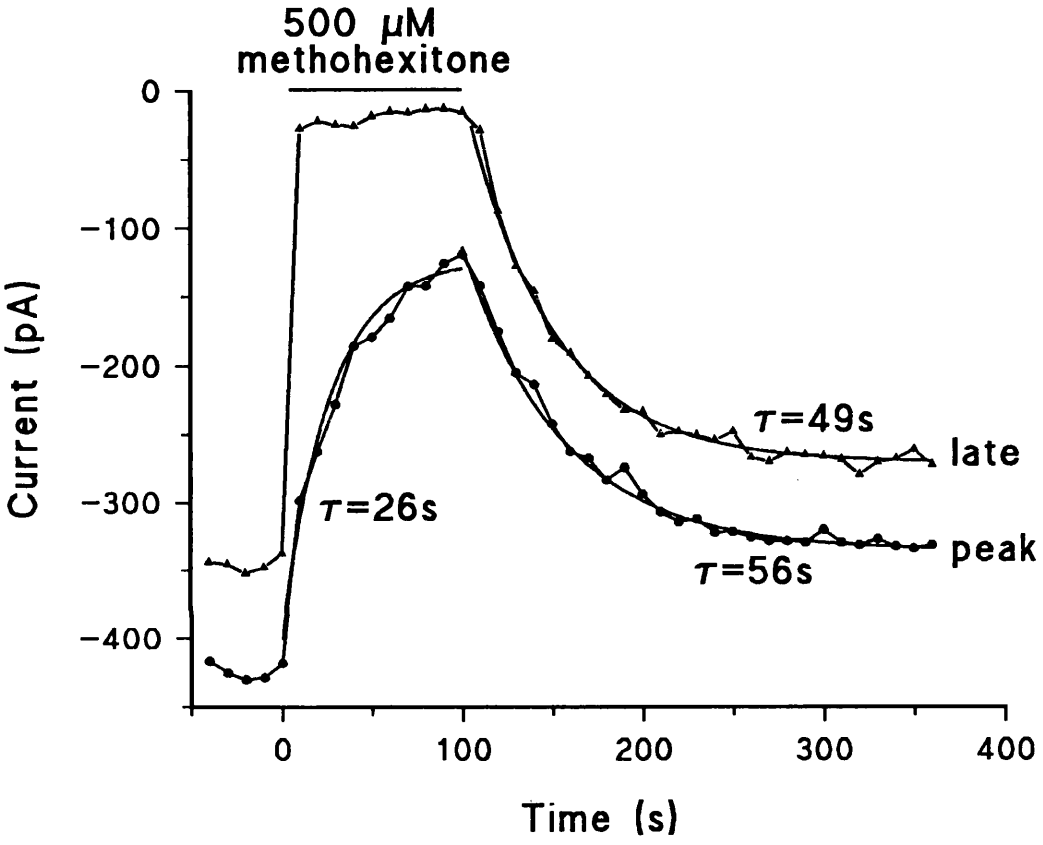

Figure 4.4.2

The time course of the onset and offset of the action of 500μM methohexitone on the voltage activated calcium current of a chromaffin cell. Single exponential curves were fitted to the peak and late current components, with the indicated time constants.

The effect of 100 μM methohexitone on the amplitude and decay rate of tail currents was examined in two cells. Tail currents were elicited by repolarisation to -80 mV following a test depolarisation to -50 to +50 mV. In the presence and absence of methohexitone, tail currents were fitted well by single exponential functions. These curves were extrapolated back to the end of the test pulse in order to estimate the peak tail current amplitude. Fig. 4.4.3 shows the relationship between peak tail current and the test potential used to activate the channels. Methohexitone reduced tail current amplitude by about 50 %, but did not alter the shape of the activation curve: half-maximal activation of the channels occurred at -5 mV in the presence and absence of anaesthetic.

Methohexitone also had no apparent effect on the decay rate of tail currents (Fig. 4.4.3., lower panel). The time constants of fitted single exponential functions did not alter after exposure to 100 μM methohexitone.

Figure 4.4.1

The effect of methohexitone on the voltage-activated calcium currents of chromaffin cells. Stimulation parameters as described previously.

The top panels show examples of currents recorded before during and after application of 50 μM (left) and 100 μM (right) methohexitone. The bottom left panel shows the time course of the action of three concentrations of methohexitone on the peak and late current components. Bars represent the period of drug application. The lower right panel shows the dose-response curve for the action of methohexitone on the total calcium current expressed as a percentage of control. The figures in brackets indicate the number of cells and error bars represent the standard error of the mean. * denotes statistical significance at the 95% confidence level.

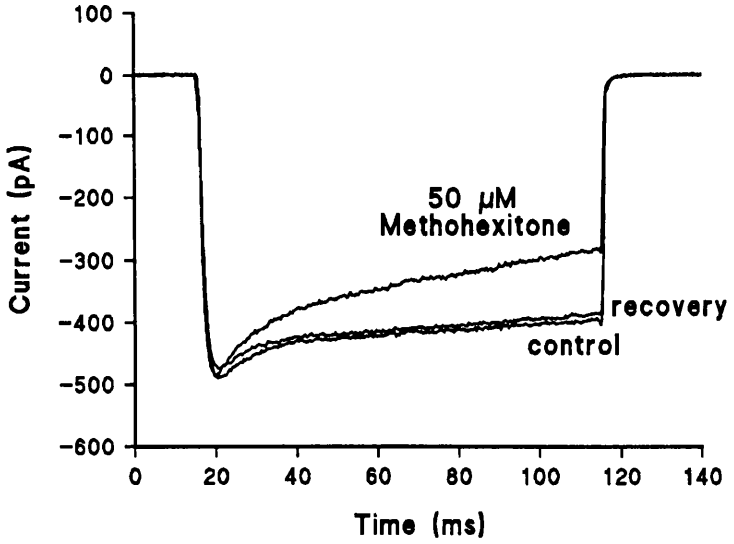
100
0
-100
-200
-300
-400
-500
-600
Current (pA)
50 μM
Methohexitone
recovery
control
0
20
40
60
80
100
120
140
Time (ms)

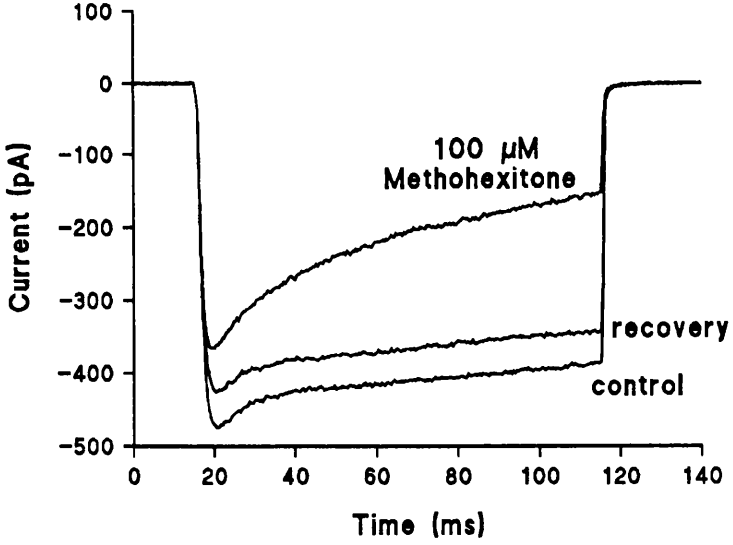
100
0
-100
-200
-300
-400
-500
Current (pA)
100 μM
Methohexitone
recovery
control
0
20
40
60
80
100
120
140
Time (ms)

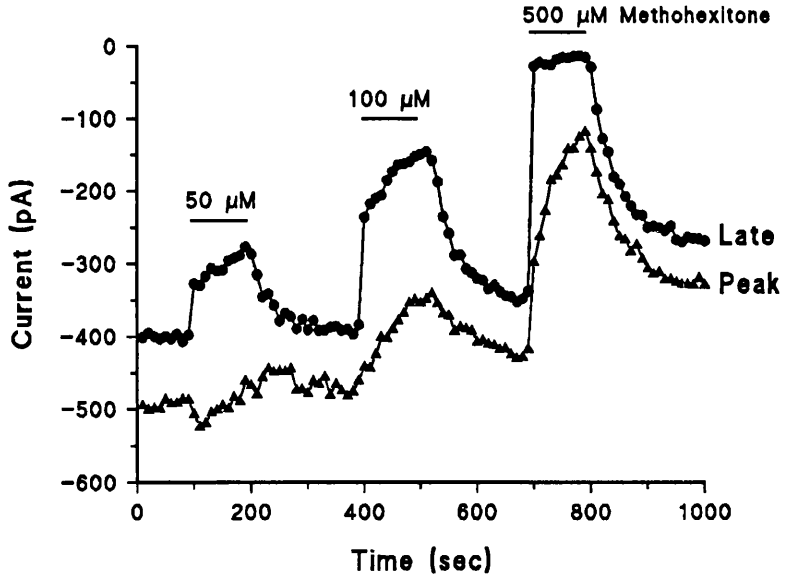
500 μM Methohexitone
100 μM
50 μM
0
-100
-200
-300
-400
-500
-600
Current (pA)
Late
Peak
0
200
400
600
800
1000
Time (sec)

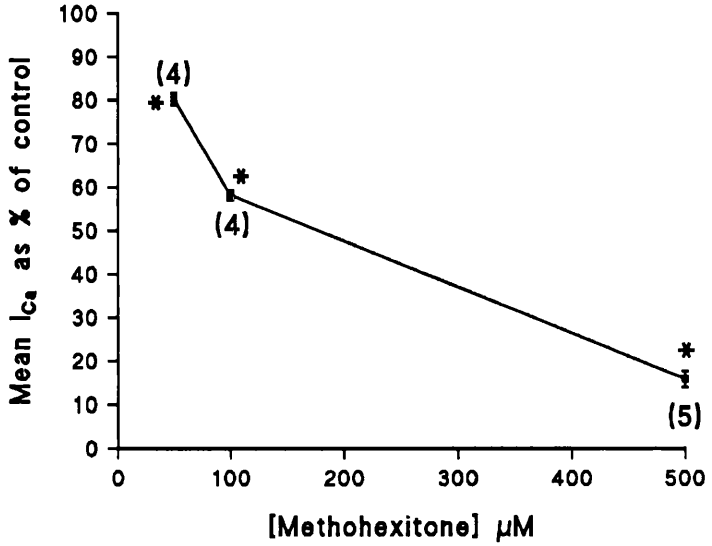
100
90
80
70
60
50
40
30
20
10
0
Mean I_{Ca} as % of control
(4)
(4)
(5)
0
100
200
300
400
500
[Methohexitone] μM

Figure 4.4.3

The effect of 100 μM methohexitone on calcium channel tail currents. Tail currents were evoked by repolarising to -80 mV from test potentials of -50 to +40 mV.

The upper panel shows a plot of peak tail current amplitude (estimated by extrapolation to the end of the test pulse) against test potential, in the presence and absence of 100 μM methohexitone. Methohexitone substantially reduces the amplitude of tail current, but does not alter the shape of the activation curve.

The lower panel shows tail currents recorded in the presence (smaller peak) and absence (larger peak) of 100 μM methohexitone. Also shown (dotted line) is the tail current recorded in the presence of methohexitone scaled to the height of the control peak. Methoxhexitone does not alter the tail current decay rate, although peak amplitude is reduced by about 50 %.

The equation of the solid line fitted to the data is:

$$y = \frac{Max}{(1+((x/x_{50})^{-p}))}$$

The parameters of the curve fits are:

	Control	100 μM methohexitone
Max (pA)	10506	5687
x_{50} (mV)	79.7	81.8
p	8.68	7.67

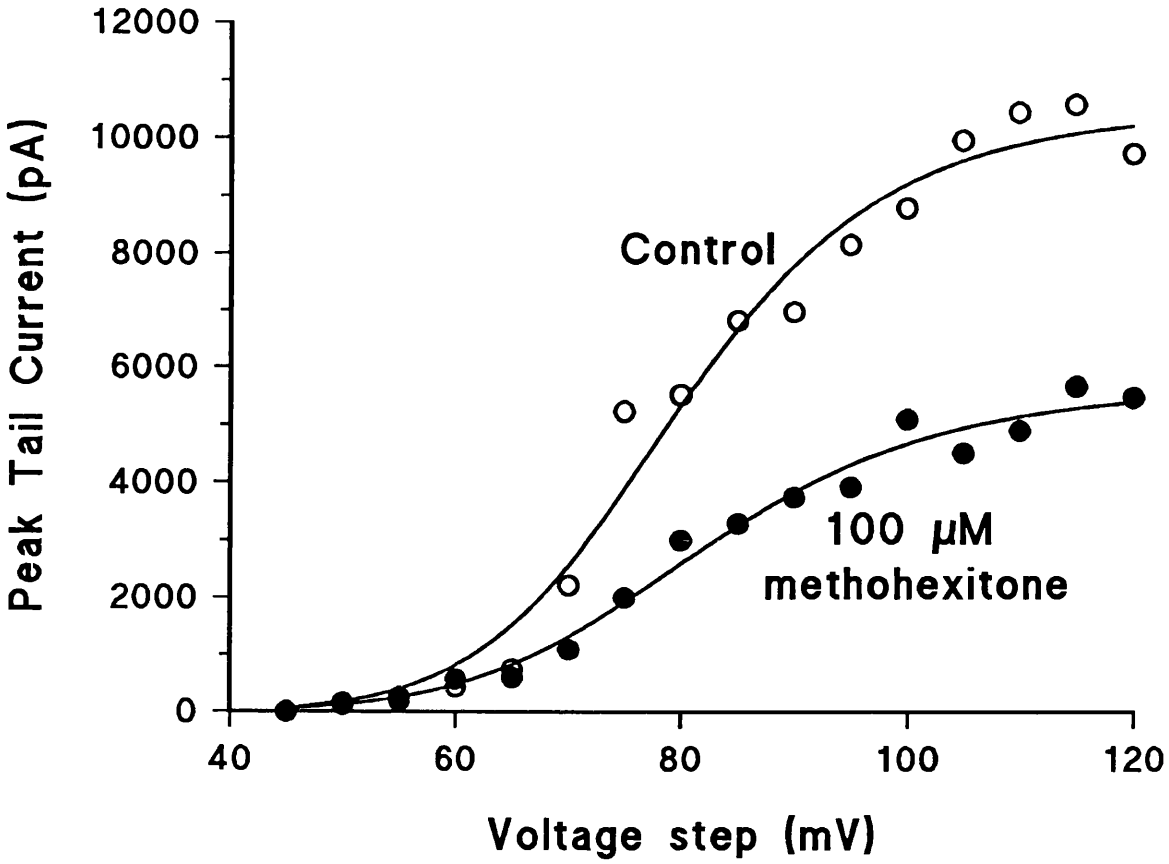
12000
10000
8000
6000
4000
2000
0
Peak Tail Current (pA)
Control
100 µM
methohexitone
40
60
80
100
120
Voltage step (mV)

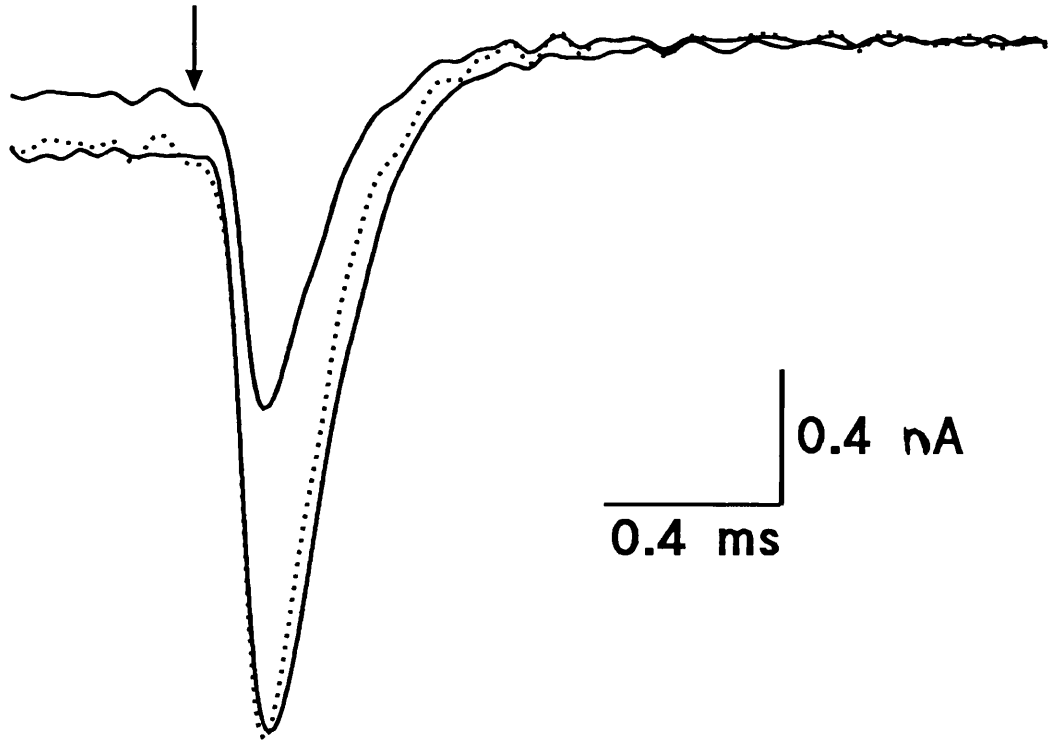
0.4 nA
0.4 ms

4.5 Etomidate

The effects of this agent on the voltage-activated calcium channel currents were studied in 8 cells. Concentrations in the range 50-200 μM reduced the peak inward current with an apparent IC_{50} close to 200 μM (Fig. 4.5.1). As with the two agents described above, application of etomidate had a slight tendency to reduce the latency to peak although the reduction was not statistically significant.

Etomidate decreased the time constant for current decay from about 55 ms in control to 45 ms in 100 μM and 48 ms in 200 μM and increased the proportion of inactivating current although it was less effective in this respect than the two previous agents (Fig. 4.6.1). In the absence of anaesthetic the inactivating current in these cells was comparable to that observed in other cells at 31.9 ± 5.9% of the peak value. The relative proportion of inactivating current increased to 42.5±8.7% in 100 μM and 53.5 ± 7.1% in the presence of 200 μM etomidate. As with the effects of methohexitone and methoxyflurane the principal effects were readily reversible (see Fig. 4.5.1).

In addition to its effects on the inward calcium currents, etomidate strongly activated a chloride current (see Fig. 4.5.1). This is observed as a displacement of the baseline at the normal holding potential of -80 mV. The chloride currents varied in magnitude from cell to cell and ranged from zero to 90pA. The magnitude of the chloride current appeared to be related to the concentration of etomidate applied although at the highest concentrations tested (200 μM) it showed a time-dependent decay. The chloride current did not contribute to the current recorded during a depolarising voltage step to zero mV as the composition of the bathing medium and pipette solutions set the chloride equilibrium potential to zero so that when the calcium current is fully activated there will be no net chloride current.

Figure 4.5.1

The effect of etomidate on the voltage-activated calcium currents of chromaffin cells. The top panels show examples of currents recorded before during and after application of 100 μM (left) and 200 μM (right) etomidate. The lower left panel shows the time course of the action of three concentrations of etomidate on voltage-activated calcium currents. All data from the same cell.

The lower right panel shows the dose-response curve for the action of etomidate on the total calcium current expressed as a percentage of control. The figures in brackets indicate the number of cells and error bars represent the standard error of the mean. * denotes statistical significance at the 95% confidence level.

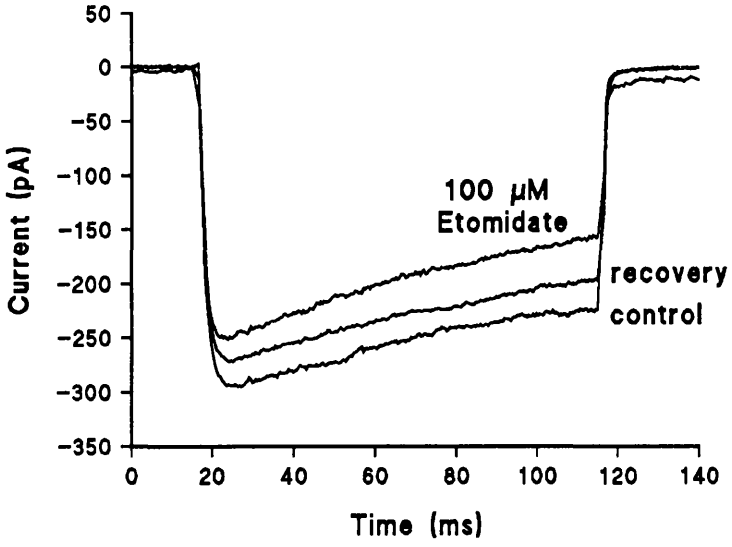
Current (pA)
Time (ms)
100 μM
Etomidate
recovery
control

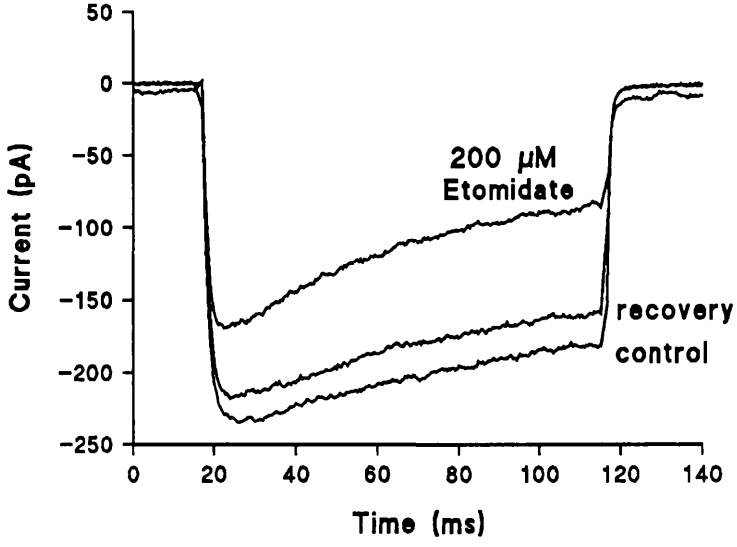
Current (pA)
Time (ms)
200 μM
Etomidate
recovery
control

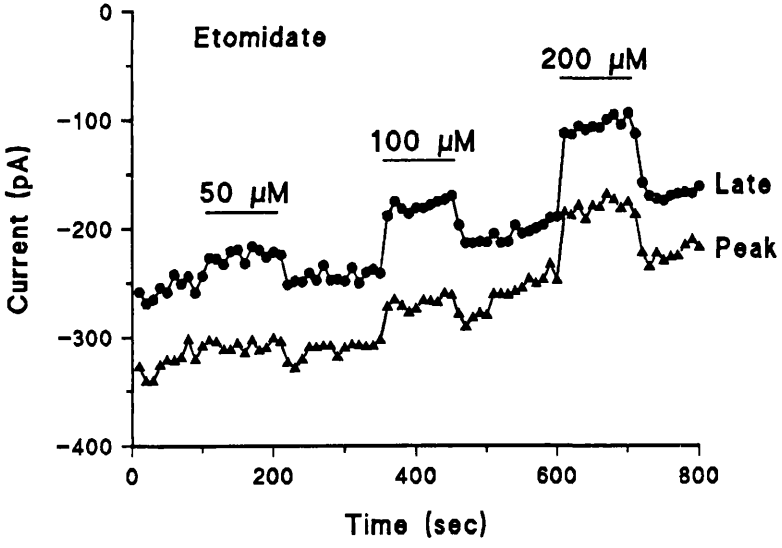
Etomidate
50 μM
100 μM
200 μM
Late
Peak
Current (pA)
Time (sec)

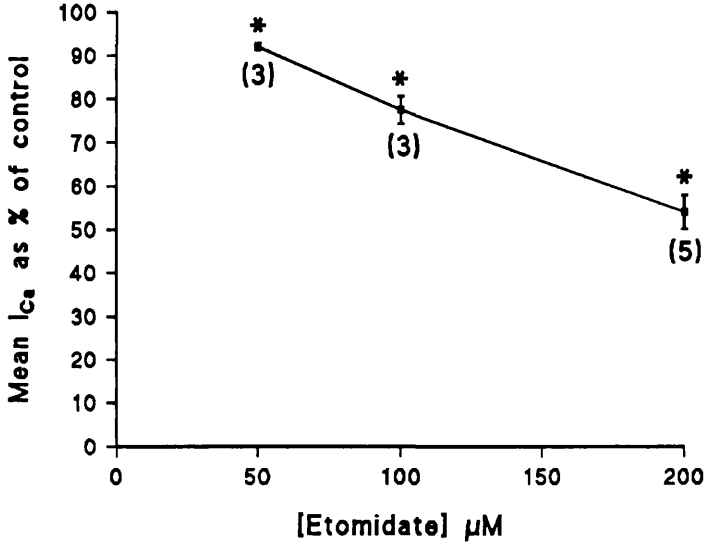
Mean I_{Ca} as % of control
[Etomidate] μM
(3)
(3)
(5)

Figure 4.6.1

Summary of the effects of anaesthetics on the stimulus-dependent inactivation of calcium currents.

The effect of anaesthetics on the time constant for calcium current inactivation is shown in the upper panel. Time constants, derived from exponential curve fitting to the current traces, are expressed as a percentage of corresponding control values. The lower panel shows the dose-dependence of anaesthetic-induced increase in the proportion of inactivating current.

Each data point represents the mean of all accepted experiments. Error bars in the lower panel represent the standard error of the mean. All controls n=54, n for other data points as in previous figures.

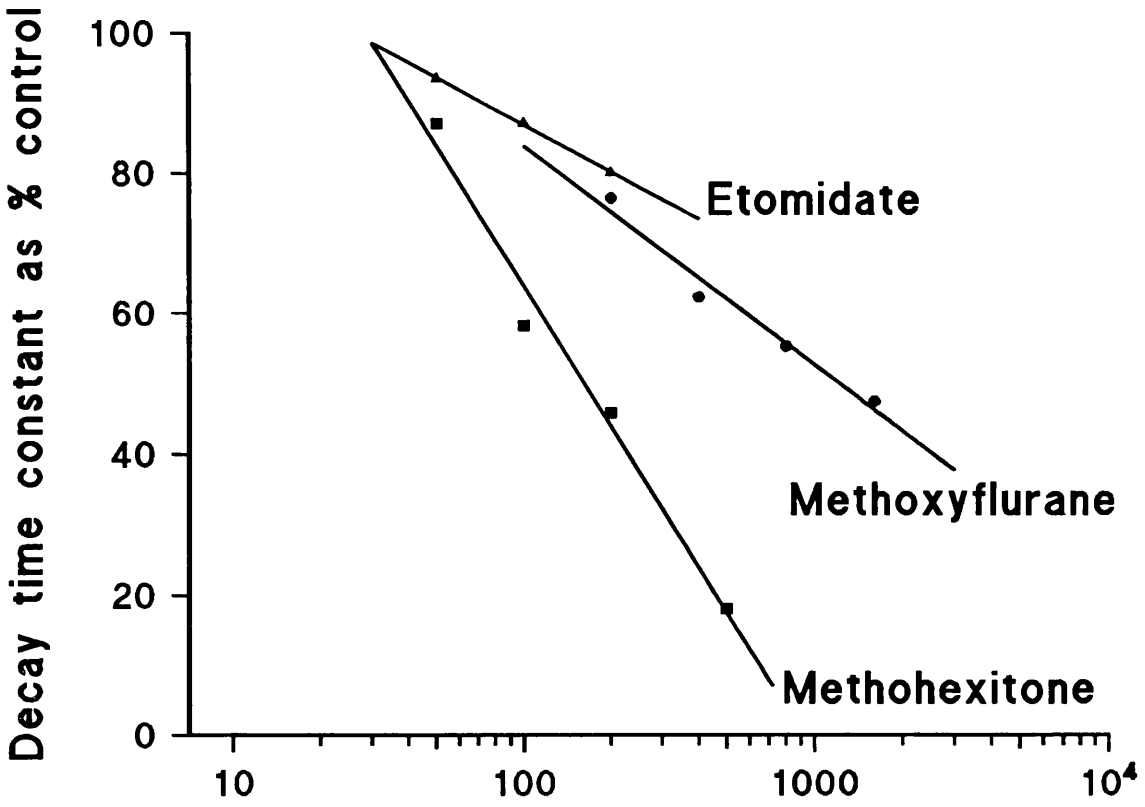
Decay time constant as % control
100
80
60
40
20
0
10
100
1000
10^4
Etomidate
Methoxyflurane
Methohexitone

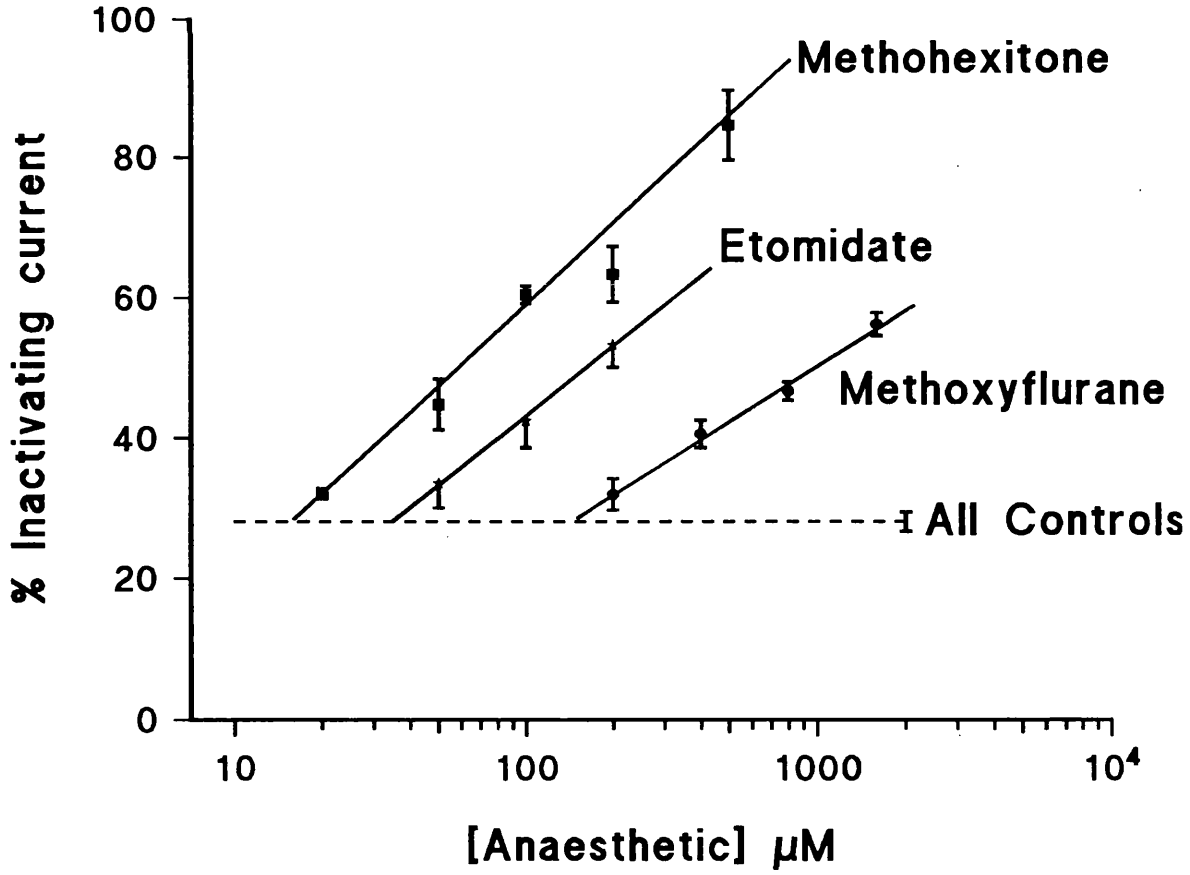
% Inactivating current
100
80
60
40
20
0
10
100
1000
10^4
[Anaesthetic] μM
Methohexitone
Etomidate
Methoxyflurane
All Controls

5. Discussion

5.1 Principal findings

The nAChR and voltage-gated calcium channels of bovine adrenal chromaffin cells are inhibited by a range of anaesthetic agents. The inhibition of the fluxes gated by these channels measured directly by electrophysiological means closely parallels the results of catecholamine secretion and radiolabelled ion studies.

Table 5.1.1

IC_{50}'s for inhibition of nAChR and voltage-gated calcium channels, and for high-K and CCh-evoked catecholamine secretion. (All values expressed as μM).

	P_o of nAChR	Voltage-gated Ca^{2+}-current	Catecholamine Secretion * K^+	CCh
Procaine	50	~2000	>3200	35
Methoxyflurane	250	1300	1200	250
Methohexitone	100	150	130	22
Etomidate	50	200	150	35

The nAChR is more sensitive than the voltage-gated Ca^{++} channels, markedly so in the case of procaine. The findings for the two channel types are discussed below.

5.2 The Nicotinic Acetylcholine Receptor

The characteristics of nicotinic gated currents recorded in the absence of drugs were very similar to those reported previously in bovine adrenal chromaffin cells (Fenwick et al 1982a, Clapham & Neher 1984 a&b, Cull-Candy et al 1988) and sympathetic ganglia (Mathie et al 1987 & 1991). The slow time

* Charlesworth et al 1992 (procaine), Pocock & Richards 1988 (methoyflurane), Pocock & Richards unpublished (methohexitone & etomidate)

constant of the burst length distribution (10.1 ms, small whole cell; 10.6 ms cell attached) and the time constant of the Lorentzian fitted to the control noise spectra (10.2 ms 10 μM CCh; 8.5 ms 25 μM CCh) agree well with values found in the above studies. Single channel conductance (from single channel studies=45 pS; estimated from noise=32 pS) was also similar to comparable values.

5.2a Anaesthetic modulation

5.2a(i) Single channel parameters

The clearest feature of the action of all four agents studied on nAChR channel gating was a dose-dependent reduction in mean open time, described by the relation 1/(mean open time) = α + f.c. (see fig. 3.6.1). The effect on the frequency of channel opening was variable, falling with methoxyflurane, but rising with etomidate and methohexitone. Despite this, the overall effect of each agent was to reduce the probability of the channel being in the open state, to a degree which accounts for the inhibition of CCh evoked catecholamine secretion. Methohexitone is an apparent exception to this correlation, the P_{open} in response to 2 μM CCh being much less sensitive to this agent than the CCh evoked secretion. However, the mean inward current evoked by 25 μM CCh was inhibited by methohexitone more strongly (IC_{50} 30 μM). This suggests that the action of methohexitone may be dependent on agonist concentration.

None of the anaesthetics altered the conductance of the open channel when the effects of filtering are taken into account.

A simple three state sequential blocking model failed to account for the actions of the anaesthetics, principally because burst length fell with increasing concentrations of each agent. An extended blocking model, allowing the closure of blocked channels, provides a reasonable framework to explain the data, though cannot provide a complete explanation

for all the agents studied.

In the case of procaine, it was found that mean blocked time was dependent on procaine concentration, and that in the presence of procaine the distribution of brief closures showed two populations. This implies the existence of two (or more) blocked states, at least one of which has an unblocking rate constant modulated by procaine.

Closed time distributions drawn from data obtained in the presence of methohexitone (fig.3.4.3) and etomidate (fig. 3.5.3) were consistent with a single population of brief closures whose mean duration was unaltered by increasing anaesthetic concentration, while their frequency relative to long closures rose. As mentioned previously the nature of these data is such that it is difficult to support firm statements based on long closed times.

It is however clear that in the presence of methohexitone and etomidate, the frequency of channel activations (burst frequency) rose. This must imply that anaesthetic destabilises a closed state of the channel relative to an open state, which clearly cannot be accommodated by models postulating only open channel states as anaesthetic targets. The most conservative change to the extended blocking model which incorporates these findings is:

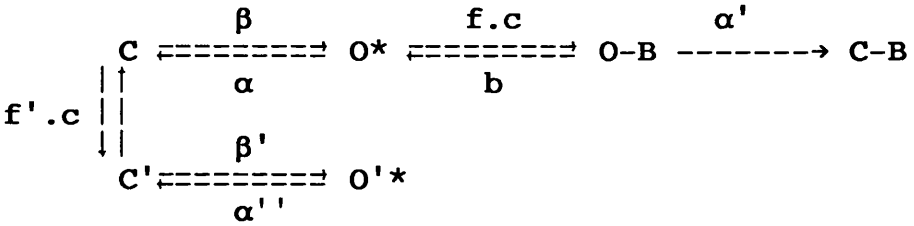

The effect of methoxyflurane on open state lifetimes can be explained by a two closed, two open state model, with no blocked states (the left-hand part of the above diagram). Such

a model however predicts that fast and slow time constants of open lifetime distributions should be independent of anaesthetic concentration, while the relative areas of the two populations changes. This was not found to be the case: while A_f/A_s does rise (modestly) with increasing methoxyflurane concentration, τ_s also falls, consistent with the extended blocking model.

Further support for this model being applicable to the action of methoxyflurane can be drawn from the findings of Dilger & Brett (1991b) and Murrell et al (1991). As a series of n-alcohols is ascended from C_4 to C_{10}, b, the unblocking rate constant, falls (approximately e-fold per C). The rate of blocked channel closure, α', varies little and shows no linear trend. Consequently b/α' falls and less oscillatory behaviour is induced as the series is ascended. In the presence of decanol, channel openings are brief, isolated events, very similar in appearance to those recorded in the presence of methoxyflurane in the present study. Decanol has a similar membrane:buffer partition coefficient to methoxyflurane; structurally similar anaesthetics (halogenated ethers) such as isoflurane and enflurane which have much lower partition coefficients dissociate from the open channel more readily and do induce channel flicker.

The correlation between the unblocking rate constant and membrane:buffer partition coefficient shows that the anesthetic/alcohol binding site(s) is very hydrophobic. This explains why highly lipophilic agents do not induce bursts of channel openings. The relative invariance of α' implies that the closure of blocked channels is relatively agent-independent.

While the rise in burst frequency seen with methohexitone and etomidate cannot be accommodated by the extended block model, the (modest) fall brought about by methoxyflurane can. If it is assumed that the release of methoxyflurane from the closed blocked channel is slow relative to the channel opening

rate, β, the number of receptor-channels capable of being activated by agonist will fall as a significant proportion of the receptor population will be in the inactive closed-blocked state at any time.

5.2a(ii) Spectral Analysis

Spectral analysis of the action of the anaesthetics on agonist induced current fluctuations demonstrated reductions in open channel lifetime consistent with the decrease observed in single channel studies. Procaine alone caused a second high frequency component to appear in the power spectra, reflecting the duration of brief individual channel openings, while the low frequency component corresponds to the duration of bursts of openings. As expected, methoxyflurane increased the corner frequency and depressed the intercept without introducing a second spectral component. Considering the appearance of single channel currents recorded in the presence of etomidate and methohexitone, it was somewhat surprising that a high frequency component was not seen in the power spectra. This was probably because the ratio of mean burst length:mean open time was not large enough in the case of these agents for two distinct components to be resolved.

The apparent discrepancy between control burst length histograms (which fitted to double exponential functions), and control power spectra, (which fitted to single Lorentzian functions), is easily explained. The ratio of the current carried by the fast and slow components of the burst length histogram is 1:9. The ratio of the power (=amplitude^2) of the two components is therefore 1:81. Hence the S_0 value of the high frequency component will be very small, consistent with the observed result.

Of the agents studied, only procaine displayed voltage-dependence in its action. This was seen as a decrease in the ratio of S_{01}:S_{02} . Since the two spectral components probably

relate to bursts of openings (S_{01}) and individual openings (S_{02}), the effect of hyperpolarisation is to increase the proportion of current carried by single channel openings relative to bursts of openings i.e the number of openings per burst falls. Examination of the equations describing the extended blocking model shows that this must be due to a decrease in b, the rate constant for channel unblocking, with hyperpolarisation, assuming α' is voltage independent. (Changes in f only influence the number of openings/burst wh en b is much higher than was found for procaine). Thus procaine binding becomes stronger at more negative potentials. However, the voltage dependence of procaine's action is rather weak. The ratio $S_{01}:S_{02}$ changed e-fold for 55 mV. However, the ratio of the amplitudes (amplitude=$\sqrt{}$power) of the two components would change e-fold for a 90 mV change, similar to that found by Gage et al (1983). This is a much weaker dependence than is found for QX222 (e-fold for 32 mV, Neher & Steinbach 1978). It is possible that procaine has a single site of action, which is weakly voltage dependent. Alternatively it may act at two sites: one strongly dependent on voltage (possibly identical to the QX222 site), the other voltage independent. The sites may be occupied by the charged and uncharged forms respectively.

5.3 Voltage-gated Calcium Channels

Calcium currents elicited by step depolarisations to potentials greater than -30 mV in chromaffin cells comprised two distinguishable components. One component displayed little stimulus-dependent inactivation, was relatively insensitive to holding potential and was blocked by nicardipine, properties characteristic of currents carried by L-type channels. A second component showed marked decay, was highly dependent on holding potential and was less sensitive to nicardipine. This component was probably carried by N-type channels. An equal proportion of both components was blocked by ω-conotoxin. No

evidence for T-type channel activity was found: calcium currents were not evoked by test pulses to voltages below those which activated the currents described above. Also no inward current remained after exposure to 50 μM $CdCl_2$, which only partly blocks T-type channels (Nowycky et al 1985).

These results are similar to the findings of Fenwick et al (1982b), Hans et al (1990) and Bossu et al (1991b), but differ from those of Hoshi et al (1984) and Artalejo (1991) (see introduction). Calcium current, particularly the inactivating component, increased markedly with hyperpolarisation and no evidence of facilitation current in response to large pre-pulses or increased stimulation frequency was observed. The bathing and recording solutions used in the present study were essentially identical to those employed by Artalejo et al (1991 a&b). At present it seems that differences in the cell populations are most likely to explain the different findings, but further work is required to clarify the issue.

5.3a Anaesthetic Modulation

Each of the anaesthetics tested reduced voltage-gated calcium currents in a dose-dependent manner and with an IC_{50} for inhibition close to that for the inhibition of K-evoked catecholamine secretion (see table 5.1.1). For the agents other than procaine, this inhibition was accompanied by a dose-related increase in the proportion of inactivating current and its rate of decay. The magnitude of these effects varied, decreasing in the order methohexitone > methoxyflurane > etomidate. Procaine had no effect on the rate of current inactivation.

All these agents (particularly methohexitone) increased the magnitude of the inactivating current component. It does not seem possible therefore that the anaesthetic induced decrease in calcium current could be attributed to a wholly selective inhibition of the non-inactivating component. This may be

compared with the action of nicardipine: in the presence of this agent, calcium current is reduced and the *relative* magnitude of the inactivating component increases, but the *absolute* magnitude remains constant, indicating selective removal of non-inactivating L-type current.

Differential effects of anaesthetics on N and L channel types based on whole cell current data have been reported by Gross & MacDonald (1988), who concluded that pentobarbitone reduced the amplitude of L-current while it increased the decay rate of N-current. In the presence of pentobarbitone, however, currents showed an increase in the absolute magnitude of inactivating current (fig.1 in above reference) appearing similar to those in the presence of methohexitone in the present study. The analysis, which ascribes components of multi-exponential curve fits to channel-types is problematic when investigating agents which alter decay rates. The observed result could have been due to an enhancement of L-current inactivation, such that it decayed in the manner of control N-current.

In the absence of single channel data it is difficult to determine the mechanism of anaesthetic-calcium channel interactions unambiguously. However, conclusions concerning likely mechanisms can be drawn from the appearance of whole cell currents:

i) Enhanced current decay rate implies that the active channel is a target for anaesthetic, whether it is blocked directly or the rate of channel closure is increased through an allosteric interaction.

ii) Reduction in peak current is explicable either by: (i) an inhibition of active channels which developes rapidly compared to the rate of channel activation, or (ii) the prevention of channel opening.

iii) Unaltered tail current decay rate implies that at the end of the depolarising pulse channels which are open close normally. Decreased tail current amplitude implies that a higher proportion are in an inactive state at the end of the test pulse, relative to control.

Moderate concentrations of methohexitone enhanced current decay with little or no depression of peak current. The action of this agent is explicable on the basis of inhibition of active channels. The rate of open channel inhibition (assuming first order kinetics) should equal f x [methohexitone] and would thus rise with increasing methohexitone concentration, explaining the depression of peak current in 500 μM. Since tail current analysis shows that the rate of channel closure is unaltered, rapid conversion of active and inactive channels is not possible. The following mechanism would account for these findings:

$$C \rightleftharpoons O^* \longrightarrow O\text{-}B \longrightarrow C\text{-}B$$

in which the rates of C-B opening and O-B unblocking are negligible, relative to the duration of the voltage pulse. The observation that the effect of methohexitone on peak current amplitude increases with successive stimuli is accommodated by such a model assuming that release of methohexitone from the closed-blocked state (C-B) is slow relative to the time between voltage pulses (10 s), such that the number of channels available for activation (i.e in the C rather than C-B state) is progressively reduced.

In contrast, methoxyflurane produced a significant depression in peak current, even at low concentrations, at which current decay rate was only moderately enhanced. While a component of methoxyflurane's action must therefore be an inhibition of open channels, it seems unlikely that it is the only, or indeed the major action. The simplest explanation is that methoxyflurane also prevents channels from opening. The

maximal effect of methoxyflurane was achieved with the first voltage pulse, consistent with closed channels being an important anaesthetic target.

Similar reasoning could explain the action of etomidate, assuming that the importance of closed channels, relative to open channels, as a site of anaesthetic action was greater. By extension, it appears that procaine acts solely by preventing resting channels from opening.

5.4 Synaptic Transmission

As described in the introduction, central excitatory synapses have been shown to be highly sensitive to clinically relevant concentrations of anaesthetics and it is pertinent to examine what implications the results presented here have in this regard.

Reduction of the calcium influx necessary to trigger neurosecretion by inhibition of voltage-gated calcium channels would be expected to depress synaptic transmission. At relevant concentrations the reduction in mean calcium current seen was relatively small, being of the order of 25 % for methohexitone, somewhat less for methoxyflurane and negligible for etomidate. The relationship between calcium influx and transmitter release from nerve endings is however very steep (Richards & Sercombe 1970, Dodge & Rahamimof 1967), thus it is possible that small reductions in calcium entry could lead to a much larger depression in neurosecretion.

There is also evidence that certain channel types may play a dominant role in mediating neurosecretion (Hirning et al 1988, Perney et al 1986, Stanley & Atrakchi 1990, Rane et al 1987). If such channels were preferentially inhibited by anaesthetics substantial inhibition of release may occur with modest reductions in total calcium current. In the absence of clear differential effects of anaesthetics on channel subtypes such mechanisms are only speculative at present.

Other factors will be important in determining the effect which modulation of calcium channels has on transmitter release and synaptic transmission. The degree to which enhanced current decay reduces the total flux will depend on the stimulus length. Depolarisation of chromaffin cells is due mainly to current flow through nAChR, rather than rapidly inactivating voltage-gated sodium channels. Depending on the longevity of secreted ACh, the 100 ms stimuli applied experimentally may be less than that experienced *in vivo*. If this were the case, the degree of current inhibition produced by anaesthetics would be greater, especially so in the case of methohexitone.

The extent to which synaptic transmission is altered will also depend on the relative quantity of transmitter released compared with the number of post-synaptic receptors. If released transmitter saturates the available receptors, anaesthetic-induced reductions in neurosecretion may have a relatively minor effect on transmission: in the reverse situation it would have a major effect.

In either case loss of post-synaptic receptor function would be expected to contribute to the depression of synaptic transmission. All the agents studied caused significant reductions in the open probability of the nAChR and would thereby impair stimulus-secretion coupling in chromaffin cells. More generally, they would be expected to impair transmission at nicotinic synapses. While there are nicotinic synapses in the CNS, there is no evidence that they are relevant to anaesthesia. Nevertheless, the chromaffin cell serves as an experimentally amenable model for excitatory synaptic transmission.

To date little work has been done at a channel level on receptors which might be expected to be involved in the development of anaesthesia, principally the sub-classes of glutamate receptors. An exception is the study of the blockade of NMDA receptor channels by ketamine (MacDonald and Nowak, 1991).

5.5 Limitations of the single channel analysis

As discussed previously (section 3.6a)there are problems inherent in accurately defining bursts of openings. This places severe restrictions on the ability to quantify models for the action of anaesthetics on the nAChR. The values derived from curve fits to the mean burst length data (p.92) are probably only relevant for comparison between agents. The conclusion that the *relative* probability of blocked channels to re-open rather than enter a long-lived closed state decreases in the order procaine > methohexitone ≈ etomidate >> methoxyflurane is likely to be valid. This is because the value of b/α' is relatively insensitive to changes in $1/(b+\alpha')$ (apparent mean blocked time), the derived value of which varies depending on the value of t_{crit} chosen.

The essential features of the extended blocking model probably describe, in outline if not in detail, the action of the agents studied on the nAChR. Inverse mean open time is linearly related to drug concentration for each of the anaesthetics studied, which is consistent with the open state of the channel being a primary target for these agents. However, a simple sequential blocking model was clearly inadequate; to be consistent with the data, a pathway from the open-blocked state (O-B) to closed state(s), without a return to the open state, must exist. The inability to define this pathway was an inherent weakness in the experimental and analytical approach adopted. As drawn on p.25 & 91 the scheme for the extended blocking model is incomplete since no pathways leading from the closed-blocked (C-B) state are indicated. It is possible that a C-B → C transition occurs; alternatively, or in addition, the C-B state may return, slowly, to the O-B state. It is not possible to distinguish between these alternatives, or to quantify them with the methods used in this study. This is because long closures cannot be interpreted meaningfully.

The rate of regeneration of drug-free, closed channels (C) can be estimated by an alternative approach. The amplitude of successive macroscopic currents, elicited by a train of brief applications of agonist, is expected to decline in the presence of a blocking drug, assuming that drug dissociation is slow relative to the interpulse interval. Current amplitude reaches a steady level when the number of channels blocked during each pulse equals the number from which drug dissociates between pulses. The rate at which this level is achieved is clearly related to the rate of drug dissociation. This can of course also be more directly determined from the rate of increase of current amplitude following removal of the blocking drug. Such methods have been used by Gurney & Rang (1984) to examine the blocking action of methonium compounds on ganglionic nAChR and by MacDonald et al (1991) to investigate the action of dissociative anaesthetics on NMDA-gated channels.

Conclusion

A representative range of anaesthetic agents have been shown to inhibit nicotinic receptor channels and voltage-gated calcium channels in bovine adrenal chromaffin cells. A common mechanism, the extended block model, was found to account for many features of the blockade of nicotinic channels by each of the agents studied. However, certain aspects of the action of the agents investigated were not compatible with this model and required additional explanation.

Macroscopic voltage-gated calcium currents were somewhat less sensitive to the anaesthetics studied. The inhibitory action of methohexitone could be explained on the basis of an inhibition of open channels, while for the other agents, both closed and open channels were anaesthetic targets.

These results show that anaesthetics are likely to depress excitatory synaptic transmission, for which the chromaffin cell serves as a model system, both at post-synaptic and pre-synaptic sites.

6. References

Anderson, C.R. and Stevens, C.F. (1973). Voltage clamp analysis of acetylcholine produced endplate current fluctuations at frog neuro-muscular junction. *J. Physiol. Lond.* **235**, 655-691.

Adams, P.R. (1975). A model for the procaine end-plate current. *J. Physiol. Lond.* **246**, 61P-63P.

Adams, P.R. (1976). Drug blockade of open end-plate channels. *J. Physiol. Lond.* **260**, 531-552.

Adams, P.R. (1977). Voltage jump analysis of procaine action at frog end-plate. *J. Physiol. Lond.* **268**, 291-318.

Artalejo, C.R., Ariano, M.A., Perlman, R.L. and Fox, A.P. (1990). Activation of facilitation calcium channels in chromaffin cells by D_1 dopamine receptors through a cAMP/protein kinase A- dependent mechanism. *Nature* **348**, 239-42.

Artalejo, C.R., Dahmer, M.K., Perlman, R.L. and Fox, A.P. (1991a). Two types of Ca^{2+} currents are found in bovine chromaffin cells: facilitation is due to the recruitment of one type. *J. Physiol. Lond.* **432**, 681-707.

Artalejo, C.R., Mogul, D.J., Perlman, R.L. and Fox, A.P. (1991b). Three types of bovine chromaffin cell Ca^{2+} channels: Facilitation increases the opening probability of a 27 pS channel. *J. Physiol. Lond.* **444**, 213-240.

Ashcroft, R.G., Coster, H.G. and Smith, J.R. (1977a). The molecular organisation of bimolecular lipid membranes. The effect of benzyl alcohol on the structure. *Biochim. Biophys. Acta* **469**, 13-22.

Ashcroft, R.G., Coster, H.G. and Smith, J.R. (1977b). Local anaesthetic benzyl alcohol increases membrane thickness. *Nature* **269**, 819-20.

Barker, J.L., Harrison, N.L., Lange, G.D. and Owen, D.G. (1987). Potentiation of γ-aminobutyric-acid-activated chloride conductance by a steroid anaesthetic in cultured rat spinal neurones. *J. Physiol. Lond.* **386**, 485-501.

Barker, J.L. and Ransom, B.R. (1978). Pentobarbitone pharmacology of mammalian central neurones grown in tissue culture. *J. Physiol. Lond.* **280**, 355-372.

Berg-Johnsen, J. and Langmoen, I.A. (1986a). Isoflurane effects in rat hippocampal cortex: a quantitative evaluation of different cellular sites of action. *Acta Physiol. Scand.* **128**, 613-618.

Berg-Johnsen, J. and Langmoen, I.A. (1986b). The effect of isoflurane on unmyelinated and myelinated fibres in the rat brain. *Acta Physiol. Scand.* **127**, 87-93.

Berg-Johnsen, J. and Langmoen, I.A. (1990). Mechanisms concerned in the direct effect of isoflurane on rat hippocampal and human neocortical neurones. *Brain Res.* **507**, 28-34.

Bigornia, L., Suozzo, M., Ryan, K.A., Napp, D. and Schneider, A.S. (1988). Dopamine receptors on adrenal chromaffin cells modulate calcium uptake and catecholamine release. *J. Neurochem.* **51**, 999-1006.

Boggs, J.M., Yoong, T. and Hsia, J.C. (1976). Site and mechanism of anesthetic action. I. Effect of anesthetics and pressure on fluidity of spin-labeled lipid vesicles. *Mol. Pharmacol.* **12**, 127-35.

Bormann, J. and Clapham, D.E. (1985). γ-Aminobutyric acid receptor channels in adrenal chromaffin cells: a patch-clamp study. *Proc. Natl. Acad. Sci. USA* **82**, 2168-72.

Charlesworth, P., Jacobson, I., Pocock, G. and Richards, C.D. (1992). The mechanism by which procaine inhibits catecholamine secretion from bovine chromaffin cells. *Br. J. Pharmacol.* **106**, 802-812.

Bosnjak, Z.J., Seagard, J.L., Wu, A. and Kampine, J.P. (1982). The effects of halothane on sympathetic ganglionic transmission. *Anesthesiology.* **57**, 473-9.

Bosnjak, Z.J., Supan, F.D. and Rusch, N.J. (1991). The effects of halothane, enflurane, and isoflurane on calcium current in isolated canine ventricular cells. *Anesthesiology.* **74**, 340-5.

Bossu, J.L., De Waard, M. and Feltz, A. (1991a). Inactivation characteristics reveal two calcium currents in adult bovine chromaffin cells. *J. Physiol. Lond.* **437**, 603-20.

Bossu, J.L., De Waard, M. and Feltz, A. (1991b). Two types of calcium channels are expressed in adult bovine chromaffin cells. *J. Physiol. Lond.* **437**, 621-34.

Brett, R.S., Dilger, J.P. and Yland, K.F. (1988). Isoflurane causes "flickering" of the acetylcholine receptor channel: observations using the patch clamp. *Anesthesiology.* **69**, 161-70.

Buch, H., Knabe, J., Buzello, W. and Rummel, W. (1970). Stereospecificity of anesthetic activity, distribution, inactivation and protein binding of the optical antipodes of two N-methylated barbiturates. *J. Pharmacol. Exp. Ther.* **175**, 709-716.

Cena, V., Nicolas, G.P., Sanchez Garcia, P., Kirpekar, S.M. and Garcia, A.G. (1983). Pharmacological dissection of receptor-associated and voltage- sensitive ionic channels involved in catecholamine release. *Neuroscience.* **10**, 1455-62.

Charlesworth, P., Pocock, G. and Richards, C.D. (1991). Calcium currents in bovine chromaffin cells. *J. Physiol. Lond.* **438**, 105P.

Colquhoun, D. and Hawkes, A.G. (1977). Relaxation and fluctuations of membrane currents that flow through drug-operated channels. *Proc. R. Soc. Lond. B.* **199**, 231-262.

Charnet, P., Labarca, C., Leonard, R.J., Vogelaar, N.J., Czyzyk, L., Gouin, A., Davidson, N. and Lester, H.A. (1990). An open-channel blocker interacts with adjacent turns of alpha- helices in the nicotinic acetylcholine receptor. *Neuron.* **4**, 87-95.

Charnet, P., Labarca, C., Cohen, B.N., Davidson, N., Lester, H.A. and Pilar, G. (1992). Pharmacological and kinetic properties of α4β2 neuronal nicotinic acetylcholine receptors expressed in *Xenopus* oocytes. *J. Physiol. Lond.* **450**, 375-394.

Cheek, T., O'Sullivan, A.J., Moreton, R.B., Berridge, M.J. and Burgoyne, R.D. (1989). Spatial localization of the stimulus-induced rise in cytosolic calcium in bovine adrenal chromaffin cells. *FEBS Lett.* **247(2)**, 429-434.

Cherkin, A. and Catchpool, J.F. (1964). Temperature dependence of anesthesia in goldfish. *Science* **144**, 1460-1462.

Clapham, D.E. and Neher, E. (1984a). Trifluoperazine reduces inward ionic currents and secretion by separate mechanisms in bovine chromaffin cells. *J. Physiol. Lond.* **353**, 541-64.

Clapham, D.E. and Neher, E. (1984b). Substance P reduces acetylcholine-induced currents in isolated bovine chromaffin cells. *J. Physiol. Lond.* **347**, 255-77.

Colquhoun, D. and Sakmann, B. (1981). Fluctuations in the microsecond time range of the current through single acetylcholine receptor ion channels. *Nature* **294**, 464-6.

Colquhoun, D., and B. Sakmann. 1983. Bursts of openings in transmitter-activated ion channels. In Single-channel recording. B. Sakmann, and E. Neher, editors. Plenum, New York. 345-363.

Connolly, J., Boulter, J. and Heinemann, S.F. (1992). α4-2β2 and other nicotinic acetylcholine receptor subtypes as targets of psychoactive and addictive drugs. *Br. J. Pharmacol.* **105**, 657-666.

Cooper, E., Couturier, S. and Ballivet, M. (1991). Pentameric structure and subunit composition of a neuronal nicotinic acetylcholine receptor. *Nature* **350**, 235-238.

Cottrell, G.A., Lambert, J.J. and Peters, J.A. (1987). Modulation of $GABA_A$ receptor activity by alphaxalone. *Br. J. Pharmacol.* **90**, 491-500.

Crawford, J.M. (1970). Anaesthetic agents and the chemical sensitivity of cortical neurones. *Neuropharmacology* **9**, 31-46.

Cull-Candy, S.G., Mathie, A. and Powis, D.A. (1988). Acetylcholine recptor channels and their block by clonidine in cultured bovine chromaffin cells. *J. Physiol. Lond.* **402**, 255-278.

Deneris, E.S., Connolly, J., Rogers, S.W. and Duvoisin, R. (1991). Pharmacalogical and functional diversity of neuronal nicotinic acetylcholine receptors. *Trends Pharmacol. Sci.* **12**, 34-40.

Derome, G., Tseng, R., Mercier, P., Lemaire, I. and Lemaire, S. (1981). Possible muscarinic regulation of catecholamine secretion mediated by cyclic GMP in isolated bovine adrenal chromaffin cells. *Biochem. Pharmacol.* **30**, 855-60.

Dilger, J.P., Brett, R.S., Poppers, D.M. and Liu, Y. (1991a). The temperature dependence of some kinetic and conductance properties of acetylcholine receptor channels. *Biochim. Biophys. Acta* **1063**, 253-8.

Dilger, J.P. and Brett, R.S. (1991b). Actions of volatile anesthetics and alcohols on cholinergic receptor channels. *Ann. N. Y. Acad. Sci.* **625**, 616-27.

Dodge, F.A. and Rahamimoff, R. (1967). Co-operative action of calcium ions in transmitter release at the neuromuscular junction. *J. Physiol. Lond.* **193**, 419-432.

Doroshenko, P. and Neher, E. (1991). Pertussis-toxin-sensitive inhibition by (-) baclofen of Ca signals in bovine chromaffin cells. *Pflugers Arch.* **419**, 444-449.

Douglas, W.W. and Rubin, R.P. (1963). The mechanism of catecholamine release from the adrenal medulla and the role of calcium in stimulus-secretion coupling. *J. Physiol. Lond.* **167**, 288-310.

el-Beheiry, H. and Puil, E. (1989). Anaesthetic depression of excitatory synaptic transmission in neocortex. *Exp. Brain Res.* **77**, 87-93.

Evans, R.H. and Hill, R.G. (1978). GABA-mimetic action of etomidate. *Experientia.* **34**, 1325-27.

Feldberg, W., Minz, B. and Tsudzimura, H. (1934). The mechanism of the nervous discharge of adrenaline. *J. Physiol. Lond.* **81**, 286-304.

Fenwick, E.M., Marty, A. and Neher, E. (1982a). A patch clamp study of bovine chromaffin cells and of their sensitivity to acetylcholine. *J. Physiol. Lond.* **331**, 577-597.

Fenwick, E.M., Marty, A. and Neher, E. (1982b). Sodium and calcium channels in bovine chromaffin cells. *J. Physiol. Lond.* **331**, 599-635.

Fieber, L.A. and Adams, D.J. (1991). Acetylcholine-evoked currents in cultured neurones dissociated from rat parasympathetic cardiac ganglia. *J. Physiol. Lond.* **434**, 215-237.

Fox, A.P., Nowycky, M.C. and Tsien, R.W. (1987a). Kinetic and pharmacological properties distinguishing three types of calcium currents in chick sensory neurones. *J. Physiol. Lond.* **394**, 149-72.

Fox, A.P., Nowycky, M.C. and Tsien, R.W. (1987b). Single-channel recordings of three types of calcium channels in chick sensory neurones. *J. Physiol. Lond.* **394**, 173-200.

Franks, N.P. and Lieb, W.R. (1978). Where do general anaesthetics act?. *Nature* **274**, 339-342.

Franks, N.P. and Lieb, W.R. (1979). The structure of lipid bilayers and the effects of general anaesthetics. *J. Mol. Biol.* **133**, 469-500.

Franks, N.P. and Lieb, W.R. (1982). Molecular mechanisms of general anaesthesia. *Nature* **300**, 487-493.

Franks, N.P. and Lieb, W.R. (1984). Do general anaesthetics act by competitive binding to specific receptors?. *Nature* **310**, 599-601.

Franks, N.P. and Lieb, W.R. (1988). Volatile general anaesthetics activate a novel neuronal K^+ current. *Nature* **333**, 662-664.

Franks, N.P. and Lieb, W.R. (1991). Stereospecific effects of inhalational general anesthetic optical isomers on nerve ion channels. *Science* **254**, 427-30.

Gage, P.W. and Hamill, O.P. (1976). Effects of several inhalation anaesthetics on the kinetics of postsynaptic conductance changes in mouse diaphragm. *Br. J. Pharmacol.* **57**, 263-72.

Gage, P.W., Hamill, O.P. and Wachtel, R.E. (1983). Sites of action of procaine at the motor end-plate. *J. Physiol. Lond.* **335**, 123-37.

Gage, P.W. and McKinnon, D. (1985). Effects of pentobarbitone on acetylcholine-activated chanels in mammalian muscle. *Br. J. Pharmac.* **85**, 229-235.

Gage, P.W. and Robertson, B. (1985). Prolongation of inhibitory currents by pentobarbitone, halothane and ketamine in CA1 pyramidal cells in rat hippocampus. *Br. J. Pharmacol.* **85**, 675-681.

Gage, P.W. and Sah, P. (1982). Postsynaptic effects of some central stimulants at the neuromuscular junction. *Br. J. Pharmacol.* **75**, 493-502.

Galindo, A. (1969). Effects of procaine, pentobarbital and halothane on synaptic transmission in the central nervous system. *J. Pharmacol. Exp. Ther.* **169**, 185-95.

Gardner, P., Ogden, D.C. and Colquhoun, D. (1984). Conductances of single ion channels opened by nicotinic agonists are indistinguishable. *Nature* **309**, 160-162.

Gross, A., Ballivet, M., Rungger, D. and Bertrand, D. (1991). Neuronal nicotinic acetylcholine receptors expressed in *Xenopus* oocytes: role of the α subunit in agonist sensitivity and desensitization. *Pflugers Arch.* **419**, 545-551.

Gurney, A.M. and Rang, H.P. (1984). The channel-blocking action of methonium compounds on rat submandibular ganglion cells. *Br. J. Pharmacol.* **82**, 623-642.

Gross, R.A. and MacDonald, R.L. (1988). Differential actions of pentobarbitone on calcium current components of mouse sensory neurones in culture. *J. Physiol. Lond.* **405**, 187-203.

Halliwell, J.V. (1990). K^+ channels in the central nervous system. In Potassium channels: structure, classification, function and therapeutic potential. N.S. Cook, editor. Ellis Horwood, Chichester. 348-381.

Halsey, M.J., Wardley Smith, B. and Green, C.J. (1978). Pressure reversal of general anaesthesia - a multi-site expansion hypothesis. *Br. J. Anaesth.* **50**, 1091-17.

Hamill, O.P., Marty, A., Neher, E., Sackmann, B. and Sigworth, F.J. (1981). Improved patchclamp techniques for high resolution current recordings from cells and cell-free membrane patches. *Pflugers Arch* **391**, 85-100.

Hans, M., Illes, P. and Takeda, K. (1990). The blocking effects of omega-conotoxin on Ca current in bovine chromaffin cells. *Neurosci. Lett.* **114**, 63-68.

Haydon, D.A., Hendry, B.M., Levinson, S.R. and Requena, J. (1977a). The molecular mechanisms of anaesthesia. *Nature* **268**, 356-8.

Haydon, D.A., Hendry, B.M., Levinson, S.R. and Requena, J. (1977b). Anaesthesia by the n-alkanes. A comparative study of nerve impulse blockage and the properties of black lipid bilayer membranes. *Biochim. Biophys. Acta* **470**, 17-34.

Herrington, J., Stern, R.C., Evers, A.S. and Lingle, C.J. (1991). Halothane inhibits two components of calcium current in clonal (GH_3) pituitary cells. *J. Neurosci.* **11**, 2226-40.

Higgins, L.S. and Berg, D.K. (1987). Immunological identification of a nicotinic acetylcholine receptor on bovine chromaffin cells. *J. Neurosci.* **7**, 1792-98.

Hirano, T., Kidokoro, Y. and Ohmori, H. (1987). Acetylcholine dose-response relation and the effect of cesium ions in the rat adrenal chromaffin cell under voltage clamp. *Pflugers. Arch.* **408**, 401-407.

Hirning, L.D., Fox, A.P., McCleskey, E.W., Olivera, B.M., Thayer, S.A., Miller, R.J. and Tsien, R.W. (1988). Dominant role of N-type calcium channels in evoked release of norepinephrine from sympathetic neurons. *Science* **239**, 57-60.

Holz, R.W., Senter, R.A. and Frye, R.A. (1982). Relationship between Ca^{2+} uptake and catecholamine secretion in primary dissociated cultures of adrenal medulla. *J. Neurochem.* **39**, 635-46.

Hoshi, T., Rothlein, J. and Smith, S.J. (1984). Facilitation of Ca^{2+}-channel currents in bovine adrenal chromaffin cells. *Proc. Natl. Acad. Sci. USA* **81**, 5871-55.

Hoshi, T. and Smith, S.J. (1987). Large depolarization induces long openings of voltage-dependent calcium channels in adrenal chromaffin cells. *J. Neurosci.* **7**, 571-80.

Hubbell, W.L., Metcalfe, J.C., Metcalfe, S.M. and McConnell, H.M. (1970). The interaction of small molecules with spin-labelled erythrocyte membranes. *Biochim. Biophys. Acta* **219**, 415-27.

Ifune, C.K. and Steinbach, J.H. (1991). Voltage-dependent block by magnesium of neuronal nicotinic acetylcholine receptor channels in rat phaechromocytoma cells. *J. Physiol. Lond.* **443**, 683-701.

Imoto, K., Methfessel, C., Sakmann, B., Mishina, M., Mori, Y., Konno, T., Fukuda, K., Kurasaki, M., Bujo, H., Fujita, Y. and Numa, S. (1986). Location of a delta-subunit region determining ion transport through the acetylcholine receptor channel. *Nature* **324**, 670-674.

Jain, M.K., Wu, N.Y. and Wray, L.V. (1975). Drug-induced phase change in bilayer as possible mode of action of membrane expanding drugs. *Nature* **255**, 494-6IS.

Jacobson, I., Pocock, G. and Richards, C.D. (1991). Effects of pentobarbitone on the properties of nicotinic channels of chromaffin cells. *Eur. J. Pharmacol.* **202**, 331-339.

Jones, M.V., Brooks, P.A. and Harrison, N.L. (1992). Enhancement of γ-aminobutyric acid-activated Cl- currents in cultured rat hippocampal neurones by three volatile anaesthetics. *J. Physiol. Lond.* **449**, 279-293.

Kao, L.S. and Schneider, A.S. (1985). Muscarinic receptors on bovine chromaffin cells mediate a rise in cytosolic calcium that is independent of extracellular calcium. *J. Biol. Chem.* **260**, 2019-22.

Katz, B. and Miledi, R. (1975). The effect of procaine on the action of acetylcholine at the neuromuscular junction. *J. Physiol. Lond.* **249**, 269-84.

Kendall, T.J.G. and Minchin, M.C.W. (1982). The effects of anaesthetics on the uptake and release of amino acid neurotransmitters in thalamic slices. *Br. J. Pharmacol.* **75**, 219-227.

Knight, D.E. and Baker, P.F. (1983). Stimulus-secretion coupling in isolated bovine adrenal medullary cells. *Q. J. Exp. Physiol.* **68**, 123-43.

Kordas, M. (1970). The effect of procaine on neuromuscular transmission. *J. Physiol. Lond.* **209**, 689-99.

Kress, H.G., Muller, J., Eisert, A., Gilge, U., Tas, P.W. and Koschel, K. (1991). Effects of volatile anesthetics on cytoplasmic Ca^{2+} signaling and transmitter release in a neural cell line. *Anesthesiology.* **74**, 309-19.

Krishtal, O.A. and Pidoplichko, V.I. (1980). A receptor for protons in the nerve cell membrane. *Neuroscience.* **5**, 2325-27.

Krnjevic, K. and Puil, E. (1988). Halothane suppresses slow inward currents in hippocampal slices. *Can. J. Physiol. Pharmacol.* **66**, 1570-1575.

Kullmann, D.M., Martin, R.L. and Redman, S.J. (1989). Reduction by general anaesthetics of group Ia excitatory postsynaptic potentials and currents in the cat spinal cord. *J. Physiol. Lond.* **412**, 277-96.

Kumakura, K., Karoum, F., Guidotti, A. and Costa, E. (1980). Modulation of nicotinic receptors by opiate receptor agonists in cultured adrenal chromaffin cells. *Nature* **283**, 489-92.

Larrabee, M.G. and Posternak, J.M. (1952). Selective action of anaesthetics on synapses and axons in mammalian sympathetic ganglia. *J. Neurophysiol.* **15**, 92-114.

Lawrence, D.K. and Gill, E.W. (1975). Structurally specific effects of some steroid anesthetics on spin-labeled liposomes. *Mol. Pharmacol.* **11**, 280-6.

Lee, A.G. (1976). Interactions between phospholipids and barbiturates. *Biochim. Biophys. Acta* **455**, 102-108.

MacDonald, J.F., Bartlett, M.C., Mody, I., Pahapill, P., Reynolds, J.N., Salter, M.W., Schneiderman, J.H. and Pennefather, P.S. (1991). Actions of ketamine, phencyclidine amd MK-801 on NMDA receptor currents in cultured mouse hippocampal neurones. *J. Physiol. Lond.* **432**, 483-508.

Leonard, R.J., Labarca, C.G., Charnet, P., Davidson, N. and Lester, H.A. (1988). Evidence that the M2 membrane-spanning region lines the ion channel pore of the nicotinic receptor. *Science* **242**, 1578-81.

Lever, M.J., Miller, K.W., Paton, W.D. and Smith, E.B. (1971). Pressure reversal of anaesthesia. *Nature* **231**, 368-71.

Lieb, W.R., Kovalycsik, M. and Mendelsohn, R. (1982). Do clinical levels of general anaesthetics affect lipid bilayers? Evidence from Raman scattering. *Biochim. Biophys. Acta* **688**, 388-98.

Livett, B.G., Kozousek, V., Mizobe, F. and Dean, D.M. (1979). Substance P inhibits nicotinic activation of chromaffin cells. *Nature* **278**, 256-257.

Lodge, D., Anis, N.A. and Burton, N.R. (1982). Effects of optical isomers of ketamine on excitation of cat and rat spinal neurones by amino acids and acetylcholine. *Neurosci. Lett.* **29**, 281-286.

Loring, R.H., Chiappinelli, V.A., Zigmond, R.E. and Cohen, J.B. (1984). Characterization of a snake venom neurotoxin which blocks nicotinic transmission in the avian ciliary ganglion. *Neuroscience.* **11**, 989-999.

MacDonald, J.F. and Nowak, M.K. (1991). Mechanisms of blockade of excitatory amino acid receptor channels. In Trends Pharm. Sci. Special report - The pharmacology of excitatory amino-acids. Elsevier, Cambridge. 25-30.

MacDonald, R.L., Rogers, C.J. and Twyman, R.E. (1989). Barbiturate regulation of kinetic properties of the $GABA_A$ receptor channel of mouse spinal neurones in culture. *J. Physiol. Lond.* **417**, 483-500.

MacIver, M.B. and Kendig, J.J. (1991). Anesthetic effects on resting membrane potential are voltage- dependent and agent-specific. *Anesthesiology*. **74**, 83-8.

Mathie, A., Colquhoun, D. and Cull Candy, S.G. (1990). Rectification of currents activated by nicotinic acetylcholine receptors in rat sympathetic ganglion neurones. *J. Physiol. Lond.* **427**, 625-55.

Mathie, A., Cull Candy, S.G. and Colquhoun, D. (1987). Single-channel and whole-cell currents evoked by acetylcholine in dissociated sympathetic neurons of the rat. *Proc. R. Soc. Lond. Biol.* **232**, 239-48.

Mathie, A., Cull Candy, S.G. and Colquhoun, D. (1991). Conductance and kinetic properties of single nicotinic acetylcholine receptor channels in rat sympathetic neurones. *J. Physiol. Lond.* **439**, 717-50.

Matthews, E.K. and Quilliam, J.P. (1964). Effects of central depressant drugs upon acetylcholine release. *Br. J. Pharmacol.* **22**, 415-440.

McLarnon, J.G., P. Pennefather, and D.M.J. Quastel. 1986. Mechanism of nicotinic channel blockade by anaesthetics. In Molecular and cellular mechanisms of anesthetics. S.H. Roth, and K.W. Miller, editors. Plenum, New York. 155-164.

Metcalfe, J.C., Seeman, P. and Burgen, A.S. (1968). The proton relaxation of benzyl alcohol in erythrocyte membranes. *Mol. Pharmacol.* **4**, 87-95.

Meyer, K.H. (1937). Contributions to the theory of narcosis. *Transactions Of The Faraday Society* **33**, 1062-1068.

Miller, K.W., Paton, W.D., Smith, E.B. and Smith, R.A. (1972). Physicochemical approaches to the mode of action of general anesthetics. *Anesthesiology*. **36**, 339-51.

Miller, R.J. (1987). Multiple calcium channels and neuronal function. *Science* **235**, 46-52.

Minchin, M.C. (1981). The effect of anaesthetics on the uptake and release of γ-aminobutyrate and D-aspartate in rat brain slices. *Br. J. Pharmacol.* **73**, 681-9.

Moss, G.W.J., Lieb, W.R. and Franks, N.P. (1991). Anesthetic inhibition of firefly luciferase, a protein model for general anesthesia, does not exhibit pressure reversal. *Biophys. J.* **60**, 1309-1314.

Mullins, L.J (1954). Some physical mechanisms in narcosis. *Chemical Reviews* **54**, 289-323.

Murphy, B.J., Rogers, C.A., Sunahara, R.K., Lemaire, S. and Tuana, B.S. (1990). Identification, characterization, and photoaffinity labeling of the dihydropyridine receptor associated with the L-type calcium channel from bovine adrenal medulla. *Mol. Pharmacol.* **37**, 173-181.

Murrell, R.D., Braun, M.S. and Haydon, D.A. (1991). Actions of n-alcohols on nicotinic acetylcholine receptor channels in cultured rat myotubes. *J. Physiol. Lond.* **437**, 431-48.

Neher, E. (1983). The charge carried by single-channel currents of rat cultured muscle cells in the presence of local anaesthetics. *J. Physiol. Lond.* **339**, 663-78.

Neher, E. and Steinbach, J.H. (1978). Local anaesthetics transiently block currents through single acetylcholine-receptor channels. *J. Physiol. Lond.* **277**, 153-76.

Nicoll, R.A. (1972). The effect of anaesthetics on synaptic excitation and inhibition in the olfactory bulb. *J. Physiol. Lond.* **223**, 803-814.

Nicoll, R.A., Eccles, J.C., Oshima, T. and Rubia, F. (1975). Prolongation of hippocampal inhibitory postsynaptic potentials by barbiturates. *Nature* **258**, 625-627.

Nicoll, R.A. and Iwamoto, E.T. (1978). Action of pentobarbitone on sympathetic ganglion cells. *J. Neurophysiol.* **41**, 977-986.

Nicoll, R.A. and Madison, D.V. (1982). General anaesthetics hyperpolarise neurons in the vertebrate central nervous system. *Science* **217**, 1055-1057.

Nishi, K. and Oyama, Y. (1983a). Accelerating effects of pentobarbitone on the inactivation process of the calcium current in Helix neurones. *Br. J. Pharmacol.* **79**, 645-54.

Nishi, K. and Oyama, Y. (1983b). Barbiturates increase the rate of voltage-dependent inactivation of the calcium current in snail neurones. *Br. J. Pharmacol.* **80**, 761-5.

Norenberg, W., Illes, P. and Takeda, K. (1991). Neuropeptide Y inhibits nicotinic cholinergic currents but not voltage-dependent calcium currents in bovine chromaffin cells. *Pflugers. Arch.* **418**, 346-52.

Nowycky, M.C., Fox, A.P. and Tsien, R.W. (1985). Three types of neuronal calcium channel with different calcium agonist sensitivity. *Nature* **316**, 440-443.

Ogden, D.C., Siegelbaum, S.A. and Coquhoun, D. (1981). Block of acetylcholine-activated ion channels by an uncharged local anaesthetic. *Nature* **289**, 596-598.

Patlak, J.B. (1988). Sodium channel subconductance levels measured with a new variance-mean analysis. *J. Gen. Physiol.* **92**, 413-430.

Oshima, E. and Richards, C.D. (1988). An *in vitro* investigation of the action of ketamine on excitatory synaptic transmission in the hippocampus of the guinea-pig. *Eur. J. Pharmac.* **148**, 25-33.

Papke, R.L. and Heinemann, S.F. (1991). The role of the β_4-subunit in determining the kinetic properties of rat neuronal nicotinic acetylcholine α_3-receptors. *J. Physiol. Lond.* **440**, 95-112.

Pearce, R.A., Stringer, J.L. and Lothman, E.W. (1989). Effect of volatile anesthetics on synaptic transmission in the rat hippocampus. *Anesthesiology* **71**, 591-598.

Pennefather, P., and D.J.M. Quastel. 1980. Actions of anesthetics on the function of nicotinic acetylcholine receptors. In Molecular Mechanismsof Anesthesia (Progress in Anesthesiology Vol.2). B.R. Fink, editor. Raven Press, New York. 45-57.

Perney, T.M., Hirning, L.D., Leeman, S.E. and Miller, R.J. (1986). Multiple calcium channels mediate neurotransmitter release from peripheral neurons. *Proc. Natl. Acad. Sci. U. S. A.* **83**, 6656-6659.

Peters, J.A., Kirkness, E.F., Callachan, H., Lambert, J.J. and Turner, A.J. (1988). Modulation of the $GABA_A$ receptor by depressant barbiturates and pregnane steroids. *Br. J. Pharmacol.* **94**, 1257-1269.

Phillips, G.H. 1974. Structure-activity relationships in steroidal anaesthetics. In Molecular mechanisms in general anaesthesia. M.J. Halsey, R.A. Millar, and J.A. Sutton, editors. Churchill Livingstone, . 32-47.

Pocock, G. (1980). Catecholamine secretion and ion movements in bovine adrenal medulla. *Ph.D. Thesis, University of London.*

Pocock, G. (1983). Ionic and metabolic requirements for stimulation of secretion by ouabain in bovine adrenal medullary cells. *Molec. Pharmac.* **23**, 671-680.

Pocock, G. and Richards, C.D. (1987). The action of pentobarbitone on stimulus-secretion coupling in adrenal chromaffin cells. *Br. J. Pharmacol.* **90**, 71-80.

Pocock, G. and Richards, C.D. (1988). The action of volatile anaesthetics on stimulus-secretion coupling in bovine adrenal chromaffin cells. *Br. J. Pharmacol.* **95**, 209-217.

Rane, S.G., Holz, G.G. and Dunlap, K. (1987). Dihydropyridine inhibition of neuronal calcium current and substance P release. *Pflugers Arch.* **409**, 361-366.

Richards, C.D. (1972). On the mechanism of barbiturate anaesthesia. *J. Physiol. Lond.* **227**, 749-767.

Richards, C.D. (1973). On the mechanism of halothane anaesthesia. *J. Physiol. Lond.* **233**, 439-456.

Richards, C.D. and Sercombe, R. (1970). Calcium, magnesium and the electrical activity of guinea-pig olfactory cortex *in vitro*. *J. Physiol. Lond.* **211**, 571-584.

Richards, C.D. and Hesketh, T.R. (1975). Implications for theories of anaesthesia of antagonism between anaesthetic and non-anaesthetic steroids. *Nature* **256**, 179-182.

Richards, C.D., Russell, W.J. and Smaje, J.C. (1975). The action of ether and methoxyflurane on synaptic transmission in isolated preparations of the mammalian cortex. *J. Physiol. Lond.* **248**, 121-142.

Richards, C.D., Martin, K., Gregory, S., Keightley, C.A., Hesketh, T.R., Smith, G.A., Warren, G.B. and Metcalfe, J.C. (1978). Degenerate perturbations of protein structure as the mechanism of anaesthetic action. *Nature* **276**, 775-9.

Richards, C.D. and White, A.E. (1975). The actions of volatile anaesthetics on synaptic transmission in the dentate gyrus. *J. Physiol. Lond.* **252**, 241-257.

Richards, C.D. and White, A.E. (1981). Additive and non-additive effects of mixtures of short-acting intravenous anaesthetic agents and their significance for theories of anaesthesia. *Br. J. Pharmacol.* **74**, 161-170.

Richards, C.D. (1982). The actions of pentobarbitone, procaine and tetrodotoxin on synaptic transmission in the olfactory cortex of the guinea-pig. *Br. J. Pharmacol.* **75**, 639-646.

Richards, C.D. and Smaje, J.C. (1976). Anaesthetics depress the sensitivity of cortical neurones to l-glutamate. *Br. J. Pharmacol.* **58**, 347-357.

Rosenberg, P.H., Jansson, S.E. and Gripenberg, J. (1977). Effects of halothane, thiopental, and lidocaine on fluidity of synaptic plasma membranes and artificial phospholipid membranes. *Anesthesiology.* **46**, 322-6.

Roth, S. and Seeman, P. (1972). Anesthetics expand erythrocyte membranes without causing loss of K +. *Biochim. Biophys. Acta* **255**, 190-8.

Ruff, R.L. (1977). A quantitative analysis of local anaesthetic alteration of miniature end-plate currents and end-plate current fluctuations. *J. Physiol. Lond.* **264**, 89-124.

Sawada, S. and Yamamoto, C. (1985). Blocking action of pentobarbital on receptors for excitatory amino acids in the guinea-pig hippocampus. *Exp. Brain Res.* **59**, 226-231.

Schneider, A.S., Herz, R. and Rosenheck, K. (1977). Stimulus-secretion coupling in chromaffin cells isolated from bovine adrenal medulla. *Proc. Natl. Acad. Sci. USA* **74**, 5036-40.

Scholfield, C.N. (1980). Potentiation of inhibition by general anaesthetics in neurones of the olfactory cortex in vitro. *Pflugers Arch* **383**, 249-255.

Seeman, P. (1972a). The membrane actions of anesthetics and tranquilisers. *Pharmacol. Rev.* **24**, 583-655.

Seeman, P. and Roth, S. (1972b). General anesthetics expand cell membranes at surgical concentrations. *Biochim. Biophys. Acta* **255**, 171-7.

Smaje, J.C. (1976). General anaesthetics and the acetylcholine sensitivity of cortical neurones. *Br. J. Pharmacol.* **58**, 359-368.

Somjen, G.G. and Gill, M. (1963). The mechanism of blockade of synaptic transmission in the mammalian spinal cord by diethyl ether and thiopental. *J. Pharmacol. Exp. Ther.* **140**, 19-30.

Sontag, J.M., Sanderson, P., Klepper, M., Aunis, D., Takeda, K. and Bader, M.F. (1990). Modulation of secretion by dopamine involves decreases in calcium and nicotinic currents in bovine chromaffin cells. *J. Physiol. Lond.* **427**, 495-517.

Southan, A.P. and Wann, K.T. (1989). Inhalational anaesthetics block accommodation of pyramidal cell discharge in the rat hippocampus. *Br. J. Anaesth.* **63**, 581-586.

Staiman, A. and Seeman, P. (1974). The impulse blocking concentrations of anaesthetics, alcohols, anticonvulsants, barbiturates and narcotics on phrenic and sciatic nerves. *Can. J. Physiol. Pharmac.* **52**, 535-550.

Stanley, E.F. and Atrakchi, A.H. (1990). Calcium currents recorded from a vertebrate presynaptic nerve terminal are resistant to the dihydropyridine nifedipine. *Proc. Natl. Acad. Sci. USA* **87**, 9683-9687.

Steinbach, A.B. (1968). A kinetic model for the action of xylocaine on receptors for acetylcholine. *J. Gen. Physiol.* **52**, 162-180.

Steinbach, J.H. and Ifune, C. (1989). How many kinds of nicotinic acetylcholine receptor are there?. *Trends in Neurosci.* **12**, 3-6.

Stern, R.C., Herrington, J., Lingle, C.J. and Evers, A.S. (1991). The action of halothane on stimulus-secretion coupling in clonal (GH3) pituitary cells. *J. Neurosci.* **11**, 2217-25.

Takara, H., Wada, M., Arita, K., Sumikawa, K. and Izumi, F. (1986). Ketamine inhibits ^{45}Ca influx and catecholamine secretion by inhibiting ^{22}Na influx in cultured bovine adrenal medullary cells. *Eur. J. Pharmacol.* **125**, 217-224.

Terrar, D.A. and Victory, J.G. (1988). Effects of halothane on membrane currents associated with contraction in single myocytes isolated from guinea-pig ventricle. *Br. J. Pharmacol.* **94**, 500-8.

Torda, T.A. and Gage, P.W. (1977). Postsynaptic effect of i.v. anaesthetic agents at the neuromuscular junction. *Br. J. Anaesth.* **49**, 771-6.

Trifaro, J.M. and Lee, R.W. (1980). Morphological characteristics and stimulus-secretion coupling in bovine adcrenal chromaffin cell cultures. *Neuroscience*. **5**, 1533-46.

Trudell, J.R., Hubbell, W.L. and Cohen, E.N. (1973). The effect of two inhalation anesthetics on the order of spin-labeled phospholipid vesicles. *Biochim. Biophys. Acta* **291**, 321-7.

Trudell, J.R. (1977). A unitary theory of anesthesia based on lateral phase separations in nerve membranes [proceedings]. *Biophys. J.* **18**, 358-9.

Ueda, I. and Kamaya, H. (1973). Kinetic and thermodynamic aspects of the mechanism of general anesthesia in a model system of firefly luminescence in vitro. *Anesthesiology.* **38**, 425-36.

Vernino, S., Amador, M., Luetje, C.W., Patrick, J. and Dani, J.A. (1992). Calcium modulation and high calcium permeability of neuronal nicotinic acetylcholine receptors. *Neuron* **8**, 127-134.

Wachtel, R.E. and Wegrzynowicz, E.S. (1991). Mechanism of volatile anesthetic action on ion channels. *Ann. N. Y. Acad. Sci.* **625**, 116-28.

Waymire, J.C., Bennett, W.F., Boehme, R., Hankins, L., Gilmer Waymire, K. and Haycock, J.W. (1983). Bovine adrenal chromaffin cells: high-yield purification and viability in suspension culture. *J. Neurosci. Methods* **7**, 329-51.

Weakly, J.N. (1969). Effect of barbiturates on quantal synaptic transmission in spinal motoneurones. *J. Physiol. Lond.* **204**, 63-77.

Werz, M.A. and MacDonald, R.L. (1985). Barbiturates decrease voltage-dependent calcium conductance of mouse neurones in dissociated cell culture. *Molec. Pharmac.* **28**, 269-277.

Yashima, N., Wada, A. and Izumi, F. (1986). Halothane inhibits the cholinergic-receptor-mediated influx of calcium in primary culture of bovine adrenal medulla cells. *Anesthesiology.* **64**, 466-72.

Yawo, H. (1989). Rectification of synaptic and acetylcholine currents in the mouse submandibular ganglion cells. *J. Physiol. Lond.* **417**, 307-22.

Zorychta, E. and Capek, R. (1978). Depression of spinal monosynaptic transmission by diethyl ether: Quantal analysis of unitary synaptic potentials. *J. Pharmacol. Exp. Ther.* **207**, 825-836.

Zorychta, E., Esplin, D. and Capek, R. (1975). Action of halothane on transmitter release in the spinal monosynaptic pathway. *Fedn. Proc.* **34**, 749.

A1. Derivation of the equations describing the extended block model

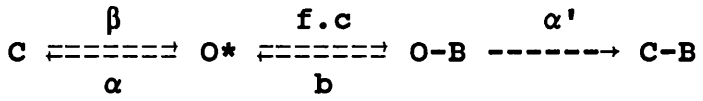

Since the mean lifetime of a single state is equal to 1/(sum of rates leading from that state):

$$\text{Mean open Time} = \frac{1}{(\alpha+f.c)}$$

$$\text{Mean blocked time} = \frac{1}{(b+\alpha')}$$

Mean burst length is equal to the mean open time per burst plus the mean shut time per burst. Mean open time per burst is the product of the mean number of openings per burst and the mean open time.

The mean number of openings per burst can be determined by first defining the probability of each state to state transition allowed by the kinetic scheme:

$$\pi_{O\rightarrow OB} = \frac{f.c}{(\alpha+f.c)}$$

$$\pi_{O\rightarrow C} = \frac{\alpha}{(\alpha+f.c)}$$

$$\pi_{OB\rightarrow O} = \frac{b}{(b+\alpha')}$$

$$\pi_{OB\rightarrow CB} = \frac{\alpha'}{(b+\alpha')}$$

The probability of there being n openings per burst is given by:

$$P_{(n)} = (\pi_{O\rightarrow OB}\cdot\pi_{OB\rightarrow O})^{n-1}\cdot(\pi_{O\rightarrow C} + \pi_{O\rightarrow OB}\cdot\pi_{OB\rightarrow CB})$$

The mean of this geometric distribution (for $1<n<\infty$), and therefore the mean number of openings per burst, is:

$$\frac{1}{(\pi_{O\rightarrow C} + \pi_{O\rightarrow OB}\cdot\pi_{OB\rightarrow CB})}$$

Replacing rates for probabilities and rearranging:

Mean number of openings/burst $= \dfrac{\alpha + f.c}{\alpha + (f.c.\alpha'/(b+\alpha'))}$

and therefore:

Mean open time/burst $= \dfrac{1}{\alpha + (f.c.\alpha'/(b+\alpha'))}$

Similarly, mean shut time per burst = mean number of gaps x mean gap length. The mean number of gaps/burst = (mean number of openings/burst) -1 , which is:

$$\frac{f.c.b}{\alpha(b+\alpha')+(f.c.\alpha')}$$

and therefore:

Mean shut time/burst $= \dfrac{f.c.b/(b+\alpha')}{\alpha(b+\alpha') + f.c.\alpha'}$

Adding the mean open and shut times per burst gives:

Mean burst length $= \dfrac{1 + (f.c.b/(b+\alpha')^2)}{\alpha + (f.c.\alpha'/(b+\alpha'))}$

A.2 The predicted spectral density function for two and three state models.

For the simple model:

$$C \underset{\alpha}{\overset{\beta}{\rightleftharpoons}} O$$

in which the binding of agonist is assumed to be rapid relative to channel opening, the spectral density function for current fluctuations is:

$$(1) \quad S_{(f)} = 4.I.\gamma.(V_m-V_r).\frac{\tau}{1+(2.\pi.f.\tau)^2}$$

I = mean current
γ = single channel conductance
V_m = holding potential
V_r = reversal potential
f = frequency

(see Anderson & Stevens 1973, Colqhoun & Hawkes 1977)

$\tau = (2.\pi.f_c)^{-1} = \alpha^{-1}$, where f_c is the frequency at which $S_{(f)} = S_{(0)}/2$ i.e the power density has fallen to half the maximum value. Therefore:

$$(2) \quad S_{(f)} = \frac{4.I.\gamma.(V_m-V_r)}{2.\pi.f_c}.\frac{1}{1+(f/f_c)^2}$$

The function reaches a maximum at f=0, when:

$$(3) \quad S_{(0)} = \frac{4.I.\gamma.(V_m-V_r)}{2.\pi.f_c}$$

and so:

$$(4) \quad \gamma = \frac{\pi.f_c.S_{(0)}}{2.I.(V_m-V_r)}$$

Expressing equation (2) as logarithms:

$$Log(S_f) = \log(S_{(0)}) - \log(1+(f/f_c)^2)$$

Therefore when $f<f_c$, $\log(S_f) \approx \log(S_{(0)})$. When $f>f_c$, $\log(S_f) \approx \log(S_{(0)}) - 2\log f + 2\log f_c$, and the function declines with slope = -2.

In general for pathways involving k states, it can be shown that the spectral density function comprises k-1 components. If all open states have the same unit conductance, γ, this is given by:

$$\gamma = \frac{\pi.S_{(0)1}.f_{c1}}{2.I.(V_m-V_r)} + \frac{\pi.S_{(0)2}.f_{c2}}{} + \ldots.$$

The spectral density function for the simple sequential model:

$$C \underset{\alpha}{\overset{\beta}{\rightleftharpoons}} O^* \underset{b}{\overset{F.c}{\rightleftharpoons}} O\text{-}B$$

Terms as previously defined. (except F= forward blocking rate constant)

is:

$$S_{(f)} = \frac{I.(V_m-V_r).\gamma.P}{\lambda_2 - \lambda_1}\left[\frac{\lambda_2-b}{\lambda_2(1+(2\pi f/\lambda_2)^2)} + \frac{b-\lambda_1}{\lambda_1(1+(2\pi f/\lambda_1)^2)}\right]$$

(see Ruff 1977)

where $P = \frac{K.A^n.\beta.b}{\lambda_1 - \lambda_2}$

K = Equilibrium constant for agonist binding
A = [Agonist] (constant)
n = Stoichiometry of agonist/receptor binding

and $\lambda_{1,2} = 0.5((\alpha+b+F.c) \pm ((\alpha+b+F.c)^2-4.\alpha.b)^{0.5})$

$f=f_{c1,2}$ when $\frac{2.\pi.f}{\lambda_{1,2}} = 1$ $\quad \therefore f_{c1,2} = \frac{\lambda_{1,2}}{2.\pi}$

and so: $\tau_{1,2} = (2.\pi.f_{c1,2})^{-1} = (\lambda_{1,2})^{-1}$

When $b+f.c > \alpha$, $\lambda_{1,2}$ are very approximately given by the following equations: (see Neher & Steinbach 1978)

$$\lambda_1 \approx \alpha+F.c+b = (M_o)^{-1} + (M_g)^{-1}$$

$$\lambda_2 \approx \alpha(1+(F.c/b))^{-1} = (M_b)^{-1}$$

M_o = mean open time
M_g = mean gap length
M_b = mean burst length

$$\tau_1 \approx \frac{M_o.M_g}{M_o + M_g}$$

$$\tau_2 \approx M_b$$

Expressions for $\lambda_{1,2}$ for the extended block model (see p.25,91) are complex:

$$\lambda_{1,2} = \{\alpha+\alpha'+b+F.c \pm [(\alpha+\alpha'+b+F.c)^2 - 4(\alpha.\alpha'+F.c.\alpha'+\alpha.b)]^{0.5}\}/2$$